Aus der Klinik für Allgemein- und Viszeralchirurgie der Medizinischen Fakultät Charité - Universitätsmedizin Berlin

DISSERTATION

Tissue-resident Lymphocytes in the Human Kidney: Signatures, Specificity and their Impact for Kidney Transplantation and Cancer
-
Gewebsständige Lymphozyten in der humanen Niere: Eigenschaften, Spezifität und ihre Bedeutung für die Nierentransplantation und den Nierenkrebs

zur Erlangung des akademischen Grades
Doctor of Philosophy (PhD)

vorgelegt der Medizinischen Fakultät
Charité - Universitätsmedizin Berlin

von
Theresa Dornieden
aus Ochtrup

Datum der Promotion: 25.11.2022

Contents

Index of abbreviations 1

Abstract 3

1. Introduction 5

1.1 Solid Organ Transplantation (SOT) 5

1.2 The concept of passenger leukocytes 5

1.3 Tissue-resident memory (T_{RM}) cells 6

1.3.1 Formation of tissue-resident memory (T_{RM}) T cells 6

1.3.2 Features of tissue-resident memory (T_{RM}) T cells 7

1.3.3 Tissue-residency of other lymphocytes 8

1.4 Renal Cell Carcinoma (RCC) 8

1.5 The role of T_{RM} cells in kidney transplantation and cancer 9

1.5.1 Impact of T_{RM} cells for transplantation 9

1.5.2 Impact of T_{RM} cells for kidney cancer 9

2. Aim of the study 10

3. Material and Methods 11

3.1 Material 11

3.1.1 Reagents 11

3.1.2 Equipment 12

3.2 Methods 13

3.2.1 Patients 13

3.2.2 Cell isolation from peripheral blood 15

3.2.3 Cell isolation from human kidney tissue 15

3.2.4 Cell counting 15

3.2.5 Freezing of isolated cells 15

3.2.6 Thawing of frozen cells 15

3.2.7 Cell staining and phenotypic analysis 16

3.2.8 Cell stimulation and functional analysis 16

3.2.9 Detection and phenotypic analysis of antigen-specific $CD8^+$ T cells 17

3.2.10 Flow cytometry 18

3.2.11 Multi-epitope ligand cartography (MELC) 19

3.2.12 Analysis and statistics 21

4. Results 22

4.1 Enrichment of effector memory T cells with an activated and pro-inflammatory phenotype in human kidney tissue 22

4.2 Tissue-resident memory (T_{RM}) T cells reside within the human kidney 23

4.3 $CD8^+$ T_{RM} T cells within the human kidney are activated 25
4.4 Renal $CD8^+$ T_{RM} T cells accumulate with increasing age 26
4.5 Increase of T_{RM} T cell frequency with elevated kidney function 27
4.6 Identification of further renal T_{RM} lymphocyte subsets 27
4.7 $CD8^+$ T_{RM} lymphocytes in renal cell carcinoma (RCC) are exhausted 28
4.8 Tumor-derived $CD8^+$ T_{RM} T cells are functionally impaired in metastasized patients 29
4.9 Antigen-specific T cells reside within the human kidney, but do not exhibit a T_{RM} phenotype.. 30
5. Discussion 31
6. Further work / Co-Authorships 35
7. Own Contributions 36
Literature 37
Eidesstaatliche Versicherung 42
Anteilserklärung 43
Auszug aus der Journal Summary List 44
Signatures and Specificity of Tissue-resident Lymphocytes Identified in Human Renal Peritumor and Tumor Tissue, Dornieden et al., JASN, 2021; 32: 2223-2241 45
Auszug aus der Journal Summary List 64
Mucosal associated invariant T cells are differentially impaired in tolerant and immunosuppressed liver transplant recipients, Sattler and Thiel et al., Am. J. Transplant., 2021; 21: 87-102 65
Lebenslauf 81
Publikationsliste 82
Danksagung 83

Index of abbreviations

Abbreviation	Meaning
%	percent
°C	degree Celsius
µl	microliter
2D	two-dimensional
3D	three-dimensional
APC	antigen-presenting cell
BKV	BK-Polyomavirus
BSA	bovine serum albumin
CD	cluster of differentiation
CM	central memory
CMV	Cytomegalovirus
CTLA4	cytotoxic T-lymphocyte-associated protein 4
CO_2	carbon dioxide
DAPI	4′,6-Diamidin-2-phenylindol
DMSO	dimethylsulfoxid
DN	double negative
EBV	Epstein-Barr virus
ECM	extracellular matrix
eGFR	estimated glomerular filtration rate
EM	effector memory
EMRA	terminally differentiated effector cells
FCS	fetal calf serum
FoxP3	Forkhead-Box-Protein P3
GvHD	graft-versus-host-disease
h	hour
HLA-A2	human leukocyte antigen serotype A2
HLA-DR	human leukocyte antigen-DR isotype
IFNγ	interferon γ
IL-2/5/13/17	interleukin 2/5/13/17
IL-12/15/18R	interleukin 12/15/18 receptor
ILC	innate lymphoid cell
L/D	live/dead

MAIT	mucosa-associated invariant T
MELC	multi-epitope ligand cartography
MFI	mean fluorescent intensity
mg	milligram
MHC	major histocompatibility complex
min	minute
ml	milliliter
MNCs	mononuclear cells
MR1	major histocompatibility complex class I-related gene protein
mTOR	mechanistic Target of Rapamycin
NaCl	sodium chloride
NK cell	natural killer cell
ns	not specified
OCT	optimal cutting temperature compound
PBMCs	blood peripheral mononuclear cells
PBS	phosphate buffered saline
PD-1	programmed cell death protein 1
PMA	phorbol myristal acetat
P/S	penicillin/streptomycin
RCC	renal cell carcinoma
ROI	region of interest
RORγt	RAR-related orphan receptor gamma
RPMI	medium developed at “Roswell Park Memorial Institute”
RT	room temperature
SD	standard deviation
SOT	solid organ transplantation
TCR	T cell receptor
TNFα	tumor necrosis factor α
TR	tissue-resident
TRM	tissue-resident memory
tSNE	t-distributed stochastic neighbor embedding
VEGF	vascular endothelial growth factor

Abstract

Tissue-resident memory (T_{RM}) lymphocytes are attracting increasing attention. Identification of T_{RM} cells in various tissues, such as skin, lung, intestine, brain or liver, suggest that they play a role in local pathogen detection and that they mediate a first line defense within the tissue. So far, no detailed investigation of the specificity and function of T_{RM} cells within the human kidney exists, as well as data related to their role in kidney transplantation and kidney cancer.

In this study, isolated lymphocytes out of blood, human peri-tumor and tumor kidney tissue were analyzed using flow cytometry and MELC histology. Using these technologies, the existence of the major T cell T_{RM} subsets characterized by $CD8^+$ $CD69^+CD103^+$ and $CD8^+$ $CD69^+CD103^-$ expression was demonstrated within the human kidney. These $CD8^+$ T_{RM} T cells displayed an activated phenotype and a pro-inflammatory effector profile, exhibiting increased IL-17 production. Interestingly, increased frequencies of $CD8^+$ T_{RM} T cells were associated with increased age and, moreover, a correlation of $CD4^+$ and $CD8^+$ T_{RM} cell frequency with eGFR could be detected. Beside the presence of T_{RM} T cells, renal $CD56^{dim}$ and $CD56^{bright}$ NK cells and mucosa-associated invariant T (MAIT) cells expressing the T_{RM} markers CD69 and CD103 were identified. Furthermore, tumor-derived $CD8^+$ T_{RM} cells were identified to upregulate the exhaustion markers PD-1 and TOX and were functionally impaired in metastasized patients. Finally, $CD8^+$ T cells specific for BKV, CMV, EBV and influenza could be detected within renal peri-tumor and tumor tissue. Interestingly, these cells did not display a T_{RM} phenotype. In summary, these data present a detailed overview of the phenotype and function of human renal T_{RM} cells for the very first time, giving indications for their potential relevance in kidney transplantation and cancer.

Gewebsständige Lymphozyten (engl.: tissue resident memory (T_{RM}) lymphocytes) stehen derzeit im Fokus der Forschung. Bislang wurden diese in verschiedenen Geweben identifiziert, darunter beispielsweise in Haut, Lunge, Darm, Gehirn und Leber. Ihre Haupteigenschaft besteht in der schnellen und lokalen Abwehr von Pathogenen und dem Schutz vor Reinfektion des jeweiligen Organs. Bislang wurden gewebsständige Lymphozyten in der humanen Niere zwar identifiziert, diese jedoch nicht hinsichtlich ihrer Spezifität und Funktion, sowie ihrer Rolle für die Nierentransplantation und Nierentumore analysiert.

Ziel dieser Studie war es, Lymphozyten, welche aus Blut, peri-Tumor und Tumorgewebe der humanen Niere isoliert wurden, mittels Durchflusszytometrie und MELC Histologie zu analysieren. Dabei konnten T_{RM} T Zell Hauptpopulationen in der humanen Niere identifiziert werden, welche durch die Expression der Marker $CD8^+$ $CD69^+CD103^+$ und $CD8^+$ $CD69^+CD103^-$ gekennzeichnet waren. Diese $CD8^+$ T_{RM} T Zellen zeigten einen aktivierten Phänotyp und ein pro-inflammatorisches Effektorprofil mit gesteigerter Produktion von IL-17. Interessanterweise konnte eine erhöhte Frequenz von $CD8^+$ T_{RM} T Zellen mit ansteigendem Alter assoziiert werden. Außerdem konnte gezeigt werden, dass die Frequenz von $CD8^+$ und $CD4^+$ T_{RM} T Zellen mit der glomerulären Filtrationsrate (eGFR) korrelierte. Neben T Zellen konnten außerdem auch $CD56^{dim}$ und $CD56^{brigh}$ NK Zellen, sowie, Mukosa-assoziierte invariante T (MAIT) Zellen identifiziert werden, welche die T_{RM} Marker CD69 und CD103 exprimierten. $CD8^+$ T_{RM} T Zellen aus dem

Tumor waren zudem durch eine gesteigerte Expression der Marker PD-1 und TOX gekennzeichnet und zeigten in metastasierten Patienten eine geschwächte Funktionalität. Schließlich wurden $CD8^+$ T Zellen, welche spezifisch für BKV, CMV, EBV sowie das Influenza Virus waren, im renalen peri-Tumor und Tumorgewebe identifiziert, welche jedoch keinen T_{RM} Phänotyp zeigten. Somit gibt diese Studie einen detaillierten Überblick über den Phänotyp und die Funktion von T_{RM} Zellen in der humanen Niere, sowie einen Hinweis darauf, welchen Einfluss sie auf die Nierentransplantation und Nierentumore haben könnten.

1. Introduction

1.1 Solid Organ Transplantation (SOT)

Solid organ transplantation (SOT) is the method of choice for end-stage organ failure. From all solid organ transplantations, kidney transplantation is the most performed one. However, the limited access to donor organs remains still an important issue. In Germany, a total number of 3270 organs of deceased donors were transplanted in 2020. Only in December 2020, 9192 patients were registered on an active waiting list, highlighting the shortage of available organs (https://statistics.eurotransplant.org/). Comparing different types of SOT and their graft survival, kidney transplantation is the most effective with a graft survival of 12-16 years (Lamb et al., 2011). Other organs exhibit lower survival half-lives, such as liver with 8.5 years, lungs with 5.2 years or intestine with 3.6 years (Lodhi et al., 2011).

Despite its effectiveness in overcoming end-stage orang failure, acute and chronic rejection of the graft remain a problem of SOT. A continuous immune defense against the graft can cause chronic rejection (Selvaggi et al., 2009). Therefore, reaching long-term survival of the graft is one of the most important aspects. An important factor is the function of T cells and other immune cells and how effective these cells are targeted by immunosuppressive reagents (Kirk et al., 2011). The aim of a successful immunosuppressive treatment is both to regulate T cell immune responses in a way that rejection processes are suppressed but protection to pathogens is still maintained, with the result that patients do not suffer from infections and gain a long-term survival of the graft (Kawai et al., 2008). Main mediators of graft rejection are effector memory (EM) T cells, which become easily activated and have access to graft tissue due to the expression of adhesion molecules such as integrins or selectins (Krummey and Ford, 2012). Interestingly, it could be demonstrated that organs used for kidney and lung recipients displaying high levels of peripheral memory T cells pre-transplantation and producing specific cytokines, are associated with a high rate of rejection and short graft survival (Heeger et al., 1999, San Segundo et al., 2013). A major goal in transplantation medicine is the improvement of the treatment of transplanted patients, which in turn assumes a better understanding of the mechanisms of rejection and associated immune reactions. Among others, an important factor for the graft survival and transplantation outcome is the function of so-called passenger leukocytes (Taylor et al., 2006, Srinivas and Meier-Kriesche, 2008).

1.2 The concept of passenger leukocytes

The concept of passenger leukocytes was first described by George Davis Snell in 1957 and further explained by Elkins and Guttmann in 1968 (Snell, 1957 and Elkins and Guttmann, 1968). It describes a theory of graft rejection after organ transplantation, indicating the ability of donor-specific leukocytes within the allograft stimulating alloreactive T cells from the recipient and thereby causing rejection of the graft (Thaunat and Morelon, 2007). It could be demonstrated that all organs contain leukocytes which reside in the interstitium of the particular organ, either temporarily or permanently. Is the organ used as an allograft, these leukocytes are carried together with the organ into the recipients' body and are called "passenger leukocytes". These cells either remain in the allograft or migrate into the recipients' body, in both cases contributing to allograft rejection (Demetris et al., 1995, Thaunat and Morelon, 2007). In the

past years, the existence and features of leukocytes residing within various organs was studied and so-called tissue-resident memory (T_{RM}) cells obtained increasing attention.

1.3 Tissue-resident memory (T_{RM}) cells

1.3.1 Formation of tissue-resident memory (T_{RM}) T cells

Passenger leukocytes include T cells, which are known to be one of the main drivers in graft rejection. To gain a better insight into the formation and function of T cells and tissue-resident memory (T_{RM}) T cells as well as into general SOT immunology, it is important to understand T cell development. Naïve T cells arise in the thymus and are characterized by $CD45RA^+$ and $CD62L/CCR7^+$ expression (Turner et al., 2014b). A naïve T cell is activated and acquires effector function due to interaction with a cognate antigen in the lymph nodes (Chang et al., 2014, Wherry et al., 2003). Interaction with an antigen is based on the interaction between the T cell receptor (TCR) and the MHC molecule expressed by an antigen presenting cell (APC) (Chang et al., 2011), whereby the specificity of the response is provided (Guerder et al., 1995, Turka et al., 1990). In addition, to avoid autoimmunity or unnecessary immune activation, the process of co-stimulation is required for activation as well. This co-stimulation is based on an interaction of B7, a protein expressed on APCs, and CD28, which is expressed on T cells. This interaction is necessary for the confirmation of the correct context of the response (Guerder et al., 1995, Turka et al., 1990). CD28 expression is downregulated, when T cells become activated and differentiated, therefore CD28 is used as a marker for antigen-experienced and differentiated cells in humans (Mou et al., 2014). This co-stimulatory pathway is also used as a target for various therapeutic agents, such as the immunosuppressive drug belatacept (Espinosa et al., 2016). Once a naïve T cell has interacted with an antigen, clonal expansion starts and an effector phenotype ($CD45RA^+$ $CD62L/CCR7^-$) is generated. Effector cells are able to migrate to peripheral sites following infection and can differentiate into memory cells (Turner et al., 2014b, Chang et al., 2014, Wherry et al., 2003, Sallusto et al., 2000). The two memory phenotypes of a T cell include the central memory (CM) ($CD45RA^-$ $CD62L/CCR7^+$) and the effector memory (EM) ($CD45RA^-CD62L/CCR7^-$) cells, which vary in several aspects. While CM T cells have the ability to move to secondary lymphoid organs and show longevity, EM T cells circulate between the periphery and non-lymphoid tissues and have a shorter lifetime. Additionally, CM T cells have a higher proliferation capacity compared to EM (Turner et al., 2014b, Weninger et al., 2001, Baron et al., 2003, Butcher and Picker, 1996, Mackay et al., 1990). The main characteristic of memory T cells is their improved efficiency in antigen response (Curtsinger et al., 1998), since they are able to respond rapidly and potently to antigen encounters (Espinosa et al., 2016). Persisting memory T cells can be grouped into two subsets: circulating cells, which migrate to tissue sites through the periphery, and non-circulating cells, which reside and remain within tissues (Mueller et al., 2013, Schenkel and Masopust, 2014). Non-circulating memory T cells are called T_{RM} T cells and can be found in various lymphoid tissues as well as in non-lymphoid tissues, such as the intestine, skin, lung or liver. It is assumed that these cells may be involved in local immune responses and regulation (Mueller et al., 2013, Masopust and Picker, 2012).

1.3.2 Features of tissue-resident memory (T_{RM}) T cells

Only 2-3% of the total amount of T cells in the human body can be detected in the blood, whereas the majority of T cells reside in lymphoid and non-lymphoid tissue sites (Ganusov and De Boer, 2007, Clark, 2010, Purwar et al., 2011). A fraction of these cells does not circulate and remain within the tissue. These so-called tissue-resident memory (T_{RM}) T cells exhibit a specific phenotype (Mueller et al., 2013, Masopust and Picker, 2012). T_{RM} cells are basically characterized by the expression of the surface markers CD69, CD49a and CD103, whereas the latter is mainly expressed on $CD8^+$ T cells. CD69 is a marker for early T cell activation and retention in tissues (Mueller et al., 2013, Gebhardt et al., 2011, Turner et al., 2014a, Shinoda et al., 2012, Strauch et al., 2001). The *integrin α1* or CD49a is an adhesion molecule binding extracellular matrix components such as collagen (Cheuk et al., 2017), whereas CD103 is an integrin (integrin α_E), which recognizes E-cadherin on epithelial cells and is relevant for adhesion, controlling localization and motility (Strauch et al., 2001, Fan and Rudensky, 2016). Another important characteristic of T_{RM} cells is their memory-like phenotype, since they are able to respond at early time points of infection due to fast production of effector cytokines, cytolytic molecules or growth factors (Fan and Rudensky, 2016). T_{RM} cells have specific features, including the ability to self-renewal within the tissue as well as the ability to recognize microbial products and respond by producing antimicrobial or tissue-protective factors (Fan and Rudensky, 2016). Altogether, T_{RM} cells are important for direct and fast responses against infections and clearance of pathogens within the tissue and play an important role in immune response and regulation. (Schenkel and Masopust, 2014, Turner et al., 2014b, Teijaro et al., 2011). Interestingly, it was demonstrated, that T_{RM} cells within the lung are highly protective against influenza virus compared to their circulating counterparts within the spleen (Turner et al., 2014b, Teijaro et al., 2011). Another relevant feature of T_{RM} cells is the maintenance of immune homeostasis, by mediating immune response against infiltrating autoimmune reactive T cells and preventing tissue destruction (Turner et al., 2014b). Moreover, it is assumed that tissue-residency is especially a feature of T cells that are specific for pathogens, which are known to infect the particular tissue. Interestingly, it was demonstrated that a high frequency of influenza-specific memory T cells exhibit a T_{RM}-phenotype in the lung, compared to the spleen in mice (Turner et al., 2014a, de Bree et al., 2005). This indicates that T_{RM} cells could be generated and differentiated due to pathogen-specific infection of the tissue: Pathogen-specific memory T cells migrate to the infected tissue, differentiate and remain as T_{RM} cells (Turner et al., 2014b). Another assumption is that T cells, which infiltrate the graft after transplantation and mediate rejection, differentiate into T_{RM} cells and remain within the tissue. Evidence for that is the upregulation of CD103 by alloreactive graft-infiltrating T cells in mouse, rat and human organs, including pancreas or kidney (Turner et al., 2014b, Feng et al., 2002, Wang et al., 2004, Yuan et al., 2005). Beside the protecting features, it is assumed that T_{RM} cells might have adverse effects and are involved in diseases such as autoimmunity, allergy, inflammation or immunopathology (Schenkel and Masopust, 2014, Masopust and Soerens, 2019). If they do not recognize a pathogenic but a self- or harmless antigen instead, activation can lead to severe and long-lasting damage. Interestingly, first experiments could already demonstrate a triggering of allergic airway disease caused by T_{RM} $CD4^+$ cells (Masopust and Soerens, 2019, Hondowicz et al., 2016). Moreover, there is evidence that they are involved in various autoimmune diseases such as inflammatory bowel diseases or multiple

sclerosis due to their triggering features such as local proliferation or production of pro-inflammatory cytokines (Masopust and Soerens, 2019, Kleinschek et al., 2009, Sasaki et al., 2014).

In summary, based on their characteristics, T_{RM} cells are important players for protection against pathogens, infections and cancer as well as for mediation of immune response within the tissue on the one hand. While they also could be drivers for several diseases or potential mediators of graft destruction and rejection in a transplantation setting on the other hand (Schenkel and Masopust, 2014, Turner et al., 2014b, Masopust and Soerens, 2019). Therefore, targeting and elimination of T_{RM} cells could be a novel and innovative approach in transplantation or disease, however further detailed studies are needed (Masopust and Soerens, 2019).

1.3.3 Tissue-residency of other lymphocytes

The feature of tissue-residency is not exclusively a characteristic of T cells. Most other lymphocyte populations reside within tissue sites as well (Masopust and Soerens, 2019). Mucosal-associated invariant T (MAIT) cells are a subpopulation of T cells expressing a semi-invariant Vα7.2 TCR and the C-type lectin receptor CD161. In addition, MAIT cells express various cytokine receptors, such as IL-12R, IL-15R and IL-18R. Activation of these cells is either triggered in a TCR-dependent manner by bacterial riboflavin biosynthesis products which are presented to the TCR by the MCH-I molecule MR1, or in a TCR-independent manner by responding to innate interleukins (Corbett et al., 2014, Kjer-Nielsen et al., 2012, Treiner et al., 2003). Key features of MAIT cells are the production of IFN-γ and IL-17, their antibacterial protection due to the ability of sensing microbial products which are bound to MR1, as well as their dominant presence in liver and intestine (Kjer-Nielsen et al., 2012, Dusseaux et al., 2011, Chua et al., 2012, Georgel et al., 2011, Le Bourhis et al., 2010, Meierovics et al., 2013). Furthermore, non-classical T cells, including TCRγδ$^+$ or CD8αα TCRαβ$^+$ T cells which control homeostasis, show tissue-residency (McDonald et al., 2018). Other populations for which residency within tissue sites could be demonstrated are memory B and plasma cells (Onodera et al., 2012, Landsverk et al., 2017) as well as Natural Killer (NK) cells (Peng and Tian, 2017). Human NK cells are characterized by the expression of the surface markers CD56 and CD16 and have the ability to kill infected or cancer cells. It was demonstrated that tissue-resident NK cells, which are distinct from conventional NK cells, reside in various tissues, such as liver or uterus (Peng and Tian, 2017). Altogether, all of these tissue-resident lymphocytes share the function of tissue site protection in various diseases and maintenance of integrity, as well as their protective role in cancer is discussed (Medzhitov, 2008, Schenkel and Masopust, 2014).

1.4 Renal Cell Carcinoma (RCC)

As already mentioned, T_{RM} cells are evaluated to be important players for the protection against pathogens, infections and various cancers (Schenkel and Masopust, 2014). However, their role in renal cell carcinoma was not investigated yet. Kidney cancer is one of the most common cancers, where renal cell carcinoma (RCC) is the most frequent form. Patients diagnosed with RCC are mostly older patients with an average age of 65 years and men are more affected than women (Siegel et al., 2017, Klatte et al., 2007, Choueiri and Motzer, 2017). The survival prognosis for patients with RCC is poor, especially for high-stage disease patients (Siegel et al., 2017, Siegel et al., 2016). Although the majority of low stage tumors can be removed due to surgical treatments and therefore have a good prognosis, a

percentage of 20 to 30 % will either develop metastatic disease after surgery or already present metastases (Patard et al., 2002, Tsui et al., 2000, Zisman et al., 2002). Due to that, RCC is incurable for most of the patients (Klatte et al., 2007). Medical treatment of RCC has improved over the past years. Several first-line and second-line therapies exist and can be chosen depending on the patient. These are for instance various drugs against the vascular endothelial growth factor (VEGF) or mTOR inhibitors with distinct effects and side effects (Choueiri and Motzer, 2017).

1.5 The role of T_{RM} cells in kidney transplantation and cancer

1.5.1 Impact of T_{RM} cells for transplantation

As previously described, solid organs, which are used for transplantation, contain a number of T_{RM} cells. Interestingly, organs which show a high number of T_{RM} cells, including lung and intestine, are associated with high rates of complications and restricted long-term survival after they have been transplanted (Lodhi et al., 2011). The role of T_{RM} cells in transplantation is diversely discussed and worth to consider for transplantation outcome and graft survival. T_{RM} cells can have both positive and negative impact on solid organ transplants. On the one hand, T_{RM} cells mediate immune responses in the tissue site. They provide protection against local acute infections and reactivation of chronic infections as well as prevention of circulating T cell infiltration and associated tissue destruction (Turner et al., 2014b). On the other hand, alloreactive recipient T cells can migrate into the graft, develop a T_{RM} phenotype and contribute to allograft rejection (Feng et al., 2002, Wang et al., 2004, Yuan et al., 2005, Hadley et al., 1999, Smyth et al., 2007). Furthermore, donor T_{RM} cells can mediate GvHD through migration into the recipient's organism (Turner et al., 2014b).

1.5.2 Impact of T_{RM} cells for kidney cancer

So far, various studies described the existence of $CD8^+$ T_{RM} T cells in different tumor entities, including urothelial, colorectal or lung cancer (Djenidi et al., 2015, Wang et al., 2015, Quinn et al., 2003). It is thought that T_{RM} cells have the function to control cancer cells (Gebhardt et al., 2018) and according to that, their accumulation is associated with a prolonged survival in plenty tumor patients and serves as a prognostic marker (Webb et al., 2014, Djenidi et al., 2015, Wang et al., 2015).

Yet, no detailed analysis of the existence and function of T_{RM} cells within kidney cancer was performed. Solely a previous study from Van den Hove et al (1997) could demonstrate that RCC tissue is infiltrated by mainly $CD3^+$ T cells, with a large amount of $CD8^+$ T cells, as well as NK cells. All detected infiltrating lymphocyte subsets expressed the surface marker CD69 significantly higher than their counterparts in the peri-tumor tissue (Van den Hove et al., 1997).

2. Aim of the study

Although organs are perfused before transplantation, it is assumed that kidney-resident cells are transplanted along with the graft and can trigger immune reactions. So far very little is known about the general immune cell composition and especially about T_{RM} cells within the human kidney and their impact for transplantation as well as kidney cancer. A recent published study from Park et al (2020) described the immune cell composition in normal human kidneys, however included a limited number of patients (Park et al., 2020). De Leur et al (2019) could first demonstrate the presence of T_{RM} T cells within human kidney allografts (de Leur et al., 2019). Furthermore, the existence of renal MAIT and T_{RM} MAIT cells was demonstrated by Law et al (2019) and Terpstra et al (2020) recently (Law et al., 2019, Terpstra et al., 2020). Nevertheless, a detailed investigation of the human renal immune cell composition and especially of T_{RM} lymphocytes within renal tissue out of a large patient cohort is still not demonstrated, as well as their presence and potential relevance in transplantation and renal cancer. Therefore, the main objectives of the study were as follows:

1. Based on the above-mentioned information, it was aimed to comprehensively characterize the various lymphocyte subsets in the human kidney tissue in a large patient cohort.
2. Further, it should be addressed how these renal derived lymphocyte subsets differ from the cells in the paired peripheral blood and if T_{RM} cells can be identified in the human kidney, which are absent in the peripheral blood.
3. Especially T_{RM} cell characteristics should be identified by analyzing their surface marker expression and cytokine profile.
4. By means of MELC histology it should be detected where the identified kidney-resident cells are located and if they interact with other cells.
5. In order to investigate if renal T_{RM} cell frequencies correlate with age or kidney function, clinical parameters of the patients should be studied and associated with obtained experimental data.
6. A further objective of the study was to investigate if renal leukocytes derived from peri-tumor and tumor tissue of RCC patients differ in their frequencies and characteristics.
7. To better understand the function of renal T_{RM} cells, it was aimed to identify antigen-specific cells within the human kidney and to address if these cells have a tissue-resident memory phenotype.
8. Finally, it should be tried to figure out the potential role of kidney-resident cells for kidney transplantation and renal cancer.

3. Material and Methods

The following description of “Material and Methods” is based on the paper Dornieden et al. Signatures and Specificity of Tissue-resident Lymphocytes Identified in Human Renal Peritumor and Tumor Tissue. 2021. JASN.

3.1 Material

3.1.1 Reagents

Following reagents were used for experiments (see table 1):

Table 1: Used reagents with particular manufacturer and location. Source: Dornieden et al. Signatures and Specificity of Tissue-resident Lymphocytes Identified in Human Renal Peritumor and Tumor Tissue. 2021. JASN.

Reagent	Manufacturer
AB serum human	Pan Biotech, Aidenbach, Germany
Bovine serum albumin (BSA)	Carl Roth, Karlsruhe, Germany
Brefeldin A	Cayman, Michigan, USA
CASY Clean	OLS, Bremen, Germany
CASY Ton	OLS, Bremen, Germany
Collagenase II	Gibco, Thermo Fisher, Darmstadt, Germany
Dimethylsulfoxid (DMSO)	Honeywell, Seelze, Germany
DNAse I	Sigma Aldrich, Merck, Darmstadt, Germany
FACS Clean	Thermo Fisher, Darmstadt, Germany
FACS Flow	Thermo Fisher, Darmstadt, Germany
FACS Rinse	Thermo Fisher, Darmstadt, Germany
Fetal calf serum (FCS)	Gibco, Thermo Fisher, Darmstadt, Germany
Fix/Perm kit	Thermo Fisher, Darmstadt, Germany
Fix/Perm kit	BD, Heidelberg, Germany
Ionomycin	Sigma Aldrich, Darmstadt, Germany
Isopentane	AppliChem, Darmstadt, Germany
Leukohuman Separating Solution	Genaxxon, Ulm, Germany
Optimal cutting temperature compound (OCT)	Sakura, Alphen aan den Rijn, Netherlands
Paraformaldehyde 2% (methanol- and RNAse-free)	Electron Microscopy Sciences, Hatfield, PA, USA
Penicillin/Streptomycin (P/S)	Sigma Aldrich, Merck, Darmstadt, Germany
Phorbol myristat acetat (PMA)	Sigma Aldrich, Darmstadt, Germany
Phosphate buffered saline (PBS)	Biochrom, Berlin, Germany
RPMI-1640 medium	Corning, Falcon, Kaiserslautern, Germany
Sodium chloride (NaCl) 0.9 % injection solution	B. Braun Melsungen AG, Melsungen, Germany

3.1.2 Equipment

Following equipment was used for experiments (see table 2):

Table 2: Used equipment with corresponding manufacturer and location. Source: Dornieden et al. Signatures and Specificity of Tissue-resident Lymphocytes Identified in Human Renal Peritumor and Tumor Tissue. 2021. JASN.

Equipment	Manufacturer
2 ml plastic pipet	VWR, Darmstadt, Germany
5 ml plastic pipet	Sarstedt, Nürnbrecht, Germany
10 ml plastic pipet	Fisher Scientific, Schwerte, Germany
25 ml plastic pipet	Fisher Scientific, Schwerte, Germany
1.5 ml reaction tube	Brand, Wertheim, Germany
5 ml reaction tube	Sarstedt, Nürnbrecht, Germany
15 ml reaction tube	Corning, Falcon, Kaiserslautern, Germany
50 ml reaction tube	Corning, Falcon, Kaiserslautern, Germany
Bench EnvairEco Safe basic Plus	Envair, Emmendingen, Germany
Bench HeraSafe	Kendro, Langenselbold, Germany
CASY Cell counter & analyser	OLS, Bremen, Germany
CASY Cups	OLS, Bremen, Germany
Centrifuge 5415 R	Eppendorf, Hamburg, Germany
Centrifuge Multifuge 3 S-R	Thermo Fisher Scientific, Schwerte, Germany
Centrifuge Universal 320 R	Hettich, Tuttlingen, Germany
Cover slides (APES-coated)	Menzel-Gläser, Braunschweig, Germany
Cryomold	Sakura, Alphen aan den Rijn, Netherlands
Cryotubes	Sarstedt, Nürnbrecht, Germany
Cryotome NX80	ThermoFisher, Waltham, MA, USA
FACS tubes	Corning, Falcon, Kaiserslautern, Germany
FlowJo Version 10	BD, Heidelberg, Germany
Fortessa X-20 flow cytometer	BD, Heidelberg, Germany
Freezer -80 °C	Heraeus, Hanau, Germany
Fridge Freezer Combination	Liebherr Medline, Bulle, Switzerland
GraphPad Prism 7	GraphPad Software, Inc., San Diego, USA
Incubator	Eppendorf, Hamburg, Germany
Liquid nitrogen tank Cyrosystem 2000	MVE, Jüchen, Germany
Lithium Heparin blood selection tubes	Greiner Bio-One, Frickenhausen, Germany
Petri dishes	Corning, Falcon, Kaiserslautern, Germany
Pipetboy	Neolab, Heidelberg, Germany
Pipette/Diluter CAVRO XL3000	Tecan GmbH, Crailsheim, Germany
Pipets	Eppendorf, Hamburg, Germany
Silicone sheets	Life Technologies, Carlsbad, CA, USA
Strainer 100 µl	Corning, Falcon, Kaiserslautern, Germany
Syringes 2 ml	B. Braun Melsungen AG, Melsungen, Germany
Tips 10 µl	VWR, Darmstadt, Germany
Tips 200 µl	Sarstedt, Nürnbrecht, Germany
Tips 1000 µl	Brand, Wertheim, Germany
Toponome Image Cycler® MM3	MelTec GmbH & Co.KG, Magdeburg, Germany
Vacuum pump	Neolab, Heidelberg, Germany
Vortex Shaker	Neolab, Heidelberg, Germany
Waterbath SW22	Julabo, Seelbach, Germany

3.2 Methods

3.2.1 Patients

All samples were obtained from the Clinic for Urology of Charité-Universitätsmedizin Berlin, Germany. Blood, peri-tumor and tumor samples (from renal cell carcinoma (RCC) patients) were collected from patients undergoing nephrectomy. Patient demographics are shown in table 3. Altogether, 62 patients were included in this study, however not all patients could be included in all experiments due to limited access to tissue and resulting cell numbers, especially tumor tissue was extremely restricted. The study was approved by the Ethics Committee of Charité-Universitätsmedizin Berlin (EA1/353/16, EA4/066/19) and all experiments described in this study were conducted in compliance with the Declarations of Helsinki and Istanbul (Dornieden et al., 2021).

Table 3: Patient Demographics. In total, 62 patients were included in this study, not all patients were included in all experiments due to limited tissue access, tissue size and cell numbers, ns = not specified. Source: Dornieden et al. Signatures and Specificity of Tissue-resident Lymphocytes Identified in Human Renal Peritumor and Tumor Tissue. 2021. JASN.

Variable	**n (%)**	**min/max**	**mean**	**SD**
Total number of included patients	62 (100)			
Age (in years)		26 / 85	63.92	13.58
Gender (female/male)	22 (35.48) / 40 (64.52)			
Clinical Parameters:				
Cause of Nephrectomy:				
Renal cell carcinoma (RCC)	46 (74.19)			
Ureter tumor	7 (11.29)			
Oncocytoma	1 (1.61)			
Nephrolithiasis	1 (1.61)			
Impaired function	4 (6.45)			
Cystic kidney	3 (4.84)			
Pre-operative kidney function (eGFR CKD-EPI):				
Stage 1 (≥90 ml/min)	8 (12.90)			
Stage 2 (60-90 ml/min)	24 (38.71)			
Stage 3 (30-60 ml/min)	17 (27.42)			
Stage 4 (15-30 ml/min)	2 (3.23)			
Stage 5 (<15 ml/min)	5 (8.06)			
ns	6 (9.68)			
Further diagnoses:				
Hypertension	37 (59.98)			
Chronic kidney disease	17 (27.42)			
Diabetes	DM1: 1 (1.61) DM2: 12 (19.35)			
Cardiac disease	11 (17.74)			
Staging by size of tumor (T):	**% of n=46 (tumor patients)*			
T1 (thereof 1a, 1b)	23 (50.00*) (11 (23.91*), 13 (28.26*))			
T2 (all 2a)	8 (17.39*)			
T3 (all 3a)	13 (28.26*)			
T4	2 (4.35*)			
Relapse or tumor patients:				
Renal cell carcinoma (RCC) remained kidney	1 (2.17*)			
Lung + Lymph nodes	1 (2.17*)			
Urinary Bladder	1 (2.17*)			
Liver	1 (2.17*)			
Larynx	1 (2.17*)			
Prostate	1 (2.17*)			
no	40 (86.96*)			
Metastases diagnosed before nephrectomy:				
Pulmonary metastases	3 (6.52*)			
Osseous metastases	2 (4.35*)			
Adrenal gland metastases	1 (2.17*)			
Lymph node metastases	2 (4.35*)			
Lymph node + pulmonary metastases	1 (2.17*)			
no	37 (80.43*)			

3.2.2 Cell isolation from peripheral blood

Blood peripheral mononuclear cells (PBMCs) were isolated from 10 ml heparinized peripheral blood with Leukohuman Separating Solution and density gradient centrifugation. Isolated PBMCs were resuspended in PBS containing 0.25 % BSA and stored at 4 °C for further use (Dornieden et al., 2021).

3.2.3 Cell isolation from human kidney tissue

After nephrectomy, kidneys were perfused with 0.9 % NaCl to remove peripheral blood. Tissue samples were separated and stored at RT in fresh 0.9 % NaCl. Peri-tumor and tumor (RCC) kidney tissues were dissected into small pieces, added to digestion medium containing RPMI 1640 medium supplemented with 0.3 mg/ml glutamine and 10 % FCS, 1 % P/S, 1 mg/ml Collagenase II and 10 U/ml DNAse I and incubated for 45 min at 37 °C, while shaking. Reaction was stopped with 10 ml cold RPMI 1640 medium containing 0.3 mg/ml glutamine, 10 % FCS and 1 % P/S. Tissue suspension was filtered through a 100µm strainer and washed at 504 xg for 15 min at 4 °C. The pellet was resuspended in 20 ml RPMI 1640 medium containing 0.3 mg/ml glutamine, 10 % FCS and 1 % P/S and mononuclear cells (MNCs) were isolated with Leukohuman Separating Solution and density gradient centrifugation. Isolated MNCs were washed with PBS containing 0.25 % BSA at 504 xg for 12 min at 4 °C. Supernatant was discarded and the pellet was resuspend in PBS containing 0.25 % BSA and stored at 4 °C for further use (Dornieden et al., 2021).

3.2.4 Cell counting

Isolated cells were counted using CASY cell counter and analyzer. For this purpose, 10 µl of cell suspension was added to 10 ml CASY ton and measured in CASY. The given amount of living cells was used for further analysis (Dornieden et al., 2021).

3.2.5 Freezing of isolated cells

Dependent on further analysis, some freshly isolated and counted cells were frozen for usage at a later time point. Therefore, cell pellets were resuspended in freezing medium containing FCS and 10 % DMSO and transferred into cryotubes. After storage for 24 h at - 80 °C, cells were transferred to liquid nitrogen tank for long term storage (Dornieden et al., 2021).

3.2.6 Thawing of frozen cells

Frozen cells, stored in cryotubes, were thawed in 37 °C waterbath. Cells were transferred into 10 ml pre-heated RPMI 1640 medium containing 0.3 mg/ml glutamine, 20 % FCS and 1 % P/S and washed at 504 xg for 10 min at RT. Afterwards, cells were resuspended in 5 ml warm medium and washed again for 6 min. Cell pellet was resuspended in required amount of PBS containing 0.25 % BSA and stored at 4 °C for further use (Dornieden et al., 2021).

3.2.7 Cell staining and phenotypic analysis

For phenotyping of PBMCs and isolated MNCs from peri-tumor and tumor kidney tissue, 1 x 10^6 freshly isolated cells were stained with a mixture of various antibodies (see table 4) for 20 min at RT in the dark. Afterwards, cells were washed at 504 xg for 6 min at 4 °C.

For the usage of intracellular antibodies, cells were fixated and permeabilized using a Fix/Perm kit (Thermo Fisher). After washing at 504 xg for 6 min at 4 °C, cells were stained with a mixture of intracellular antibodies (see table 4) for 30 min at RT in the dark. Stained cells were washed at 504 xg for 6 min at 4 °C and measured with a BD Fortessa X-20 flow cytometer (Dornieden et al., 2021).

Table 4: Antibodies used for phenotyping with corresponding manufacturer and location. Source: Dornieden et al. Signatures and Specificity of Tissue-resident Lymphocytes Identified in Human Renal Peritumor and Tumor Tissue. 2021. JASN.

Antibody	Clone	Fluorochrome	Manufacturer
CD3	SK7	PerCP/Cy5.5	Biolegend, San Diego, USA
CD4	SK3	BUV395	BD, Heidelberg, Germany
CD8	SK1	APCeFluor780	ThermoFisher,Darmstadt, Germany
CD14	63D3	BV510	Biolegend, San Diego, USA
CD19	SJ25C1	BV510	Biolegend, San Diego, USA
CD25	BC96	PE/Cy7	Biolegend, San Diego, USA
CD28	CD28.2	BV711	Biolegend, San Diego, USA
CD38	HIT2	BV605	Biolegend, San Diego, USA
CD45RA	HI100	BV650	Biolegend, San Diego, USA
CD45RO	UCHL1	BV650	Biolegend, San Diego, USA
CD49a	TS2/7	PE/Cy7	Biolegend, San Diego, USA
CD56	5.1H11	BV785	Biolegend, San Diego, USA
CD62L	DREG-56	BV605	BD, Heidelberg, Germany
CD69	FN50	Alexa700	Biolegend, San Diego, USA
CD69	FN50	BV711	Biolegend, San Diego, USA
CD69	FN50	FITC	Biolegend, San Diego, USA
CD103	Ber-ACT8	BV785	Biolegend, San Diego, USA
CD103	Ber-ACT8	PE	Biolegend, San Diego, USA
CD161	HP-3G10	PE/Dazzle594	Biolegend, San Diego, USA
CTLA4	BNI3	BV421	Biolegend, San Diego, USA
FoxP3	150D	Alexa647	Biolegend, San Diego, USA
HLA-DR	L243	FITC	Biolegend, San Diego, USA
HLA-DR	L243	PE/Cy7	Biolegend, San Diego, USA
Ki67	B56	Alexa700	BD, Heidelberg, Germany
L/D	-	Aqua (BV510)	Biolegend, San Diego, USA
NKG2D	1D11	BV421	Biolegend, San Diego, USA
PD1	EH12.1	BV711	BD, Heidelberg, Germany
Tox	REA473	APC	Miltenyi, Bergisch Gladbach, Germany
Vα7.2	3C10	APC	Biolegend, San Diego, USA
Vα7.2	3C10	BV711	Biolegend, San Diego, USA

3.2.8 Cell stimulation and functional analysis

For functional analysis, 4 x 10^6 freshly isolated cells were stained with CD69 antibody (see table 5) for 20 min at RT in the dark. CD69 staining was performed before culture to prevent a stimulus-dependent

increase by PMA/Ionomycin. After washing at 504 xg for 6 min at 4 °C, cells were resuspended in 500µl RPMI 1640 medium containing 0.3 mg/ml glutamine, 10 % AB and 1 % P/S and stimulated with 1:100,000 phorbol myristat acetat (PMA) and 1:1000 ionomycin. Unstimulated controls remained without PMA and ionomycin. In all samples Brefeldin A was used in a concentration of 1:500 and served for accumulation of intracellular cytokines. Cells were stimulated for 6 h at 37 °C and 5 % CO_2.

After stimulation, cells were washed at 504 xg for 6 min at 4 °C and stained with a mixture of various surface antibodies (see table 5) for 20 min at RT in the dark. After washing at 504 xg for 6 min at 4°C, cells were fixated and permeabilized using a Fix/Perm kit (BD). After washing at 504 xg for 6 min at 4°C, cells were stained with a mixture of intracellular antibodies (see table 5) for 30 min at RT in the dark. Stained cells were washed at 504 xg for 6 min at 4 °C and measured with a BD Fortessa X-20 flow cytometer (Dornieden et al., 2021).

Table 5: Antibodies used for functional analysis with corresponding manufacturer and location. Source: Dornieden et al. Signatures and Specificity of Tissue-resident Lymphocytes Identified in Human Renal Peritumor and Tumor Tissue. 2021. JASN.

Antibody	Clone	Fluorochrome	Manufacturer
CD3	SK7	PerCP/Cy5.5	Biolegend, San Diego, USA
CD4	SK3	BUV395	BD, Heidelberg, Germany
CD8	SK1	APCeFluor780	Thermo Fisher, Darmstadt, Germany
CD14	63D3	BV510	Biolegend, San Diego, USA
CD19	SJ25C1	BV510	Biolegend, San Diego, USA
CD45RO	UCHL1	BV650	Biolegend, San Diego, USA
CD49a	TS2/7	PE/Cy7	Biolegend, San Diego, USA
CD69	FN50	BV711	Biolegend, San Diego, USA
CD103	Ber-ACT8	PE	Biolegend, San Diego, USA
CD161	HP-3G10	PE/Dazzle594	Biolegend, San Diego, USA
Granzyme B	GB11	FITC	Biolegend, San Diego, USA
IFN-γ	4S.B3	eFluor450	Thermo Fisher, Darmstadt, Germany
IL-2	MQ1-17H12	BV605	Biolegend, San Diego, USA
IL-17	BL168	BV785	Biolegend, San Diego, USA
L/D	-	Aqua (BV510)	Biolegend, San Diego, USA
TNFα	MAb11	Alexa700	Biolegend, San Diego, USA
Vα7.2	3C10	APC	Biolegend, San Diego, USA

3.2.9 Detection and phenotypic analysis of antigen-specific $CD8^+$ T cells

For detection of $CD8^+$ antigen-specific T cells in peripheral blood and human kidney tissue, PE labelled HLA-A*0201 MHC I Dextramers containing epitopes of BK-virus (BKV), Influenza, Epstein-Barr virus (EBV) and cytomegalovirus (CMV) were used (see table 6).

For the assessment of HLA-A2 positivity, 100 µl whole blood was stained with CD3 and HLA-A2 antibodies (see table 7) for 10 min at RT. Cells were lysed with 900 µl lysing solution (BD) for 10 min at RT and afterwards measured with a BD Fortessa X-20 flow cytometer. Samples of $HLA\text{-}A2^+$ patients were used for this experiment. For each antigen and negative control, 1-3 x 10^6 thawed cells were washed with 2 ml PBS containing 5 % FCS at 504 xg for 6 min at 4 °C. Pellet was resuspended in 50 µl PBS containing 5 % FCS and stained with MHC I Dextramer for 10 min at RT in the dark. A mixture of additional antibodies (see table 7) was added and cells were incubated for further 20 min at 4 °C in the

dark. After two washing steps, cells were measured with a BD Fortessa X-20 flow cytometer (Dornieden et al., 2021).

Table 6: Used MHC I Dextramers for detection of antigen-specific CD8⁺ T cells. Source: Dornieden et al. Signatures and Specificity of Tissue-resident Lymphocytes Identified in Human Renal Peritumor and Tumor Tissue. 2021. JASN.

Virus	Allele	Peptide	Antigen	Manufacturer
CMV	HLA-A*0201	NLVPMVATV	pp65	Immudex, Copenhagen, Denmark
Influenza	HLA-A*0201	GILGFVFFL	MP	Immudex, Copenhagen, Denmark
BKV	HLA-A*0201	LLMWEAVTV	VP1	Immudex, Copenhagen, Denmark
EBV	HLA-A*0201	GLCTLVAML	BMLF1	Immudex, Copenhagen, Denmark

Table 7: Antibodies used for detection of antigen-specific CD8⁺ T cells and their phenotypic analysis. Corresponding manufacturers and location are listed. Source: Dornieden et al. Signatures and Specificity of Tissue-resident Lymphocytes Identified in Human Renal Peritumor and Tumor Tissue. 2021. JASN.

Antibody	Clone	Fluorochrome	Manufacturer
CD3	SK7	PerCP/Cy5.5	Biolegend, San Diego, USA
CD4	SK3	BUV395	BD, Heidelberg, Germany
CD8	SK1	APCeFluor780	ThermoFisher,Darmstadt, Germany
CD14	63D3	BV510	Biolegend, San Diego, USA
CD19	SJ25C1	BV510	Biolegend, San Diego, USA
CD45RA	HI100	BV650	Biolegend, San Diego, USA
CD62L	DREG-56	BV605	BD, Heidelberg, Germany
CD69	FN50	Alexa700	Biolegend, San Diego, USA
CD103	Ber-ACT8	BV785	Biolegend, San Diego, USA
CTLA4	BNI3	BV421	Biolegend, San Diego, USA
HLA-A2	BB7.2	APC/Cy7	Biolegend, San Diego, USA
HLA-DR	L243	PE/Cy7	Biolegend, San Diego, USA
L/D	-	Aqua (BV510)	Biolegend, San Diego, USA
PD1	EH12.1	BV711	BD, Heidelberg, Germany

3.2.10 Flow cytometry

The usage of flow-cytometry enables the analysis of single cells. In this study, cells were stained with various surface and intracellular markers, binding to receptors on the surface of or within the cell. These used markers were labelled with different fluorescent molecules, which in turn can be detected by flow cytometer measurement. Single cells pass a ray of light in a high speed and according to their structure, size and staining, the cells show a certain signal and can be analyzed (Cossarizza et al., 2017). All analyses were performed according to the same gating strategy (Fig 1) (Dornieden et al., 2021).

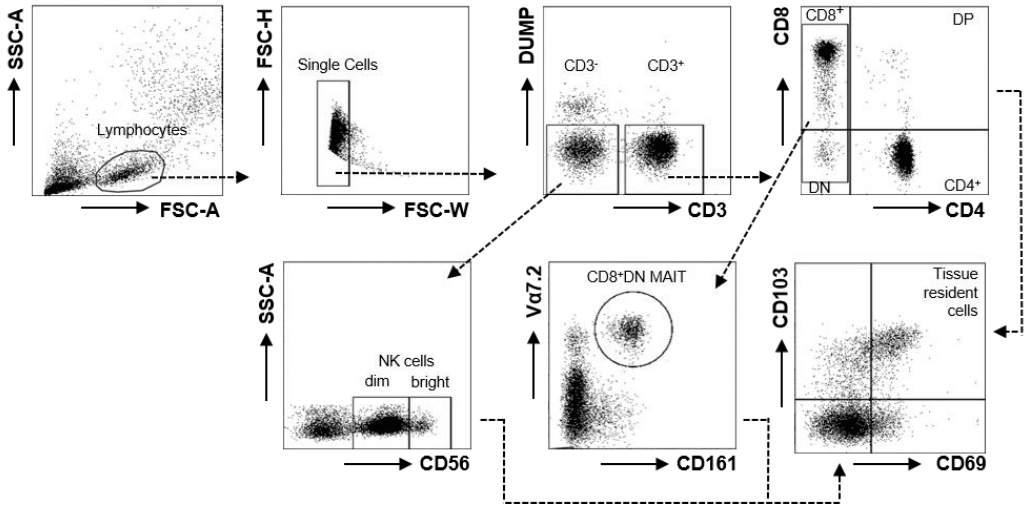

Figure 1. Used gating strategy for flow cytometer analysis. Cell subsets were detected by using flow cytometry. Lymphocytes were gated, followed by single cells and living $CD14^-CD19^-$ ($DUMP^-$) $CD3^+$ or $CD3^-$ cells. Within the $CD3^+$ subset, conventional $CD8^+$ and $CD4^+$ T cells were identified, as well as double-positive (DP,$CD8^+CD4^+$), double-negative (DN,$CD8^-CD4^-$) and MAIT ($CD8^+$DN $V\alpha7.2^+CD161^+$) cells. NK cells were detected within $CD3^-$ population. Tissue-resident cells were identified according to CD69 and CD103 single- or co-expression. Source: Dornieden et al. Signatures and Specificity of Tissue-resident Lymphocytes Identified in Human Renal Peritumor and Tumor Tissue. 2021. JASN.

3.2.11 Multi-epitope ligand cartography (MELC)

MELC sample preparation until freezing and storage of samples at -80 °C was performed by the author, all other steps of MELC histology were performed in close collaboration with Dr. rer. nat. Anna Pascual-Reguant (DRFZ, Berlin).

Sample preparation

For MELC histology, fresh peri-tumor and tumor tissue samples in a size of about 1x1x1.5 cm were frozen using tissue snap-freezing method. Therefore, fresh tissue samples were covered with OCT for a few minutes. After samples were transferred into fresh OCT in a cryomold, tissues were frozen using isopentane in a metal beaker, which was cooled down while placed in a liquid nitrogen dewar container. Samples were placed into cold isopentane till OCT was frozen and were afterwards stored at -80 °C.

The fresh frozen tissue was cut in 5-µm sections on cover slides coated with APES (24 x 60 mm), wherefore a NX80 cryotome was used. Next, fixation of the samples was performed for 10 min at RT with 2 % paraformaldehyde, which was methanol- and RNAse-free. After a washing step, permeabilization with 0.2 % Triton X-100 in PBS for 10 min at RT was performed and followed by blocking with 10 % goat serum and 1 % BSA in PBS for at least 20 min. Afterwards, the samples were placed in a fluid chamber with 100 µl of PBS and “press-to-seal” silicone sheets, which were attached to the cover slip (Dornieden et al., 2021, Pascual-Reguant et al., 2021).

MELC Image Acquisition

For generating multiplexed histology data, a modified Toponome Image Cycler® MM3 (TIC) was used. The components of the used robotic microscopic system were the following: 1. an inverted wide field (epi)fluorescence microscope Leica DM IRE2 with a CMOS camera and a motor-controlled XY stage;

2. CAVRO XL3000 Pipette/Diluter; 3. a MelTec TIC-Control software used for microscope control and pipetting system as well as for synchronized image acquisition. The MELC run consisted of different cycles, each with the following four steps: 1. incubation of the antibody, which was fluorescence-coupled and washing; 2. cross-correlation-based auto-focusing; 3. photo-bleaching of the fluorophore; 4. a second autofocusing step and followed acquisition of a 3D stack post-bleaching fluorescence image. In each four-step cycle, another fluorescence-labeled antibody of interest was used. After the sample was labeled with all antibodies of interest, the experiment was completed. Used antibodies for MELC histology are listed in table 8. The antibodies were stained in the indicated order (Dornieden et al., 2021, Pascual-Reguant et al., 2021).

Table 8: Used antibodies for MELC histology. Source: Dornieden et al. Signatures and Specificity of Tissue-resident Lymphocytes Identified in Human Renal Peritumor and Tumor Tissue. 2021. JASN.

Molecule	Clone	Fluorochrome	Manufacturer
AQP2 (E-2)		PE	Santa Cruz Biotechnology, Dallas, USA
CD3	REA613	PE	Miltenyi, Bergisch Gladbach, Germany
CD4	VIT4	PE	Miltenyi, Bergisch Gladbach, Germany
CD8	BW135/80	PE	Miltenyi, Bergisch Gladbach, Germany
CD11c	MJ4-27G12	PE	Miltenyi, Bergisch Gladbach, Germany
CD14	Tük4	PE	Miltenyi, Bergisch Gladbach, Germany
CD16	REA423	PE	Miltenyi, Bergisch Gladbach, Germany
CD31	9G11	PE	R&D Systems, Minneapolis, USA
CD45RA	REA562	PE	Miltenyi, Bergisch Gladbach, Germany
CD45RO	UCHL1	PE	DRFZ, Berlin, Germany
CD49a	TS2/7	PE	Biolegend, San Diego, USA
CD56	AF12-7H3	PE	Miltenyi, Bergisch Gladbach, Germany
CD69	REA824	PE	Miltenyi, Bergisch Gladbach, Germany
CD103	Ber-ACT8	PE	Miltenyi, Bergisch Gladbach, Germany
CD161	191B8	PE	Miltenyi, Bergisch Gladbach, Germany
CD163	RM3/1	PE	Biolegend, San Diego, USA
DAPI			Miltenyi, Bergisch Gladbach, Germany
HLA-DR	REA332	PE	Miltenyi, Bergisch Gladbach, Germany
Ki67	MIB1	FITC	Miltenyi, Bergisch Gladbach, Germany
TCR Vα7.2	3C10	PE	Biolegend, San Diego, USA

Image pre-processing

At the beginning of the measurement, a phase contrast image was taken used for alignment of all images. After alignment, processing of each fluorescence MELC image by background subtraction and illumination correction, based on the bleaching images, was performed. To capture slice thickness, an “Extended Depth of Field” algorithm was applied to the 3D fluorescence stack in each cycle. Normalization of images was performed in ImageJ, using a rolling ball algorithm for background estimation, as well as removing of edges and stretching of fluorescence intensities to the full intensity

range (16 bit). In this way, 2D fluorescence images were generated and subsequently segmented and analyzed (Dornieden et al., 2021, Pascual-Reguant et al., 2021).

Cell segmentation and single-cell feature extraction

Cell segmentation was divided into two steps, containing a signal-classification step using Ilastik 1.3.2 followed by an object-recognition step using CellProfiler 3.1.8. Ilastik was used for classification of pixels in the three classes nuclei, membrane, and extracellular matrix (ECM), as well as for generation of maps for each class. Combined images were summed up and used to classify membranes and ECM, for classification of nuclei only the DAPI images were used. In a small region of a data-set (approx. 6 % of the image), the random forest algorithm (machine-learning, Ilastik) was trained by manual pixel classification, while the rest of the data-set was classified in an unsupervised manner using the random forest algorithm. Afterwards, CellProfiler was used for segmentation of the nuclei and membrane probability maps and for generating nuclei and cellular binary masks. While these masks were superimposed on the individual fluorescence images acquired for each marker, single-cell information such as mean fluorescent intensity (MFI) of each marker per segmented cell was extracted (Dornieden et al., 2021, Pascual-Reguant et al., 2021).

Unsupervised clustering and data-driven analysis

With the help of Orange, segmented cells analysis was performed, using several algorithms for dimensionality reduction, which use the list of MFI values as single-cell features. By analyzing all segmented cells, unsupervised clustering of the kidney single-cell data was performed. T-SNE plots were created with 18 principal components, a perplexity of 30 and 1000 iterations (Dornieden et al., 2021, Pascual-Reguant et al., 2021).

Data transformation and normalization

For the presented data, raw measurements were used. Normalization of the presented data was performed at various steps. Fluorescence intensities per pixel were normalized to the full 16-bit range in ImageJ and brought to a 0 to 1 scale in CellProfiler. Fluorescence intensities per cell were normalized for individual columns on a 0 to 1 scale in Orange (Dornieden et al., 2021, Pascual-Reguant et al., 2021).

3.2.12 Analysis and statistics

Data derived from flow cytometry measurements were analyzed using FlowJo Version 10. For all statistical analyses, GraphPad Prism 8 was used. Data were tested for normal distribution with Kolmogorov-Smirnov test. Following statistical tests were used for calculating statistical significance: For the comparison of two groups: two-tailed paired t-test or two-tailed Wilcoxon Signed Ranks test for paired samples and two-tailed Mann-Whitney U test or two-tailed unpaired t test for unpaired groups. For comparison of three or four groups: Friedman test or one-way ANOVA for paired groups and Ordinary one-way ANOVA or Kruskal-Wallis test for unpaired groups. P-values below 0.05 were considered as significant. All present bar graphs show means ± SD. Cytobank software was used for further analyses, including viSNE, heatmaps or FlowSOM (data not shown here) (Dornieden et al., 2021).

4. Results

4.1 Enrichment of effector memory T cells with an activated and pro-inflammatory phenotype in human kidney tissue

So far, little is known about the immune cell composition of the human kidney. To gain a deeper insight into this field, bulk $CD3^+$ $CD8^+$ and $CD4^+$ T cells from peri-tumor tissue of nephrectomized kidneys and paired peripheral blood samples were analyzed. Regarding their differentiation subsets, it could be demonstrated that effector memory ($CD45RA^-CD62L^-$) $CD8^+$ and $CD4^+$ T cells were significantly enriched in the renal tissue compared to their counterparts in the peripheral blood. In contrast, the blood was characterized by increased frequencies of $CD8^+$ and $CD4^+$ central memory ($CD45RA^-CD62L^+$) and naïve ($CD45RA^+CD62L^+$) T cells (Fig. 2A). Furthermore, $CD8^+$ and $CD4^+$ renal T cells expressed significantly higher HLA-DR, being indicative for an activated phenotype. In addition, elevated expression of the co-stimulatory molecules PD-1 and CTLA4 was detected on $CD8^+$ and $CD4^+$ T cells within kidney derived cells compared to their counterparts in peripheral blood, as well as an increase of $CD4^+$ renal T cells negative for CD28, displaying a differentiated phenotype (Fig. 2B). Interestingly, functional analysis showed a significant enrichment of IL-17 production for both $CD8^+$ and $CD4^+$ kidney T cells compared to blood-derived cells, indicating a pro-inflammatory status of these renal cells. In addition, a down-regulation of granzyme B producing $CD8^+$ renal T cells could be demonstrated, whereas an increase of IFNγ and TNFα producing $CD4^+$ renal T cells could be indicated (data not shown).

(2A)

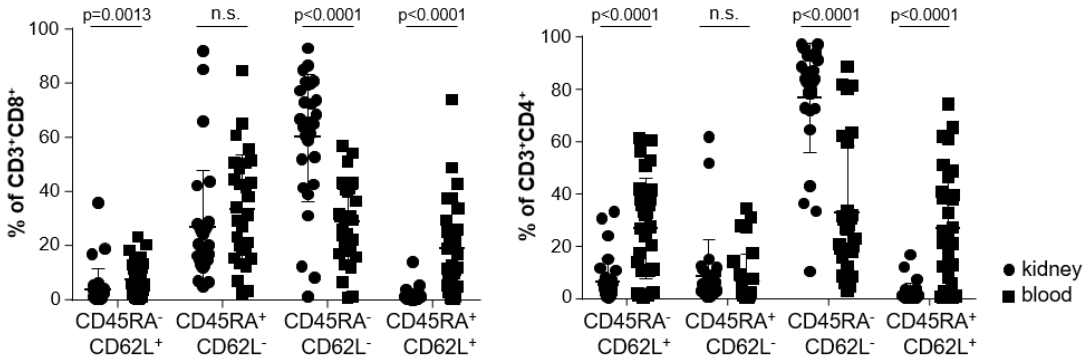

(2B)

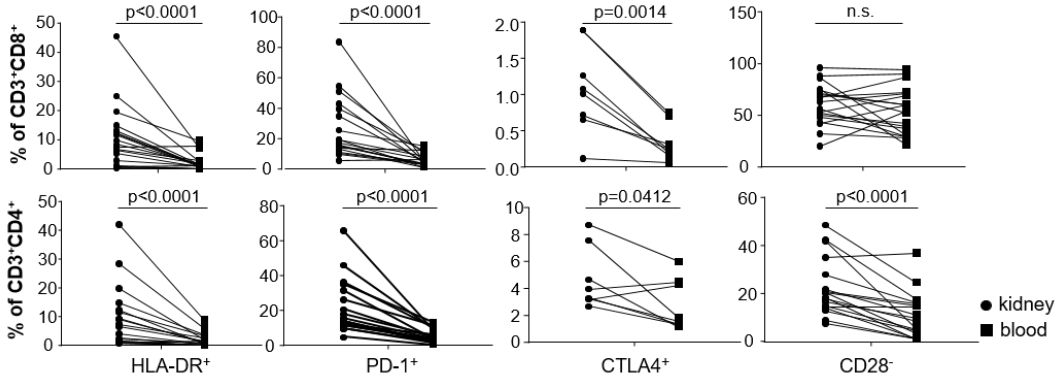

Figure 2. Increase of effector memory T cells within the human kidney displaying an activated and pro-inflammatory phenotype. Freshly isolated mononuclear cells derived from kidney peri-tumor tissue and peripheral blood were stained with surface markers. (A) Frequencies of $CD8^+$ and $CD4^+$ T cells expressing CD45RA and CD62L were quantified by flow cytometry (n=29), presenting the differentiation subsets of $CD8^+$ and $CD4^+$ T cells: central memory cells ($CD45RA^-CD62L^+$), terminally differentiated effector cells ($CD45RA^+CD62L^-$), effector memory cells ($CD45RA^-CD62L^-$) and naïve ($CD45RA^+CD62L^+$) cells. (B) Frequencies of $CD8^+$ and $CD4^+$ T cells expressing HLA-DR (n=19), PD-1 (n=19), CLTA4 (n=8) and CD28 (n=19) were detected by flow cytometry. All statistically significant differences were presented as means ± SD. A value of $p<0.05$ was considered significant. Source: Dornieden et al. Signatures and Specificity of Tissue-resident Lymphocytes Identified in Human Renal Peritumor and Tumor Tissue. 2021. JASN.

4.2 Tissue-resident memory (T_{RM}) T cells reside within the human kidney

So far, T_{RM} cells could be detected in various human tissues (Ganusov and De Boer, 2007, Clark, 2010, Purwar et al., 2011) as well as in renal nephrectomies (de Leur et al., 2019) but their presence in "healthy" kidney tissue was not proven yet. Therefore, the classical markers of tissue-residency CD69, CD103 and CD49a were analyzed in $CD8^+$ and $CD4^+$ T cells derived from kidney tissue compared with their counterparts in peripheral blood. As presumed, $CD8^+$ and $CD4^+$ $CD69^+CD103^+$ and $CD69^+CD103^-$ T cells were significantly enriched in kidney, while these cells were nearly absent in blood, demonstrating their T_{RM} phenotype. Whereas, $CD69^-CD103^+$ single-positive cells were only elevated in the renal $CD8^+$ T cell subset, not for $CD4^+$ T cells (Fig. 3A). Furthermore, a significant upregulation of $CD8^+$ and $CD4^+$ $CD49a^+$ T cells could be detected within the kidney compared to paired blood (Fig. 3B). The presence of $CD8^+$ and $CD4^+$ T_{RM} cells was confirmed by multi-epitope ligand cartography (MELC), a novel automatized multiplex microscopy technology for high-throughput histological studies. Therefore, a sequential co-staining of CD3, CD69, CD103, CD49a and CD45RO with CD8 or CD4 in the same peri-tumor tissue section was performed (Fig. 3C). Altogether, these data give evidence for the presence of T_{RM} $CD8^+$ and $CD4^+$ T cells within "healthy" human kidney tissue for the first time by using various markers and methods. Characterized by distinctly higher frequencies, $CD8^+$ T_{RM} T cells seem to represent the majority of renal T_{RM} subsets.

(3A)

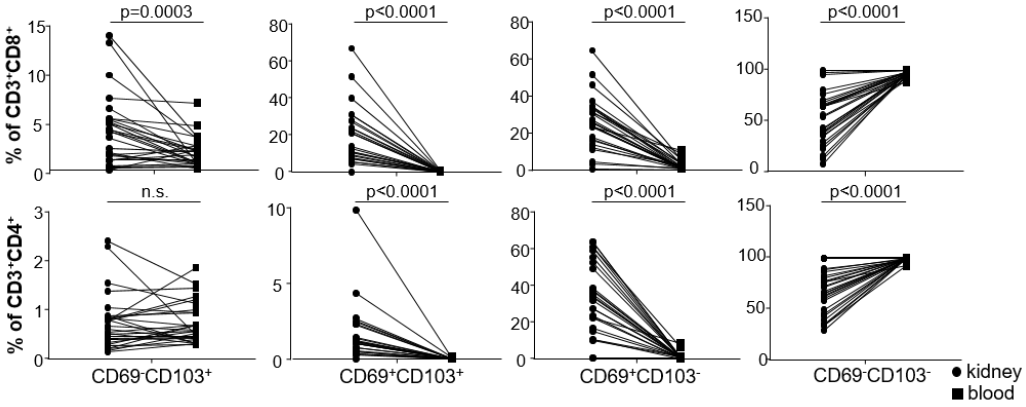

(3B)

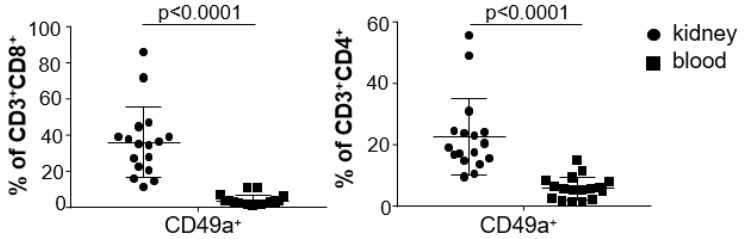

(3C)

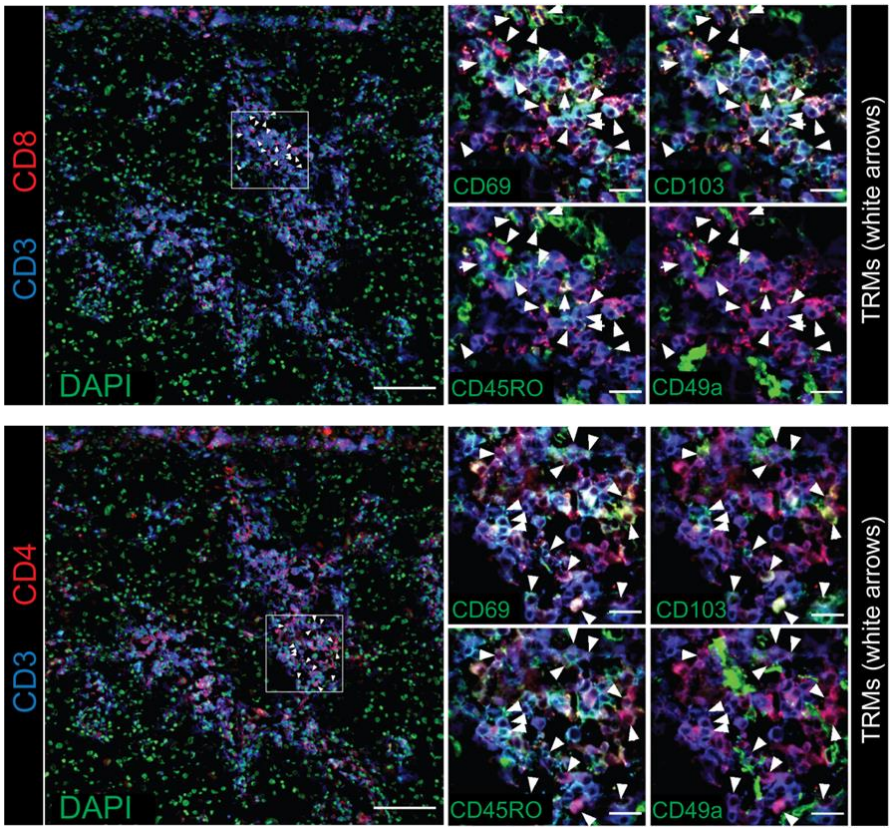

Figure 3: Detection of T_{RM} $CD8^+$ and $CD4^+$ T cells within the human kidney. (A,B) Mononuclear cells isolated from peripheral blood and kidney peri-tumor tissue were stained with surface markers CD69 and CD103 (n=28) (A), as well as CD49a (n=17) (B) and quantified by flow cytometry. Statistically significant differences were presented as means ± SD. A value of $p<0.05$ was considered significant. (C) Fresh frozen peri-tumor kidney tissue was used for MELC histology. Markers for the identification of

T_{RM} cells were stained and an overlay of the fluorescent images was performed. CD3 (blue), CD8 (red, top) or CD4 (red, bottom) and DAPI (green) stainings are shown for the whole field of view (FOV), the scale bar is 100 µm. DAPI (green) is exchanged for CD69, CD103, CD45RO or CD49a in the selected region (scale bar 20µm). White arrows hint at T_{RM} cells. Four independent experiments were performed, one out of these is shown here. Source: Dornieden et al. Signatures and Specificity of Tissue-resident Lymphocytes Identified in Human Renal Peritumor and Tumor Tissue. 2021. JASN.

4.3 CD8⁺ T_{RM} T cells within the human kidney are activated

To further investigate the function of CD8⁺ T_{RM} T cells within the human kidney, a comparative analysis of the two present T_{RM} subsets CD69⁺CD103⁺ and CD69⁺CD103⁻ compared to CD69⁻CD103⁻ cells was performed. Indicating a higher expression of HLA-DR and PD-1 of T_{RM} CD8⁺ T cells compared to their CD69-CD103- counterpart, as well as a reduction of CD28, presenting their antigen-experience and differentiation. Contrarily significantly higher CTLA4 expression could be detected solely for CD69⁺CD103⁻ cells compared to the double-negative subset (Fig. 4A). Regarding their effector cytokine profile, T_{RM} CD8⁺ T cells displayed a significant reduced production of the cytotoxic mediator granzyme B, compared the CD69⁻CD103⁻ counterpart, whereas production of IL-2 and IL-17 was significant enriched for both T_{RM} CD8⁺ T cell subsets. CD69⁺CD103⁺ cells showed a higher production of TNFα compared to the CD69⁺CD103⁻ cell subset, while no difference could be demonstrated for IFNγ (Fig 4B).

(4A)

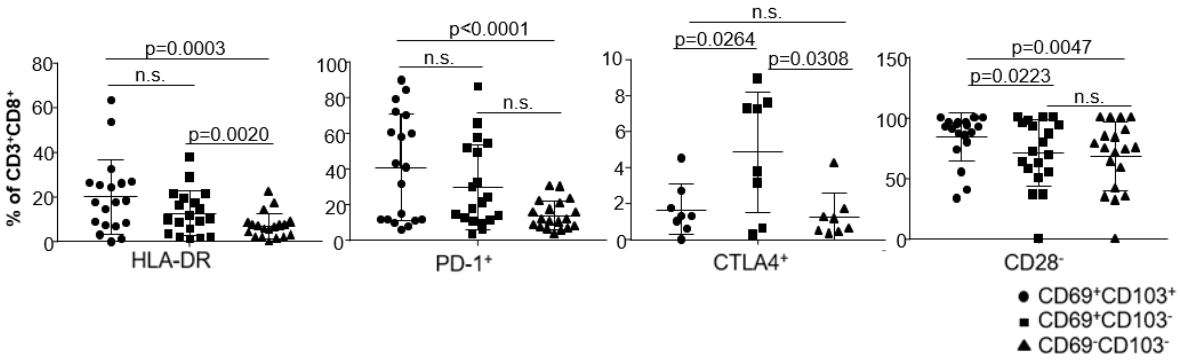

(4B)

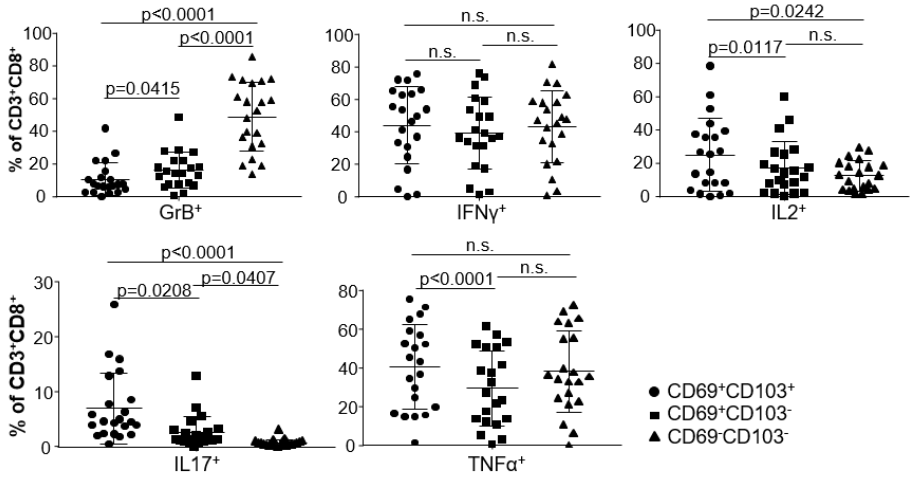

Figure 4: Renal CD8⁺ T_{RM} T cells exhibit an activated phenotype. (A) Mononuclear cells isolated from peri-tumor kidney tissue were stained with surface markers HLA-DR (n=19), PD-1 (n=19), CTLA4 (n=8) and CD28 (n=19) and CD8⁺ T_{RM} T cell subsets were analyzed regarding this marker expression by FACS. (B) Mononuclear cells derived from peri-tumor tissue were stimulated

with PMA and ionomycin and afterwards the effector cytokine profile of $CD8^+$ T_{RM} T cell subsets was quantified by FACS (n=21). Statistically significant differences were presented as mean values ± SD. A value of $p<0.05$ was considered significant. Source: Dornieden et al. Signatures and Specificity of Tissue-resident Lymphocytes Identified in Human Renal Peritumor and Tumor Tissue. 2021. JASN.

4.4 Renal $CD8^+$ T_{RM} T cells accumulate with increasing age

As it is already known that the pool of memory T cells increases with age, we assumed that also T_{RM} T cells in the kidney accumulate with rising age. Therefore, a cohort of n=35 patients was divided into two age groups regarding to the calculated mean age of 63 years: Group I (n=13) being ≤63 years and Group II (n=22) being > 63 years. As presumed, $CD8^+$ $CD69^+CD103^+$ and $CD69^+CD103^-$ T_{RM} T cells were significantly enriched in the advanced age group (group II) compared to the lower age group (group I) (Fig 5A). Furthermore, it could be demonstrated that the increase of both T_{RM} cell subsets significantly correlated with age (Fig 5B).

(5A)

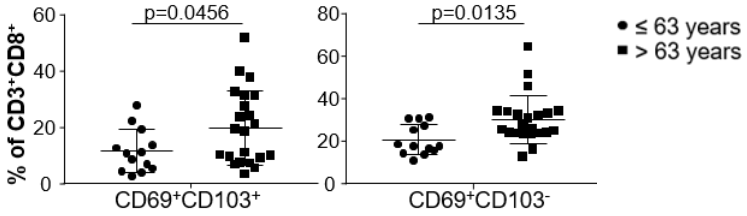

(5B)

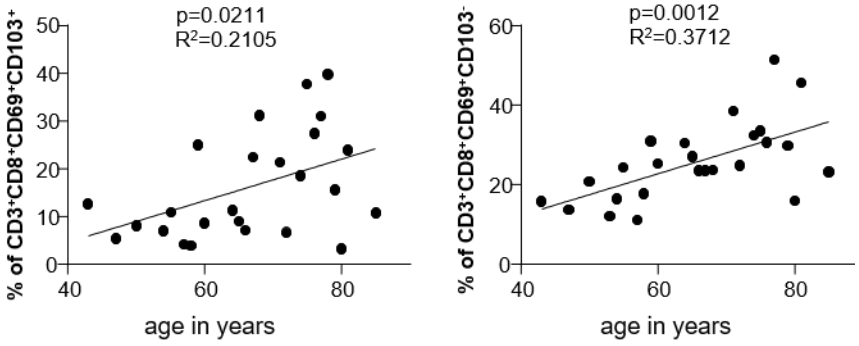

Figure 5: $CD8^+$ T_{RM} T cells within the human kidney accumulate with increasing age. (A) Mononuclear cells isolated from peri-tumor kidney tissue were stained with tissue-resident markers CD69 and CD103. Two age groups were defined according to the calculated mean age of 63 years: Group I being ≤ 63 years (n=13) and Group II being > 63 years (n=22) and frequencies of $CD8^+$ T_{RM} T cell subsets were compared between the groups. Statistically significant differences were presented as mean values ± SD. A value of $p<0.05$ was considered significant. (B) Correlation analysis of both $CD69^+CD103^+$ and $CD69^+CD103^-$ $CD8^+$ T_{RM} T cell frequencies with patient age (n=35). From patients with same age, mean values of T_{RM} cell frequencies were calculated. Source: Dornieden et al. Signatures and Specificity of Tissue-resident Lymphocytes Identified in Human Renal Peritumor and Tumor Tissue. 2021. JASN.

4.5 Increase of T_{RM} T cell frequency with elevated kidney function

Patients were grouped concerning their stage of estimated glomerular filtration rate (eGFR) into five stages and corresponding frequencies of $CD8^+$ and $CD4^+$ $CD69^+CD103^+$ T_{RM} T cells were displayed. Interestingly, both $CD8^+$ and $CD4^+$ T_{RM} cell frequencies were significantly increased in patients with an elevated kidney function (here eGFR stage 2) compared to patients with a restricted kidney function (here eGFR stages 3 and 5). Moreover, the frequencies of $CD8^+$ and $CD4^+$ $CD69^+CD103^+$ T_{RM} cells significantly correlated with eGFR. However, a result which was only significant for $CD4^+$ T cells (Fig 6).

(6)

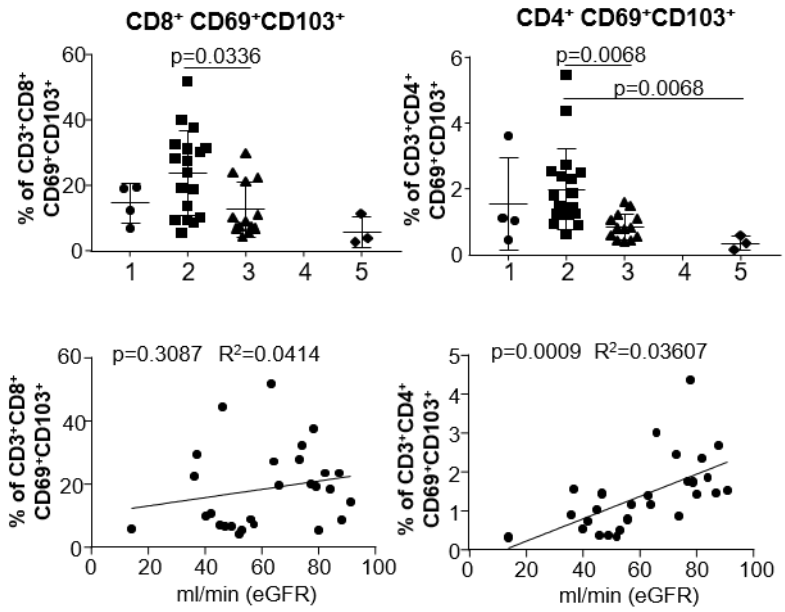

Figure 6: Increase of T_{RM} T cell frequency with elevated kidney function. Mononuclear cells isolated from peri-tumor kidney tissue were stained with tissue-resident markers CD69 and CD103. Patients were divided according to the five stages of kidney function (eGFR CKD-EPI, stage 1 n=4, stage 2 n=18, stage 3 n=13, stage 4 n=0, stage 5 n=3) and frequencies of $CD69^+CD103^+$ $CD8^+$ and $CD4^+$ T_{RM} T cells were compared between the five groups. Statistically significant differences were presented as mean values ± SD. A value of $p<0.05$ was considered significant. Moreover, correlation analyses of the same cell population frequencies with eGFR (ml/min) (n=42) were displayed. Source: Dornieden et al. Signatures and Specificity of Tissue-resident Lymphocytes Identified in Human Renal Peritumor and Tumor Tissue. 2021. JASN.

4.6 Identification of further renal T_{RM} lymphocyte subsets

Interestingly, tissue-residency could be identified in human renal lymphocyte subsets apart from conventional $CD8^+$ and $CD4^+$ T cells for the first time. The classical NK cell subsets, $CD56^{bright}$ and $CD56^{dim}$, expressing tissue-resident markers CD69 and CD103 were detected within kidney tissue, while these T_{RM} cells were absent in peripheral blood. The same holds true for mucosal-associated invariant T (MAIT) cells within kidney tissue, an observation which confirms the published data from Law et al (2019) regarding the existence of renal-resident MAIT cells (Fig. 7). With the help of MELC histology, the presence of T_{RM} NK and MAIT cells within kidney peri-tumor tissue could be approved (data not shown here).

(7)

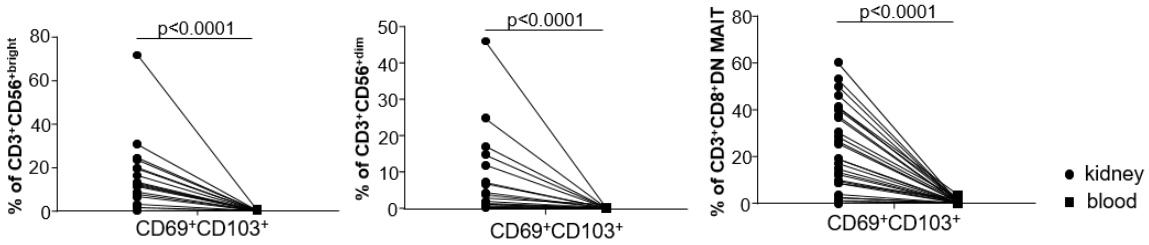

Figure 7: Identification of renal T_{RM} NK and MAIT cells. Mononuclear cells isolated from peripheral blood and peri-tumor kidney tissue were stained with tissue-resident markers CD69 and CD103. Frequencies of T_{RM} $CD56^{bright}$ and $CD56^{dim}$ NK cells (n=19) and MAIT cells ($CD3^+CD8^+$DN $TCRV\alpha7.2^+CD161^+$) (n=29) were measured in FACS. Statistically significant differences were presented as mean values ± SD. A value of $p<0.05$ was considered significant. Source: Dornieden et al. Signatures and Specificity of Tissue-resident Lymphocytes Identified in Human Renal Peritumor and Tumor Tissue. 2021. JASN.

4.7 $CD8^+$ T_{RM} lymphocytes in renal cell carcinoma (RCC) are exhausted

So far, the general function of T_{RM} cells in the kidney as well their impact in cancer, especially in RCC is unknown. Previous studies could demonstrate an enrichment of T_{RM} cells within tumor tissues (Djenidi et al., 2015, Wang et al., 2015, Webb et al., 2014). Therefore, T_{RM} lymphocyte frequencies and properties within renal cell carcinoma tissue were compared with adjacent peri-tumor tissue.

By means of MELC histology a significant enrichment of whole $CD69^+CD103^+$ T_{RM} lymphocytes and $CD69^+CD103^-$ $CD8^+$ T_{RM} T cells as well as a non-significant increase of $CD69^+CD103^-$ $CD4^+$ T_{RM} T cells within tumor tissue compared to peri-tumor tissue could be demonstrated (data not shown). Interestingly, it could be demonstrated that groups of 10 or more $CD69^+CD103^-$ $CD4^+$ and $CD8^+$ T_{RM} T cells clustered along endothelial cells (vessels) within the tumor tissue, however not in peri-tumor tissue (data not shown). A further feature of tumor-derived $CD8^+$ T_{RM} T cells was their exhausted phenotype and function, demonstrated by a significant upregulation of PD-1 and TOX co-expression (Fig. 8A), a feature not documented for RCC cells so far, as well as by downregulation of IL-2, TNFα and IL-17 production, even so the latter one was not significant. However, an upregulation of granzyme B production was detected (Fig. 8B).

(8A)

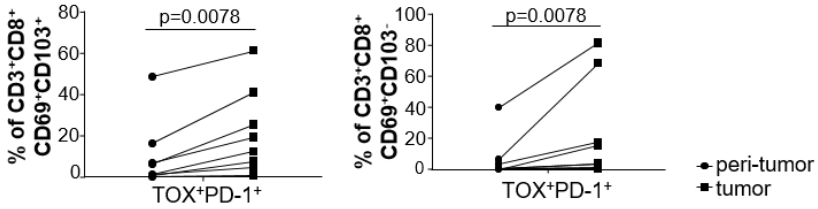

(8B)

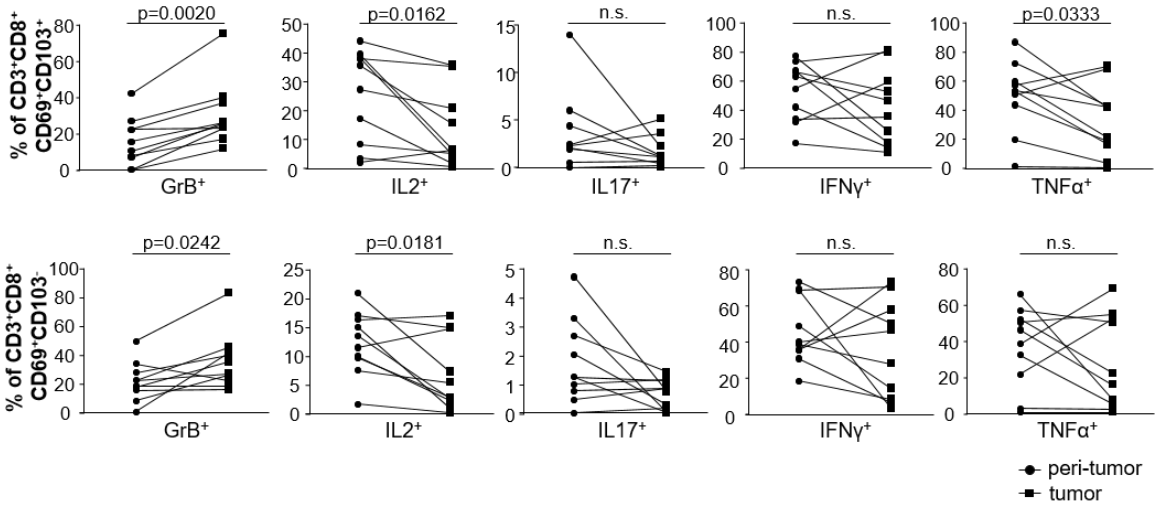

Figure 8: CD8⁺ T_{RM} T cells in RCC are exhausted. (A) Mononuclear cells isolated from peripheral peri-tumor and tumor kidney tissue were stained with exhaustion markers PD-1 and TOX. Frequencies of CD8⁺ T_{RM} T cell subsets co-expressing both markers were measured in FACS (n=8). (B) Mononuclear cells derived from peri-tumor and tumor tissue were stimulated with PMA and ionomycin and the effector cytokine profile of CD8⁺ T_{RM} T cell subsets was quantified by FACS (n=10). Statistically significant differences were presented as mean values ± SD. A value of $p<0.05$ was considered significant. Source: Dornieden et al. Signatures and Specificity of Tissue-resident Lymphocytes Identified in Human Renal Peritumor and Tumor Tissue. 2021. JASN.

4.8 Tumor-derived CD8⁺ T_{RM} T cells are functionally impaired in metastasized patients

Patients were divided into two groups regarding their metastasis's status before nephrectomy. Interestingly, tumor-derived CD8⁺ CD69⁺CD103⁺ and CD69⁺CD103⁻ T_{RM} T cells in metastasized patients displayed an impaired function compared to patients without metastases, represented by a significant downregulation of IL-2, TNFα and IFNγ production, even so the latter one was only significantly decreased for CD8⁺ CD69⁺CD103⁺ T_{RM} T cells (Fig. 9).

(9)

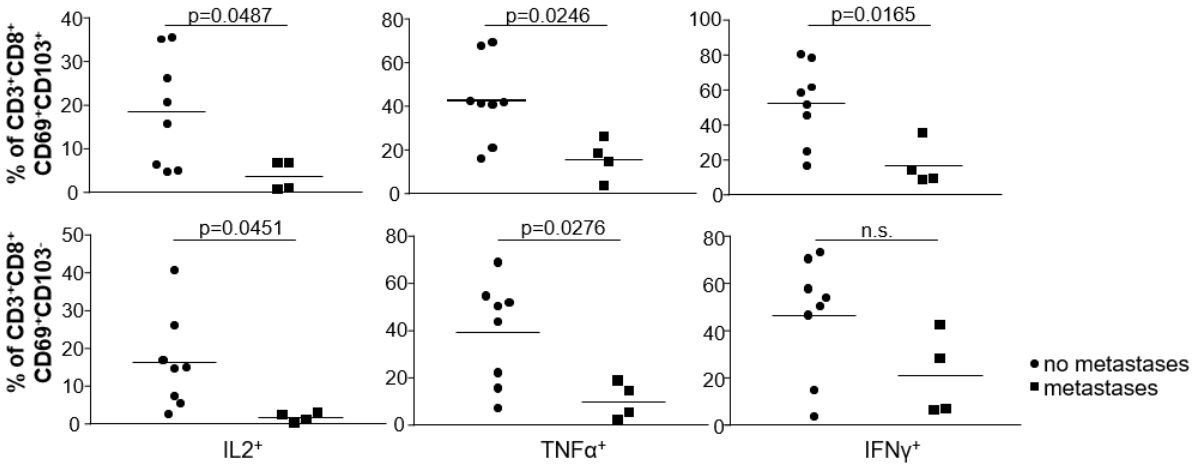

Figure 9: Tumor-derived CD8⁺ T_{RM} T cells are functionally impaired in patients with metastases. Patients were divided into two groups according to their diagnosis of metastases before nephrectomy: one group without metastases (n=8) and one group with metastases (n=4). Mononuclear cells derived from tumor tissue were stimulated with PMA and ionomycin and the effector cytokine profile of CD8⁺ CD69⁺CD103⁺ and CD69⁺CD103⁻ T cells was quantified by FACS. Statistically significant differences were

presented as mean values ± SD. A value of p<0.05 was considered significant. Source: Dornieden et al. Signatures and Specificity of Tissue-resident Lymphocytes Identified in Human Renal Peritumor and Tumor Tissue. 2021. JASN.

4.9 Antigen-specific T cells reside within the human kidney, but do not exhibit a T_{RM} phenotype

To further investigate the function of T_{RM} T cells within the human kidney, their antigen-specificity was examined. Therefore, isolated cells out of peripheral blood, peri-tumor and tumor tissue were stained with MHCII multimers for cytomegalovirus (CMV), Epstein-Barr virus (EBV), BK virus (BKV) and influenza A, the latter representing a non-persisting virus, compared to the other persisting viruses. Interestingly, $CD8^+$ T cells specific for all four tested antigens could be identified in renal peri-tumor and tumor tissue, whereby frequencies between 0.6 % (BKV) and 2.5 % (CMV, EBV) of total $CD8^+$ T cells were measured (data not shown here). The mainly amount of these cells showed a $CD45RA^-CD62L^-$ effector memory phenotype (Fig. 10A) and were negative for the tissue-resident markers CD69 and CD103. Frequencies of antigen-specific $CD8^+$ $CD69^-CD103^-$ T cells were significantly elevated compared to $CD8^+$ $CD69^+CD103^+$ T cells for EBV and CMV (Fig. 10B).

(10A)

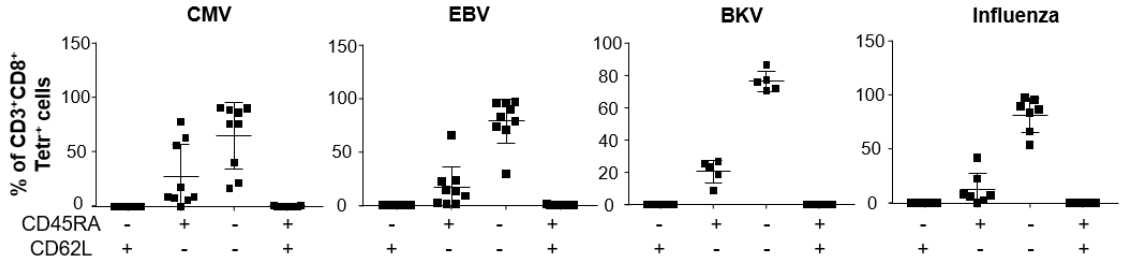

(10B)

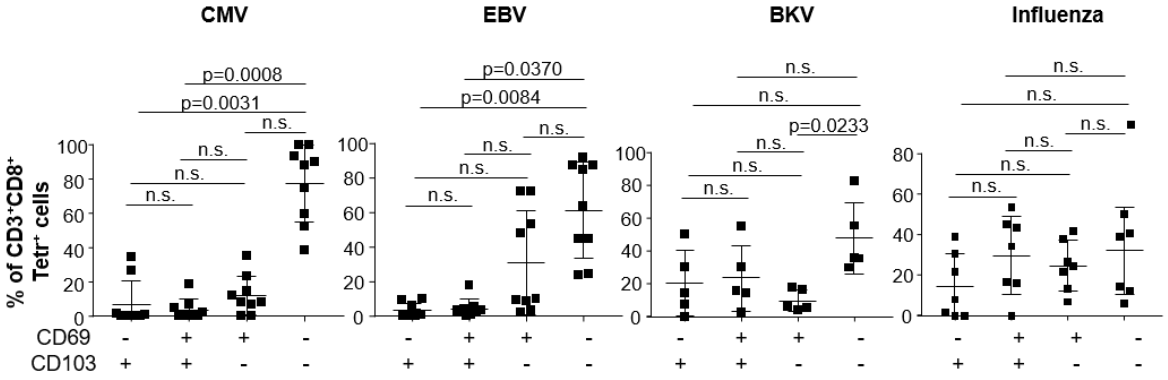

Figure 10: Presence of antigen-specific $CD8^+$ T cells within the human kidney. (A) $CD8^+$ antigen-specific T cells derived from peri-tumor tissue were stained for differentiation subsets: central memory cells ($CD45RA^-CD62L^+$), terminally differentiated effector cells ($CD45RA^+CD62L^-$), effector memory cells ($CD45RA^-CD62L^-$) and naïve ($CD45RA^+CD62L^+$) cells (CMV n=9, EBV n=9, BKV n=5, Influenza n=7) and measured in FACS. (B) Peri-tumor $CD8^+$ antigen-specific T cells were investigated for tissue-resident marker expression (CMV n=9, EBV n=9, BKV n=5, Influenza n=7) by FACS. Statistically significant differences were presented as mean values ± SD. A value of p<0.05 was considered significant. Source: Dornieden et al. Signatures and Specificity of Tissue-resident Lymphocytes Identified in Human Renal Peritumor and Tumor Tissue. 2021. JASN.

5. Discussion

So far, little is known about the immune cell composition of the human kidney in comparison with other human organs. A recent study from Park et al (2020) demonstrated the immune cell composition in normal human kidneys, however the patient cohort with n=15 patients was quite limited (Park et al., 2020). Therefore, an increased number of 62 patients were analyzed in this study. To address the first objective of the study, an analysis of renal-derived bulk $CD8^+$ and $CD4^+$ T cells was performed. Interestingly, an enrichment of effector memory T cells and an activated and pro-inflammatory phenotype of the kidney-derived T cells was demonstrated, providing an insight into kidney cell composition. However, the enrichment of effector memory cells could be explained by the increased age of the included patients, as with increasing age also the frequency of effector memory cells accumulates in the kidney (Weninger et al., 2001, Baron et al., 2003).

Another main objective of the study was the investigation of human renal tissue-resident cells in order to acquire more insight into their characteristics and their potential role in kidney transplantation and tumor pathology. So far, the existence of T_{RM} T cells in human kidney allografts and in a limited number of “healthy” kidneys was demonstrated by de Leur et al in 2019 (de Leur et al., 2019). However, a verification of their presence in a larger cohort of “healthy” human kidneys was still lacking, as well as a detailed analysis of their phenotype and function. Although the kidney is not a barrier tissue, it is known that it can be infected with pathogens by passing the urinary tract. Therefore, on the one hand kidney tissue needs to be protected by T_{RM} cells to prevent these renal infections. On the other hand, formation of T_{RM} cells within kidney tissue could be enabled due to these infections, since recruited cells can enter the infected tissue, develop T_{RM} features and reside.

In this study, renal T_{RM} lymphocytes were identified through the expression of the tissue-resident markers CD69, CD103 and CD49a. Especially for $CD4^+$ and $CD8^+$ T cells, the two main T_{RM} subsets expressing $CD69^+CD103^+$ and $CD69^+CD103^-$ were detected. Frequencies of $CD8^+$ T_{RM} T cells were distinctly higher compared to their $CD4^+$ counterparts, suggesting that these cells represent the major T_{RM} cell subset within the human kidney. The existence of two main T_{RM} T cell subsets is comparable with previous studies out of the kidney and brain (de Leur et al., 2019, Smolders et al., 2018). Smolders et al. investigated T_{RM} T cells in the human brain, a tissue which is highly encapsulated by the blood-cerebral-barrier. They examined various markers on bulk and T_{RM} $CD8^+$ and $CD4^+$ T cells. Particular results were quite close to what we detected for renal bulk and T_{RM} T cells, including increased PD-1 and CTLA-4 expression of T_{RM} cells (Smolders et al., 2018). In addition to flow cytometry analysis, the existence of T_{RM} $CD4^+$ and $CD8^+$ T cells was verified using MELC histology, a new complex histology method creating overlays of various measured markers allowing verification and localization. Therefore, this study gives proof of renal T_{RM} T cell existence applying two independent methods.

$CD8^+$ T_{RM} T cell subsets were characterized by an activated phenotype, reflected by increased HLA-DR expression, as well as by an upregulation of the co-stimulatory molecule PD-1. In addition, they displayed an activated and pro-inflammatory effector profile, producing significantly more IL-17, and a decreased cytotoxicity, indicated by a decrease of granzyme B production. Especially the latter feature

could already be observed for CD69$^+$ T cells in the human liver (Stelma et al., 2017). With regard to kidney transplantation, these features would be worth to consider for transplantation outcome and graft survival. Despite kidney perfusion peri-operatively, donor-derived renal-resident activated and pro-inflammatory T_{RM} T cells are transplanted along with the graft and could contribute to inflammatory processes through stimulation of recipient´s alloreactive T cells resulting in graft rejection (Thaunat and Morelon, 2007).

Interestingly, an enrichment of CD8$^+$ T_{RM} T cell subsets was correlated with increasing age. CD8$^+$ T_{RM} T cells display an effector memory phenotype (data not shown here), a cell subset which is already known to accumulate with increasing age and associated increased antigen experience (Weninger et al., 2001, Baron et al., 2003). Therefore, an accumulation of T_{RM} T cells with increased age seems predictable, however it was not demonstrated for the human kidney before. Furthermore, several studies indicated that CD8$^+$ T_{RM} T cells in the lung lose their protecting features with increasing age (Goplen et al 2021, Goplen et al 2020), a fact which could not be investigated in this study, however, which would be interesting to consider in further studies.

Moreover, an increase of CD4$^+$ and CD8$^+$ T_{RM} T cell frequencies in kidneys with elevated kidney function (eGFR) could be observed, indicating that T_{RM} T cells could be involved in processes of kidney protection or function. Obviously, further analyses would be necessary to confirm this hypothesis and to identify their exact functions and pathway involvements. However, considering these findings, it would be possible to target T_{RM} T cells in order to increase kidney function in patients with impaired renal function in the future.

Beside kidney-derived T_{RM} T cells, NK and MAIT cells displaying a tissue-resident phenotype could be detected by flow cytometry and MELC histology, indicating that expression of CD69 and CD103 is not unique for T_{RM} T cells. Renal MAIT cells displaying a T_{RM} phenotype were already investigated in the context of renal fibrosis and chronic kidney disease (Law et al., 2019). However, our results could verify the existence of intra-renal MAIT cells in “healthy” human kidneys for a larger number of patients. The presence of NK cells displaying a T_{RM} phenotype was already investigated for the murine kidney, as well as for the human liver and gut (Peng and Tian, 2017), here we could demonstrate the existence of intra-renal NK cells in the human kidney for the first time. However, both subsets did not accumulate with increasing age (data not shown here). These results demonstrate that not exclusively cells from the adaptive but also cells from the innate immune system exhibit the feature of tissue-residency in the kidney, suggesting that rapid response after pathogen infiltration is ensured directly within the tissue, preventing infections and tissue damage immediately.

CD8$^+$ T_{RM} T cells were already detected in various cancers and serve as prognostic markers (Djenidi et al., 2015, Wang et al., 2015, Quinn et al., 2003), while their presence in kidney tumors was not examined yet. Using flow cytometry and MELC histology, an enrichment of bulk CD69$^+$CD103$^+$ lymphocytes, as well as CD4$^+$ and CD8$^+$ CD69$^+$CD103$^-$ T cells in kidney tumor tissue could be detected. The investigated accumulation of T_{RM} cells within RCC tissue leads to the assumption that T_{RM} cell formation could be a result of recruiting processes, in which immune cells are recruited to the site of inflammation, such as cancer, and develop tissue-resident features afterwards in order to keep local control (Turner et al.,

2014b). Furthermore, tumor-derived $CD8^+$ T_{RM} T cells were characterized by an exhausted phenotype, upregulating the exhaustion markers PD-1 and TOX, as well as downregulating IL-2 and TNFα production. However, cytotoxicity was increased, measured by upregulated release of granzyme B. Exhaustion of tumor-derived lymphocytes is already known from various studies (McLane et al., 2019) and the recently identified transcription factor TOX was already investigated in hepatocellular carcinoma (Wang et al., 2019), however its upregulation in T_{RM} kidney cancer cells could be demonstrated for the very first time in this study. In summary, renal tumor-derived T_{RM} cells are both: accumulated within the tumor and impaired in function, nevertheless displaying elevated cytotoxicity; features which do not differ from other cancer entities (McLane et al., 2019). By use of MELC histology, it could be demonstrated that especially $CD4^+$ and $CD8^+$ T_{RM} T cells were clustered along the vessels, suggesting their recruitment via the vessels and their fast development of tissue-resident features and residency directly after entrance. These investigated exhaustion features would be worth to consider for the treatment of RCC patients since T_{RM} cells could serve as a potential therapeutical target. Boosting their activity could improve their anti-tumor response and initiate defense mechanisms directly within the tumor tissue in order to enhance patient's outcome.

Interestingly, a functional impairment of tumor-derived $CD8^+$ T_{RM} T cells in patients suffering from metastases compared to metastases-free patients could be demonstrated, pointing out their potential relevance for RCC patient's outcome. Hence, renal $CD8^+$ T_{RM} T cells seem to be protective and control tumor-spreading by producing cytokines involved in anti-tumor responses (IFNγ) and cell growth (IL-2, TNFα). Recombinant IL-2 is already used for treatment of metastatic RCC and leads to activation of defense mechanisms (Klapper et al., 2008), pointing out that functional activation of tumor-derived T_{RM} T cells could be a promising therapeutic option for treating RCC patients, especially in metastasized patients. However, further investigation would be necessary.

Finally, to figure out the specific role of T_{RM} cells within the kidney, antigen-specificity was proven. Interestingly, $CD8^+$ T cells specific for BKV, CMV, EBV and influenza were detected in both kidney peri-tumor and tumor tissue. In contrast to a study of tissue-resident antigen-specific cells in the human lung (Pizzolla et al., 2018), identified renal antigen-specific $CD8^+$ T cells did not display a tissue-resident phenotype, but were $CD69^-CD103^-$. Therefore, it was not possible to associate the role of renal T_{RM} cells with antigen-specificity and specialized pathogen control within the tissue, instead their function seems to be more general, including controlling various types of inflammation.

While most T_{RM} cell data are derived from infectious mouse models and human data are limited, this study presents a comprehensive analysis of renal-derived T_{RM} cells out of the human kidney. However, also this study has certain limitations: The included and investigated kidneys cannot be considered as "healthy". All kidneys were removed due to different diseases, most commonly renal cell carcinoma. However, as it is absolutely impossible to investigate completely healthy kidneys, exclusively tissue portions which were examined by a pathologist and were pronounced as "healthy" were used in this study. It needs to be considered that this could result in differences between the immune cell composition within kidney tissue and peripheral blood, particularly in respect of their activation and effector molecule status. Additionally, the majority of included patients had an increased age since nephrectomy is performed mostly in older patients. Moreover, correlation analysis of cell frequencies

with various patient parameters was limited, including correlation of T_{RM} cell frequencies with patient's outcome. The timeframe of this study was 3.5 years. During this time solely 6 out of 62 patients (9.7 %) were diagnosed with a relapse and a total number of 9 patients (14.5 %) suffered from metastases before nephrectomy. Furthermore, the standard therapy for kidney cancer is surgery performing nephrectomy, therefore correlation analysis of T_{RM} cell frequencies and various applied therapies could not be conducted. Moreover, due to extremely limited access to peri-tumor and especially tumor tissue, various experiments could not be performed, including measuring the cytokine profile of renal $CD4^+$ T_{RM} cells and $CD8^+$ antigen-specific cells as well as potential cell culture experiments using sorted renal derived peri-tumor or tumor T_{RM} cells.

In summary, this study presented the existence of various T_{RM} lymphocyte subsets within the human kidney for the very first time for a large patient cohort and by the use of two different highly complex methods. Phenotypic and functional signatures were analyzed comprehensively in both peri-tumor and tumor kidney tissue, demonstrating the existence of activated and pro-inflammatory T_{RM} T cell subsets that increase with age, but may become exhausted within kidney cancer. Considering these features in processes of graft rejection or kidney cancer could improve the understanding of these mechanisms. Nevertheless, further experiments are needed to figure out their exact impact, as well as their possible prospective therapeutic potential for transplantation or cancer, by either modifying, triggering or inhibiting them.

6. Further work / Co-Authorships

Mucosal associated invariant T cells are differentially impaired in tolerant and immunosuppressed liver transplant recipients

Arne Sattler, Lion G. Thiel, Annkathrin Helena Ruhm, Yasmin Bergmann, **Theresa Dornieden**, Mira Choi, Fabian Halleck, Frank Friedersdorff, Dennis Eurich and Katja Kotsch

Am J Transplant. 2021; 21: 87-102

Summary

Mucosal associated invariant T (MAIT) cells are a subset of T cells which are responsible for protection and repair of border tissues. They are characterized by the expression of a semi-invariant TCR Vα7.2 and the C-type lectin CD161. MAIT cells can be found among others in blood, mucosal surfaces and the liver and can be activated via two pathways. The TCR-dependent activation is restricted to the MHC-I protein MR1 which presents vitamin B metabolites, whereas the TCR-independent activation proceeds via inflammatory cytokines such as IL-12, IL-15, Il-18 and TL1A.

So far, it is not known if immunosuppressive drugs and SOT have an impact on the MAIT cell biology. Therefore, this study included two main investigations. First, an in vitro TCR-dependent and –independent activation of peripheral MAIT cells in the presence of different immunosuppressive medications in healthy individuals. Second, an ex vivo analysis of MAIT cells isolated out of the peripheral blood from liver transplanted patients who were either immunosuppressed or tolerant.

This work could demonstrate an impairment of the in vitro cytokine activation of MAIT cells caused by glucocorticoids, as well as of the antigen-specific activation triggered by calcineurin inhibitors in healthy donors. Moreover, a depletion of MAIT cells in the peripheral blood of liver transplanted patients was determined, an observation which was true for all types of measured immunosuppressive drugs and concentrations, as well as for investigated kidney transplanted patients. In addition, MAIT cells from these liver transplanted patients featured a functional impairment.

In summary, this study could demonstrate an interference of liver disease and immunosuppressive treatment after liver transplantation on the MAIT cell biology, affecting their phenotypical and functional features.

7. Own Contributions

Detailed listing of my contributions to the work "*Signatures and Specificity of Tissue-Resident Lymphocytes Identified in Human Renal Peritumor and Tumor Tissue*":

- Research design
- Sample collection
    - Patient information and sample preparation during surgery was done by Prof. Dr. Frank Friedersdorff (Clinic for Urology, Charité, Berlin).
- Experimental performance
    - Lymphocyte isolation
    - Staining
    - Stimulations
    - Flow cytometry measurement
    - MELC histology: Collection and preparation of samples (snap freezing) were done by the author. All other procedures of MELC histology were done in a close collaboration with Dr. rer. nat. Anna Pascual-Reguant (DRFZ, Berlin).
- Data analysis
    - Evaluation
    - Creation of tables, figures, statistics
    - Elicitation of patient data and correlation analyses
    - MELC histology: Analyses of MELC histology data was done in a close collaboration with Dr. rer. nat. Anna Pascual-Reguant (DRFZ, Berlin).
- Paper writing and publication

Detailed listing of my contributions to the work "*Mucosal associated invariant T cells are differentially impaired in tolerant and immunosuppressed liver transplant recipients*":

- Experimental performance
    - Lymphocyte isolation
    - Staining
    - Stimulations

Literature

https://www.eurotransplant.org/statistics/statistics-library/ > https://statistics.eurotransplant.org/
Stand: 19.01.2021, 9:13 Uhr.

BARON, V., BOUNEAUD, C., CUMANO, A., LIM, A., ARSTILA, T. P., KOURILSKY, P., FERRADINI, L. & PANNETIER, C. 2003. The repertoires of circulating human CD8(+) central and effector memory T cell subsets are largely distinct. *Immunity,* 18**,** 193-204.

BUTCHER, E. C. & PICKER, L. J. 1996. Lymphocyte homing and homeostasis. *Science,* 272**,** 60-6.

CHANG, J. T., CIOCCA, M. L., KINJYO, I., PALANIVEL, V. R., MCCLURKIN, C. E., DEJONG, C. S., MOONEY, E. C., KIM, J. S., STEINEL, N. C., OLIARO, J., YIN, C. C., FLOREA, B. I., OVERKLEEFT, H. S., BERG, L. J., RUSSELL, S. M., KORETZKY, G. A., JORDAN, M. S. & REINER, S. L. 2011. Asymmetric proteasome segregation as a mechanism for unequal partitioning of the transcription factor T-bet during T lymphocyte division. *Immunity,* 34**,** 492-504.

CHANG, J. T., WHERRY, E. J. & GOLDRATH, A. W. 2014. Molecular regulation of effector and memory T cell differentiation. *Nat Immunol,* 15**,** 1104-15.

CHEUK, S., SCHLUMS, H., GALLAIS SEREZAL, I., MARTINI, E., CHIANG, S. C., MARQUARDT, N., GIBBS, A., DETLOFSSON, E., INTROINI, A., FORKEL, M., HOOG, C., TJERNLUND, A., MICHAELSSON, J., FOLKERSEN, L., MJOSBERG, J., BLOMQVIST, L., EHRSTROM, M., STAHLE, M., BRYCESON, Y. T. & EIDSMO, L. 2017. CD49a Expression Defines Tissue-Resident CD8(+) T Cells Poised for Cytotoxic Function in Human Skin. *Immunity,* 46**,** 287-300.

CHOUEIRI, T. K. & MOTZER, R. J. 2017. Systemic Therapy for Metastatic Renal-Cell Carcinoma. *N Engl J Med,* 376**,** 354-366.

CHUA, W. J., TRUSCOTT, S. M., EICKHOFF, C. S., BLAZEVIC, A., HOFT, D. F. & HANSEN, T. H. 2012. Polyclonal mucosa-associated invariant T cells have unique innate functions in bacterial infection. *Infect Immun,* 80**,** 3256-67.

CLARK, R. A. 2010. Skin-resident T cells: the ups and downs of on site immunity. *J Invest Dermatol,* 130**,** 362-70.

CORBETT, A. J., ECKLE, S. B., BIRKINSHAW, R. W., LIU, L., PATEL, O., MAHONY, J., CHEN, Z., REANTRAGOON, R., MEEHAN, B., CAO, H., WILLIAMSON, N. A., STRUGNELL, R. A., VAN SINDEREN, D., MAK, J. Y., FAIRLIE, D. P., KJER-NIELSEN, L., ROSSJOHN, J. & MCCLUSKEY, J. 2014. T-cell activation by transitory neo-antigens derived from distinct microbial pathways. *Nature,* 509**,** 361-5.

COSSARIZZA, A., CHANG, H. D., RADBRUCH, A., AKDIS, M., ANDRA, I., ANNUNZIATO, F., BACHER, P., BARNABA, V., BATTISTINI, L., BAUER, W. M., BAUMGART, S., BECHER, B., BEISKER, W., BEREK, C., BLANCO, A., BORSELLINO, G., BOULAIS, P. E., BRINKMAN, R. R., BUSCHER, M., BUSCH, D. H., BUSHNELL, T. P., CAO, X., CAVANI, A., CHATTOPADHYAY, P. K., CHENG, Q., CHOW, S., CLERICI, M., COOKE, A., COSMA, A., COSMI, L., CUMANO, A., DANG, V. D., DAVIES, D., DE BIASI, S., DEL ZOTTO, G., DELLA BELLA, S., DELLABONA, P., DENIZ, G., DESSING, M., DIEFENBACH, A., DI SANTO, J., DIELI, F., DOLF, A., DONNENBERG, V. S., DORNER, T., EHRHARDT, G. R. A., ENDL, E., ENGEL, P., ENGELHARDT, B., ESSER, C., EVERTS, B., DREHER, A., FALK, C. S., FEHNIGER, T. A., FILBY, A., FILLATREAU, S., FOLLO, M., FORSTER, I., FOSTER, J., FOULDS, G. A., FRENETTE, P. S., GALBRAITH, D., GARBI, N., GARCIA-GODOY, M. D., GEGINAT, J., GHORESCHI, K., GIBELLINI, L., GOETTLINGER, C., GOODYEAR, C. S., GORI, A., GROGAN, J., GROSS, M., GRUTZKAU, A., GRUMMITT, D., HAHN, J., HAMMER, Q., HAUSER, A. E., HAVILAND, D. L., HEDLEY, D., HERRERA, G., HERRMANN, M., HIEPE, F., HOLLAND, T., HOMBRINK, P., HOUSTON, J. P., HOYER, B. F., HUANG, B., HUNTER, C. A., IANNONE, A., JACK, H. M., JAVEGA, B., JONJIC, S., JUELKE, K., JUNG, S., KAISER, T., KALINA, T., KELLER, B., KHAN, S., KIENHOFER, D., KRONEIS, T., et al. 2017. Guidelines for the use of flow cytometry and cell sorting in immunological studies. *Eur J Immunol,* 47**,** 1584-1797.

CURTSINGER, J. M., LINS, D. C. & MESCHER, M. F. 1998. CD8+ memory T cells (CD44high, Ly-6C+) are more sensitive than naive cells to (CD44low, Ly-6C-) to TCR/CD8 signaling in response to antigen. *J Immunol,* 160**,** 3236-43.

DE BREE, G. J., VAN LEEUWEN, E. M., OUT, T. A., JANSEN, H. M., JONKERS, R. E. & VAN LIER, R. A. 2005. Selective accumulation of differentiated CD8+ T cells specific for respiratory viruses in the human lung. *J Exp Med,* 202**,** 1433-42.

DE LEUR, K., DIETERICH, M., HESSELINK, D. A., CORNETH, O. B. J., DOR, F., DE GRAAV, G. N., PEETERS, A. M. A., MULDER, A., KIMENAI, H., CLAAS, F. H. J., CLAHSEN-VAN GRONINGEN, M. C., VAN DER LAAN, L. J. W., HENDRIKS, R. W. & BAAN, C. C. 2019. Characterization of donor and recipient CD8+ tissue-resident memory T cells in transplant nephrectomies. *Sci Rep,* 9**,** 5984.

DEMETRIS, A. J., MURASE, N., RAO, A. S., FUNG, J. J., STARZL, T. E. 1995. The dichotomous functions of passenger leukocytes in solid-organ transplantation. *Adv. Nephrol Necker Hosp.,* 24, 341-54.

DJENIDI, F., ADAM, J., GOUBAR, A., DURGEAU, A., MEURICE, G., DE MONTPREVILLE, V., VALIDIRE, P., BESSE, B. & MAMI-CHOUAIB, F. 2015. CD8+CD103+ tumor-infiltrating lymphocytes are tumor-specific tissue-resident memory T cells and a prognostic factor for survival in lung cancer patients. *J Immunol,* 194**,** 3475-86.

DORNIEDEN, T., SATTLER, A., PASCUAL-REGUANT, A., RUHM, A. H., THIEL, L. G., BERGMANN, Y. S., THOLE, L. M. L., KÖHLER, R., KÜHL, A. A., HAUSER, A. E., BORAL, S., FRIEDERSDORFF, F., KOTSCH, K. 2021. Signatures and specificity of tissue-resident lymphocytes identified in human renal peritumor and tumor tissue. *JASN*, 32: 2223-2241.

DUSSEAUX, M., MARTIN, E., SERRIARI, N., PEGUILLET, I., PREMEL, V., LOUIS, D., MILDER, M., LE BOURHIS, L., SOUDAIS, C., TREINER, E. & LANTZ, O. 2011. Human MAIT cells are xenobiotic-resistant, tissue-targeted, CD161hi IL-17-secreting T cells. *Blood,* 117**,** 1250-9.

ELKINS, W. L. & GUTTMANN, R. D. 1968. Pathogenesis of a local graft versus host reaction: immunogenecity of circulating host leukocytes. *Science,* 159, 1250-1.

ESPINOSA, J. R., SAMY, K. P. & KIRK, A. D. 2016. Memory T cells in organ transplantation: progress and challenges. *Nat Rev Nephrol,* 12**,** 339-47.

FAN, X. & RUDENSKY, A. Y. 2016. Hallmarks of Tissue-Resident Lymphocytes. *Cell,* 164**,** 1198-1211.

FENG, Y., WANG, D., YUAN, R., PARKER, C. M., FARBER, D. L. & HADLEY, G. A. 2002. CD103 expression is required for destruction of pancreatic islet allografts by CD8(+) T cells. *J Exp Med,* 196**,** 877-86.

GANUSOV, V. V. & DE BOER, R. J. 2007. Do most lymphocytes in humans really reside in the gut? *Trends Immunol,* 2**8,** 514-8.

GEBHARDT, T., PALENDIRA, U., TSCHARKE, D. C. & BEDOUI, S. 2018. Tissue-resident memory T cells in tissue homeostasis, persistent infection, and cancer surveillance. *Immunol Rev,* 283**,** 54-76.

GEBHARDT, T., WHITNEY, P. G., ZAID, A., MACKAY, L. K., BROOKS, A. G., HEATH, W. R., CARBONE, F. R. & MUELLER, S. N. 2011. Different patterns of peripheral migration by memory CD4+ and CD8+ T cells. *Nature,* 477**,** 216-9.

GEORGEL, P., RADOSAVLJEVIC, M., MACQUIN, C. & BAHRAM, S. 2011. The non-conventional MHC class I MR1 molecule controls infection by Klebsiella pneumoniae in mice. *Mol Immunol,* 48**,** 769-75.

GOPLEN, N. P., WU, Y., SON, Y. M., LI, C., WANG, Z., CHEON, I. S., JIANG, L., ZHU, B., AYASOUFI, K., CHINI, E. N., JOHNSON, A. J., VASSALLO, R., LIMPER, A. H., ZHANG, N. & SUN, J. 2020. Tissue-resident CD8+ T cells drive age-associated chronic lung sequelae after viral pneumonia. *Science Immunology*, 5 (53)

GOPLEN, N. P., CHEON, I. S. & SUN, J. 2021. Age-related dynamics of lung-resident memory CD8+ T cells in the age of COVD-19. *Front. Immunol*., 12:636118.

GUERDER, S., CARDING, S. R. & FLAVELL, R. A. 1995. B7 costimulation is necessary for the activation of the lytic function in cytotoxic T lymphocyte precursors. *J Immunol,* 155**,** 5167-74.

HADLEY, G. A., ROSTAPSHOVA, E. A., GOMOLKA, D. M., TAYLOR, B. M., BARTLETT, S. T., DRACHENBERG, C. I. & WEIR, M. R. 1999. Regulation of the epithelial cell-specific integrin, CD103, by human CD8+ cytolytic T lymphocytes. *Transplantation,* 67**,** 1418-25.

HEEGER, P. S., GREENSPAN, N. S., KUHLENSCHMIDT, S., DEJELO, C., HRICIK, D. E., SCHULAK, J. A. & TARY-LEHMANN, M. 1999. Pretransplant frequency of donor-specific, IFN-gamma-producing lymphocytes is a manifestation of immunologic memory and correlates with the risk of posttransplant rejection episodes. *J Immunol,* 163**,** 2267-75.

HONDOWICZ, B. D., AN, D., SCHENKEL, J. M., KIM, K. S., STEACH, H. R., KRISHNAMURTY, A. T., KEITANY, G. J., GARZA, E. N., FRASER, K. A., MOON, J. J., ALTEMEIER, W. A., MASOPUST, D. & PEPPER, M. 2016. Interleukin-2-Dependent Allergen-Specific Tissue-Resident Memory Cells Drive Asthma. *Immunity,* 44**,** 155-166.

KAWAI, T., COSIMI, A. B., SPITZER, T. R., TOLKOFF-RUBIN, N., SUTHANTHIRAN, M., SAIDMAN, S. L., SHAFFER, J., PREFFER, F. I., DING, R., SHARMA, V., FISHMAN, J. A., DEY, B., KO, D. S., HERTL, M., GOES, N. B., WONG, W., WILLIAMS, W. W., JR., COLVIN, R. B., SYKES,

M. & SACHS, D. H. 2008. HLA-mismatched renal transplantation without maintenance immunosuppression. *N Engl J Med,* 358**,** 353-61.
KIRK, A. D., KNECHTLE, S. J., LARSEN, C. P., NEWELL, K. A. & PEARSON, T. C. 2011. Miles to go. *Am J Transplant,* 11**,** 1119-20.
KJER-NIELSEN, L., PATEL, O., CORBETT, A. J., LE NOURS, J., MEEHAN, B., LIU, L., BHATI, M., CHEN, Z., KOSTENKO, L., REANTRAGOON, R., WILLIAMSON, N. A., PURCELL, A. W., DUDEK, N. L., MCCONVILLE, M. J., O'HAIR, R. A., KHAIRALLAH, G. N., GODFREY, D. I., FAIRLIE, D. P., ROSSJOHN, J. & MCCLUSKEY, J. 2012. MR1 presents microbial vitamin B metabolites to MAIT cells. *Nature,* 491**,** 717-23.
KLAPPER, J. A., DOWNEY, S. G., SMITH, F. O., YANG, J. C., HUGHES, M. S., KAMMULA, U. S., SHERRY, R. M., ROYAL, R. E., STEINBERG, S. M. & ROSENBERG, S. 2008. High-dose interleukin-2 for the treatment of metastatic renal cell carcinoma : a retrospective analysis of response and survival in patients treated in the surgery branch at the National Cancer Institute between 1986 and 2006. *Cancer,* 113**,** 293-301.
KLATTE, T., PANTUCK, A. J., KLEID, M. D. & BELLDEGRUN, A. S. 2007. Understanding the natural biology of kidney cancer: implications for targeted cancer therapy. *Rev Urol,* 9**,** 47-56.
KLEINSCHEK, M. A., BONIFACE, K., SADEKOVA, S., GREIN, J., MURPHY, E. E., TURNER, S. P., RASKIN, L., DESAI, B., FAUBION, W. A., DE WAAL MALEFYT, R., PIERCE, R. H., MCCLANAHAN, T. & KASTELEIN, R. A. 2009. Circulating and gut-resident human Th17 cells express CD161 and promote intestinal inflammation. *J Exp Med,* 206**,** 525-34.
KRUMMEY, S. M. & FORD, M. L. 2012. Heterogeneity within T Cell Memory: Implications for Transplant Tolerance. *Front Immunol,* 3**,** 36.
LAMB, K. E., LODHI, S. & MEIER-KRIESCHE, H. U. 2011. Long-term renal allograft survival in the United States: a critical reappraisal. *Am J Transplant,* 11**,** 450-62.
LANDSVERK, O. J., SNIR, O., CASADO, R. B., RICHTER, L., MOLD, J. E., REU, P., HORNELAND, R., PAULSEN, V., YAQUB, S., AANDAHL, E. M., OYEN, O. M., THORARENSEN, H. S., SALEHPOUR, M., POSSNERT, G., FRISEN, J., SOLLID, L. M., BAEKKEVOLD, E. S. & JAHNSEN, F. L. 2017. Antibody-secreting plasma cells persist for decades in human intestine. *J Exp Med,* 214**,** 309-317.
LAW, B. M. P., WILKINSON, R., WANG, X., KILDEY, K., GIULIANI, K., BEAGLEY, K. W., UNGERER, J., HEALY, H. & KASSIANOS, A. J. 2019. Human Tissue-Resident Mucosal-Associated Invariant T (MAIT) Cells in Renal Fibrosis and CKD. *J Am Soc Nephrol,* 30**,** 1322-1335.
LE BOURHIS, L., MARTIN, E., PEGUILLET, I., GUIHOT, A., FROUX, N., CORE, M., LEVY, E., DUSSEAUX, M., MEYSSONNIER, V., PREMEL, V., NGO, C., RITEAU, B., DUBAN, L., ROBERT, D., HUANG, S., ROTTMAN, M., SOUDAIS, C. & LANTZ, O. 2010. Antimicrobial activity of mucosal-associated invariant T cells. *Nat Immunol,* 11**,** 701-8.
LODHI, S. A., LAMB, K. E. & MEIER-KRIESCHE, H. U. 2011. Solid organ allograft survival improvement in the United States: the long-term does not mirror the dramatic short-term success. *Am J Transplant,* 11**,** 1226-35.
MACKAY, C. R., MARSTON, W. L. & DUDLER, L. 1990. Naive and memory T cells show distinct pathways of lymphocyte recirculation. *J Exp Med,* 171**,** 801-17.
MASOPUST, D. & PICKER, L. J. 2012. Hidden memories: frontline memory T cells and early pathogen interception. *J Immunol,* 188**,** 5811-7.
MASOPUST, D. & SOERENS, A. G. 2019. Tissue-Resident T Cells and Other Resident Leukocytes. *Annu Rev Immunol,* 37**,** 521-546.
MCDONALD, B. D., JABRI, B. & BENDELAC, A. 2018. Diverse developmental pathways of intestinal intraepithelial lymphocytes. *Nat Rev Immunol,* 18**,** 514-525.
MCLANE, L. M., ABDEL-HAKEEM, M. S. & WHERRY, E. J. 2019. CD8 T Cell Exhaustion During Chronic Viral Infection and Cancer. *Annu Rev Immunol,* 37**,** 457-495.
MEDZHITOV, R. 2008. Origin and physiological roles of inflammation. *Nature,* 454**,** 428-35.
MEIEROVICS, A., YANKELEVICH, W. J. & COWLEY, S. C. 2013. MAIT cells are critical for optimal mucosal immune responses during in vivo pulmonary bacterial infection. *Proc Natl Acad Sci U S A,* 110**,** E3119-28.
MOU, D., ESPINOSA, J., LO, D. J. & KIRK, A. D. 2014. CD28 negative T cells: is their loss our gain? *Am J Transplant,* 14**,** 2460-6.
MUELLER, S. N., GEBHARDT, T., CARBONE, F. R. & HEATH, W. R. 2013. Memory T cell subsets, migration patterns, and tissue residence. *Annu Rev Immunol,* 31**,** 137-61.
ONODERA, T., TAKAHASHI, Y., YOKOI, Y., ATO, M., KODAMA, Y., HACHIMURA, S., KUROSAKI, T. & KOBAYASHI, K. 2012. Memory B cells in the lung participate in protective humoral immune responses to pulmonary influenza virus reinfection. *Proc Natl Acad Sci U S A,* 109**,** 2485-90.

PARK, J. G., NA, M., KIM, M. G., PARK, S. H., LEE, H. J., KIM, D. K., KWAK, C., KIM, Y. S., CHANG, S., MOON, K. C., LEE, D. S. & HAN, S. S. 2020. Immune cell composition in normal human kidneys. *Sci Rep,* 10**,** 15678.

PASCUAL-REGUANT, A., KÖHLER, R., MOTHES, R., BAUHERR, S., HERNANDEZ, D. C., UECKER, R., HOLZWARTH, K., KOTSCH, K., SEIDL, M., PHILIPSEN, L., MÜLLER, W., ROMAGNANI, C., NIESNER, R., HAUSER, A. E. 2021. Multiplexed histology analyses for the phenotypic and spatial characterization of human innate lymphoid cells. *Nat Commun,* 12, 1737.

PATARD, J. J., RODRIGUEZ, A., RIOUX-LECLERCQ, N., GUILLE, F. & LOBEL, B. 2002. Prognostic significance of the mode of detection in renal tumours. *BJU Int,* 90**,** 358-63.

PENG, H. & TIAN, Z. 2017. Diversity of tissue-resident NK cells. *Semin Immunol,* 31**,** 3-10.

PIZZOLLA, A., NGUYEN, T. H., SANT, S., JAFFAR, J., LOUDOVARIS, T., MANNERING, S. I., THOMAS, P. G., WESTALL, G. P., KEDZIERSKA, K. & WAKIM, L. M. 2018. Influenza-specific lung-resident memory T cells are proliferative and polyfunctional and maintain diverse TCR profiles. *J Clin Invest,* 128**,** 721-733.

PURWAR, R., CAMPBELL, J., MURPHY, G., RICHARDS, W. G., CLARK, R. A. & KUPPER, T. S. 2011. Resident memory T cells (T(RM)) are abundant in human lung: diversity, function, and antigen specificity. *PLoS One,* 6**,** e16245.

QUINN, E., HAWKINS, N., YIP, Y. L., SUTER, C. & WARD, R. 2003. CD103+ intraepithelial lymphocytes--a unique population in microsatellite unstable sporadic colorectal cancer. *Eur J Cancer,* 39**,** 469-75.

SALLUSTO, F., LANGENKAMP, A., GEGINAT, J. & LANZAVECCHIA, A. 2000. Functional subsets of memory T cells identified by CCR7 expression. *Curr Top Microbiol Immunol,* 251**,** 167-71.

SAN SEGUNDO, D., BALLESTEROS, M. A., NARANJO, S., ZURBANO, F., MINAMBRES, E. & LOPEZ-HOYOS, M. 2013. Increased numbers of circulating CD8 effector memory T cells before transplantation enhance the risk of acute rejection in lung transplant recipients. *PLoS One,* 8**,** e80601.

SASAKI, K., BEAN, A., SHAH, S., SCHUTTEN, E., HUSEBY, P. G., PETERS, B., SHEN, Z. T., VANGURI, V., LIGGITT, D. & HUSEBY, E. S. 2014. Relapsing-remitting central nervous system autoimmunity mediated by GFAP-specific CD8 T cells. *J Immunol,* 192**,** 3029-42.

SATTLER, A., THIEL, L. G., RUHM, A. H., BERGMANN, Y., DORNIEDEN, T., CHOI, M., HALLECK, F., FRIEDERSDORFF, F., EURICH, D., KOTSCH, K., 2021. Mucosal associated invariant T cells are differentially impaired in tolerant and immunosuppressed liver transplant recipients. *Am J Transplant,* 21: 87-102.

SCHENKEL, J. M. & MASOPUST, D. 2014. Tissue-resident memory T cells. *Immunity,* 41**,** 886-97.

SELVAGGI, G., NISHIDA, S., LEVI, D., MOON, J., ISLAND, E., TEKIN, A., WEPPLER, D. & TZAKIS, A. 2009. Intestinal and multivisceral transplantation at the University of Miami. *Clin Transpl***,** 211-7.

SHINODA, K., TOKOYODA, K., HANAZAWA, A., HAYASHIZAKI, K., ZEHENTMEIER, S., HOSOKAWA, H., IWAMURA, C., KOSEKI, H., TUMES, D. J., RADBRUCH, A. & NAKAYAMA, T. 2012. Type II membrane protein CD69 regulates the formation of resting T-helper memory. *Proc Natl Acad Sci U S A,* 109**,** 7409-14.

SIEGEL, R. L., MILLER, K. D. & JEMAL, A. 2016. Cancer statistics, 2016. *CA Cancer J Clin,* 66**,** 7-30.

SIEGEL, R. L., MILLER, K. D. & JEMAL, A. 2017. Cancer Statistics, 2017. *CA Cancer J Clin,* 67**,** 7-30.

SMOLDERS, J., HEUTINCK, K. M., FRANSEN, N. L., REMMERSWAAL, E. B. M., HOMBRINK, P., TEN BERGE, I. J. M., VAN LIER, R. A. W., HUITINGA, I. & HAMANN, J. 2018. Tissue-resident memory T cells populate the human brain. *Nat Commun,* 9**,** 4593.

SMYTH, L. J., KIRBY, J. A. & CUNNINGHAM, A. C. 2007. Role of the mucosal integrin alpha(E)(CD103)beta(7) in tissue-restricted cytotoxicity. *Clin Exp Immunol,* 149**,** 162-70.

SNELL, G. D. 1957. The homograft reaction. *Annual Review of Microbiology,* 11, 439-58.

SRINIVAS, T. R. & MEIER-KRIESCHE, H. U. 2008. Minimizing immunosuppression, an alternative approach to reducing side effects: objectives and interim result. *Clin J Am Soc Nephrol,* 3 Suppl 2**,** S101-16.

STELMA, F., DE NIET, A., SINNIGE, M. J., VAN DORT, K. A., VAN GISBERGEN, K. P. J. M., VERHEIJ, J., VAN LEEUWEN, E. M. M., KOOTSTRA, N. A. and REESINK, H. W. 2017. Human intrahepatic CD69+CD8+ T cells have a tissue resident memory T cell phenotype with reduced cytolytic capacity. *Sci Rep*, 7:6172.

STRAUCH, U. G., MUELLER, R. C., LI, X. Y., CERNADAS, M., HIGGINS, J. M., BINION, D. G. & PARKER, C. M. 2001. Integrin alpha E(CD103)beta 7 mediates adhesion to intestinal microvascular endothelial cell lines via an E-cadherin-independent interaction. *J Immunol,* 166**,** 3506-14.

TAYLOR, D. O., EDWARDS, L. B., BOUCEK, M. M., TRULOCK, E. P., WALTZ, D. A., KECK, B. M., HERTZ, M. I., INTERNATIONAL SOCIETY FOR, H. & LUNG, T. 2006. Registry of the International Society for Heart and Lung Transplantation: twenty-third official adult heart transplantation report--2006. *J Heart Lung Transplant,* 25**,** 869-79.

TEIJARO, J. R., TURNER, D., PHAM, Q., WHERRY, E. J., LEFRANCOIS, L. & FARBER, D. L. 2011. Cutting edge: Tissue-retentive lung memory CD4 T cells mediate optimal protection to respiratory virus infection. *J Immunol,* 187**,** 5510-4.

TERPSTRA, M. L., REMMERSWAAL, E. B. M., VAN DER BOM-BAYLON, N. D., SINNIGE, M. J., KERS, J., VAN AALDEREN, M. C., GEERLINGS, S. E. & BEMELMAN, F. J. 2020. Tissue-resident Mucosal-associated invariant T (MAIT) cells in the human kidney represent a functionally distinct subset. *Eur J Immunol*.

THAUNAT, O. & MORELON, E. 2007. Modulation of immunogenicity. *Hand transplantation. Springer*, 210-1.

TREINER, E., DUBAN, L., BAHRAM, S., RADOSAVLJEVIC, M., WANNER, V., TILLOY, F., AFFATICATI, P., GILFILLAN, S. & LANTZ, O. 2003. Selection of evolutionarily conserved mucosal-associated invariant T cells by MR1. *Nature,* 422**,** 164-9.

TSUI, K. H., SHVARTS, O., SMITH, R. B., FIGLIN, R., DE KERNION, J. B. & BELLDEGRUN, A. 2000. Renal cell carcinoma: prognostic significance of incidentally detected tumors. *J Urol,* 163**,** 426-30.

TURKA, L. A., LEDBETTER, J. A., LEE, K., JUNE, C. H. & THOMPSON, C. B. 1990. CD28 is an inducible T cell surface antigen that transduces a proliferative signal in CD3+ mature thymocytes. *J Immunol,* 144**,** 1646-53.

TURNER, D. L., BICKHAM, K. L., THOME, J. J., KIM, C. Y., D'OVIDIO, F., WHERRY, E. J. & FARBER, D. L. 2014a. Lung niches for the generation and maintenance of tissue-resident memory T cells. *Mucosal Immunol,* 7**,** 501-10.

TURNER, D. L., GORDON, C. L. & FARBER, D. L. 2014b. Tissue-resident T cells, in situ immunity and transplantation. *Immunol Rev,* 258**,** 150-66.

VAN DEN HOVE, L. E., VAN GOOL, S. W., VAN POPPEL, H., BAERT, L., COOREVITS, L., VAN DAMME, B. & CEUPPENS, J. L. 1997. Phenotype, cytokine production and cytolytic capacity of fresh (uncultured) tumour-infiltrating T lymphocytes in human renal cell carcinoma. *Clin Exp Immunol,* 109**,** 501-9.

WANG, B., WU, S., ZENG, H., LIU, Z., DONG, W., HE, W., CHEN, X., DONG, X., ZHENG, L., LIN, T. & HUANG, J. 2015. CD103+ Tumor Infiltrating Lymphocytes Predict a Favorable Prognosis in Urothelial Cell Carcinoma of the Bladder. *J Urol,* 194**,** 556-62.

WANG, D., YUAN, R., FENG, Y., EL-ASADY, R., FARBER, D. L., GRESS, R. E., LUCAS, P. J. & HADLEY, G. A. 2004. Regulation of CD103 expression by CD8+ T cells responding to renal allografts. *J Immunol,* 172**,** 214-21.

WANG, X., HE, Q., SHEN, H., XIA, A., TIAN, W., YU, W. & SUN, B. 2019. TOX promotes the exhaustion of antitumor CD8(+) T cells by preventing PD1 degradation in hepatocellular carcinoma. *J Hepatol,* 71**,** 731-741.

WEBB, J. R., MILNE, K., WATSON, P., DELEEUW, R. J. & NELSON, B. H. 2014. Tumor-infiltrating lymphocytes expressing the tissue resident memory marker CD103 are associated with increased survival in high-grade serous ovarian cancer. *Clin Cancer Res,* 20**,** 434-44.

WENINGER, W., CROWLEY, M. A., MANJUNATH, N. & VON ANDRIAN, U. H. 2001. Migratory properties of naive, effector, and memory CD8(+) T cells. *J Exp Med,* 194**,** 953-66.

WHERRY, E. J., TEICHGRABER, V., BECKER, T. C., MASOPUST, D., KAECH, S. M., ANTIA, R., VON ANDRIAN, U. H. & AHMED, R. 2003. Lineage relationship and protective immunity of memory CD8 T cell subsets. *Nat Immunol,* 4**,** 225-34.

YUAN, R., EL-ASADY, R., LIU, K., WANG, D., DRACHENBERG, C. B. & HADLEY, G. A. 2005. Critical role for CD103+CD8+ effectors in promoting tubular injury following allogeneic renal transplantation. *J Immunol,* 175**,** 2868-79.

ZISMAN, A., PANTUCK, A. J., WIEDER, J., CHAO, D. H., DOREY, F., SAID, J. W., DEKERNION, J. B., FIGLIN, R. A. & BELLDEGRUN, A. S. 2002. Risk group assessment and clinical outcome algorithm to predict the natural history of patients with surgically resected renal cell carcinoma. *J Clin Oncol,* 20**,** 4559-66.

Eidesstaatliche Versicherung

„Ich, Theresa Dornieden, versichere an Eides statt durch meine eigenhändige Unterschrift, dass ich die vorgelegte Dissertation mit dem Thema: “Tissue-resident Lymphocytes in the Human Kidney: Signatures, Specificity and their Impact for Kidney Transplantation and Cancer” / „Gewebsständige Lymphozyten in der humanen Niere: Eigenschaften, Spezifität und ihre Bedeutung für die Nierentransplantation und den Nierenkrebs“ selbstständig und ohne nicht offengelegte Hilfe Dritter verfasst und keine anderen als die angegebenen Quellen und Hilfsmittel genutzt habe.
Alle Stellen, die wörtlich oder dem Sinne nach auf Publikationen oder Vorträgen anderer Autoren/innen beruhen, sind als solche in korrekter Zitierung kenntlich gemacht. Die Abschnitte zu Methodik (insbesondere praktische Arbeiten, Laborbestimmungen, statistische Aufarbeitung) und Resultaten (insbesondere Abbildungen, Graphiken und Tabellen) werden von mir verantwortet.

[Für den Fall, dass Sie die Forschung für Ihre Promotion ganz oder teilweise in Gruppenarbeit durchgeführt haben:] Ich versichere ferner, dass ich die in Zusammenarbeit mit anderen Personen generierten Daten, Datenauswertungen und Schlussfolgerungen korrekt gekennzeichnet und meinen eigenen Beitrag sowie die Beiträge anderer Personen korrekt kenntlich gemacht habe (siehe Anteilserklärung). Texte oder Textteile, die gemeinsam mit anderen erstellt oder verwendet wurden, habe ich korrekt kenntlich gemacht.

Meine Anteile an etwaigen Publikationen zu dieser Dissertation entsprechen denen, die in der untenstehenden gemeinsamen Erklärung mit dem/der Erstbetreuer/in, angegeben sind. Für sämtliche im Rahmen der Dissertation entstandenen Publikationen wurden die Richtlinien des ICMJE (International Committee of Medical Journal Editors; www.icmje.og) zur Autorenschaft eingehalten. Ich erkläre ferner, dass ich mich zur Einhaltung der Satzung der Charité – Universitätsmedizin Berlin zur Sicherung Guter Wissenschaftlicher Praxis verpflichte.

Weiterhin versichere ich, dass ich diese Dissertation weder in gleicher noch in ähnlicher Form bereits an einer anderen Fakultät eingereicht habe.

Die Bedeutung dieser eidesstattlichen Versicherung und die strafrechtlichen Folgen einer unwahren eidesstattlichen Versicherung (§§156, 161 des Strafgesetzbuches) sind mir bekannt und bewusst.“

Datum Unterschrift

Anteilserklärung

Ausführliche Anteilserklärung an der erfolgten Publikation als Top-Journal im Rahmen der Promotionsverfahren zum PhD bzw. MD/PhD

Signatures and Specificity of Tissue-Resident Lymphocytes Identified in Human Renal Peritumor and Tumor Tissue. Dornieden T, Sattler A, Pascual-Reguant A, Ruhm AH, Thiel LG, Bergmann YS, Thole LML, Köhler R, Kühl AA, Hauser AE, Boral S, Friedersdorff F, Kotsch K. *JASN*. 2021; 32: 2223-2241.

Beitrag im Einzelnen:

Mein Beitrag zu dieser Arbeit war die Erstellung des Forschungsdesigns, bei der Prof. Dr. Katja Kotsch und Dr. Arne Sattler mich unterstützt haben, sowie die Organisation und Abholung der Patientenproben, bei der Prof. Dr. Frank Friedersdorff die Patientenaufklärung und die Probenentnahme im OP übernommen hat. Zudem die Durchführung der Experimente nach genanntem Protokoll, wobei die Experimente zur MELC Analyse in enger Kooperation mit Dr. rer. nat. Anna Pascual-Reguant (DRFZ, Berlin) erfolgt sind, sowie die statistische Auswertung. Aus meiner statistischen Auswertung sind alle Tabellen und Abbildungen entstanden, ausgenommen die Abbildungen 2C, 4B, 5, sowie die Supplemental Figures 2, 10, 11. Diese sind in enger Absprache durch eine Kooperation mit Dr. rer. nat. Anna Pascual-Reguant (DRFZ, Berlin) entstanden. Außerdem habe ich in Zusammenarbeit mit Prof. Dr. Katja Kotsch das Paper geschrieben und publiziert.

Mucosal associated invariant T cells are differentially impaired in tolerant and immunosuppressed liver transplant recipients. Sattler A, Thiel LG, Ruhm AH, Bergmann Y, Dornieden T, Choi M, Halleck F, Friedersdorff F, Eurich D, Kotsch K. *Am J Transplant.* 2021; 21: 87-102.

Beitrag im Einzelnen:

Mein Beitrag zu dieser Arbeit war die Durchführung von einigen Experimenten. Hierbei habe ich aus dem Blut einiger Patienten Lymphozyten isoliert, diese anschließend nach Protokoll gefärbt und stimuliert.

_____
Unterschrift, Datum und Stempel des/der erstbetreuenden Hochschullehrers/in

_____
Unterschrift des Doktoranden/der Doktorandin

Auszug aus der Journal Summary List

Publikation im Journal „Journal of the American Society of Nephrology “

Journal Data Filtered By: **Selected JCR Year: 2019** Selected Editions: SCIE,SSCI Selected Categories: **“UROLOGY and NEPHROLOGY”** Selected Category Scheme: WoS

Gesamtanzahl: 85 Journale

Rank	Full Journal Title	Total Cites	Journal Impact Factor	Eigenfactor Score
1	Nature Reviews Nephrology	6,911	20.711	0.019590
2	EUROPEAN UROLOGY	33,096	17.947	0.063030
3	Kidney International Supplements	2,001	12.818	0.002190
4	Nature Reviews Urology	3,761	11.000	0.008810
5	JOURNAL OF THE AMERICAN SOCIETY OF NEPHROLOGY	39,047	9.274	0.057390
6	KIDNEY INTERNATIONAL	43,892	8.945	0.044100
7	Clinical Journal of the American Society of Nephrology	17,405	6.628	0.032450
8	AMERICAN JOURNAL OF KIDNEY DISEASES	23,230	6.618	0.032320

BASIC RESEARCH www.jasn.org

Signatures and Specificity of Tissue-Resident Lymphocytes Identified in Human Renal Peritumor and Tumor Tissue

Theresa Dornieden,[1] Arne Sattler,[1] Anna Pascual-Reguant,[2,3] Annkathrin Helena Ruhm,[1] Lion Gabriel Thiel,[1] Yasmin Samira Bergmann,[1] Linda Marie Laura Thole,[1] Ralf Köhler,[2] Anja Andrea Kühl,[4] Anja Erika Hauser,[2,3] Sengül Boral,[5] Frank Friedersdorff,[6] and Katja Kotsch[1]

[1] Department of General and Visceral Surgery, Charité–Universitätsmedizin Berlin, Corporate Member of Freie Universität Berlin, Humboldt Universität zu Berlin, and Berlin Institute of Health, Berlin, Germany
[2] German Rheumatism Research Centre Berlin, Leibniz Institute, Berlin, Germany
[3] Department of Rheumatology and Clinical Immunology, Charité–Universitätsmedizin Berlin, Corporate Member of Freie Universität Berlin, Humboldt Universität zu Berlin, and Berlin Institute of Health, Berlin, Germany
[4] iPath.Berlin—Immunopathology for Experimental Models, Charité–Universitätsmedizin Berlin, Corporate Member of Freie Universität Berlin, Humboldt-Universität zu Berlin, and Berlin Institute of Health, Berlin, Germany
[5] Department of Pathology, Charité–Universitätsmedizin Berlin, Corporate Member of Freie Universität Berlin and Humboldt Universität zu Berlin, Berlin, Germany
[6] Department of Urology, Charité–Universitätsmedizin Berlin, Corporate Member of Freie Universität Berlin, Humboldt Universität zu Berlin, and Berlin Institute of Health, Berlin, Germany

ABSTRACT

Background Tissue-resident memory T (T_{RM}) cells are known to be important for the first line of defense in mucosa-associated tissues. However, the composition, localization, effector function, and specificity of T_{RM} cells in the human kidney and their relevance for renal pathology have not been investigated.

Methods Lymphocytes derived from blood, renal peritumor samples, and tumor samples were phenotypically and functionally assessed by applying flow cytometry and highly advanced histology (multi-epitope ligand cartography) methods.

Results $CD69^+CD103^+CD8^+$ T_{RM} cells in kidneys display an inflammatory profile reflected by enhanced IL-2, IL-17, and TNFα production, and their frequencies correlate with increasing age and kidney function. We further identified mucosa-associated invariant T and $CD56^{dim}$ and $CD56^{bright}$ natural killer cells likewise expressing CD69 and CD103, the latter significantly enriched in renal tumor tissues. $CD8^+$ T_{RM} cell frequencies were not elevated in kidney tumor tissue, but they coexpressed PD-1 and TOX and produced granzyme B. Tumor-derived $CD8^+$ T_{RM} cells from patients with metastases were functionally impaired. Both $CD69^+CD103^-CD4^+$ and $CD69^+CD103^-CD8^+$ T_{RM} cells form distinct clusters in tumor tissues in proximity to antigen-presenting cells. Finally, EBV, CMV, BKV, and influenza antigen-specific $CD8^+$ T cells were enriched in the effector memory T cell population in the kidney.

Conclusions Our data provide an extensive overview of T_{RM} cells' phenotypes and functions in the human kidney for the first time, pointing toward their potential relevance in kidney transplantation and kidney disease.

JASN 32: 2223–2241, 2021. doi: https://doi.org/10.1681/ASN.2020101528

Currently, the identification and description of $CD8^+$ tissue-resident memory T (T_{RM}) cells in various tissues are attracting increasing attention.[1–3] Originally, T_{RM} cells were identified primarily at barrier sites, such as mucosal tissue or skin, but their presence has meanwhile been documented in a number of nonmucosal sites, including lymphoid and peripheral

Received October 29, 2020. Accepted April 21, 2021.

Published online ahead of print. Publication date available at www.jasn.org.

Correspondence: Prof. Katja Kotsch, Department of General and Visceral Surgery, Charité–Universitätsmedizin Berlin, Campus Benjamin Franklin, Hindenburgdamm 30, 12203 Berlin, Germany. Email: katja.kotsch@charite.de

Copyright © 2021 by the American Society of Nephrology

tissues such as thymus, skin, spleen, liver, pancreas, heart, and brain.[4–6] In general, $CD8^+$ T_{RM} cells have been characterized by expression of the *integrin-αE* (CD103), the activation/retention marker CD69, and the *collagen-binding integrin-α1* (CD49a). They are described as a distinct memory population generated at the site of infection, where their main function relies on their strategic localization and scanning of barrier tissues, thus allowing early detection of reinfection by pathogens and possibly constituting the first line of cellular defense.[7–11]

Although the human kidney can be affected by bacterial pathogens generally resulting from urinary tract infections, it does not represent a typical border tissue, such as lung or intestine. T_{RM} cells have been already mentioned as being present in resected kidneys and transplant nephrectomies, illustrating that both donor-resident $CD8^+$ T cells as well as graft-infiltrating recipient-derived $CD8^+$ T cells display a T_{RM} phenotype.[12,13] However, no detailed investigation of $CD8^+$ T_{RM} cells in human kidneys and their potential relevance with respect to renal pathology is available so far. We, therefore, performed a comprehensive analysis of tissue-resident T cell subsets in the kidney and provide detailed information on their phenotype, effector profile, and antigen specificity.

Significance Statement

Tissue-resident memory T (T_{RM}) cells are important for localized immune responses, but their phenotypic and functional diversity in human kidneys is poorly understood. In this study, $CD4^+$ and $CD8^+$ T_{RM} and other resident lymphocytes from tumor- and nontumor-containing kidney tissue samples of 62 patients with nephrectomy were extensively analyzed. It was shown that intrarenal $CD8^+$ T_{RM} cells express an activated, proinflammatory phenotype and become more numerous with age. Within tumors, however, $CD8^+$ T_{RM} cells more frequent express markers of exhaustion and become functionally impaired in patients with metastasis. Multiple viral antigen specificities were also demonstrated for intrarenal $CD8^+$ T_{RM}. These and other observations from the study provide novel insights into the complex repertoire of human kidney–resident lymphocytes with relevance for renal cancers and transplants.

METHODS

Patients

Macroscopic portions of kidney tumor tissue and adjacent peritumor tissue as well as paired blood samples were collected from patients undergoing nephrectomy at the Clinic for Urology, Charité–Universitätsmedizin Berlin, Germany. The study was approved by the Ethics Committee of Charité–Universitätsmedizin Berlin (EA1/353/16 and EA4/066/19), and all experiments described in this study were conducted in compliance with the Declarations of Helsinki and Istanbul. In total, 62 patients were included in this study. GFR was calculated using the Chronic Kidney Disease Epidemiology Collaboration creatinine equation. Patient demographics are summarized in Table 1.

Cell Isolation and Flow Cytometry

Resected peritumor and tumor tissues were perfused with 0.9% NaCl and immediately processed. To obtain single-cell suspensions, tissue was dissected into small pieces. Digestion medium was added, consisting of RPMI 1640 medium supplemented with 0.3 mg/ml glutamine, 10% FCS, 1% penicillin-streptomycin, 1 mg/ml collagenase II, and 10 U/ml DNAse I. Samples were incubated for 45 minutes at 37°C in a shaking water bath followed by separation through a 100-µm cell strainer. Subsequently, mononuclear cells from kidney and blood were isolated with LEUCO Human Separating Solution (Genaxxon Bioscience GmbH, Ulm, Germany) by means of density gradient centrifugation. For analysis of surface molecules, 1×10^6 mononuclear cells were stained with the antibodies listed in Supplemental Table 1. For intracellular staining, cells were fixed, permeabilized (Fixation Permeabilization Kit; Thermo Fisher, Darmstadt, Germany), and stained with respective antibodies (Supplemental Table 1). Cells were measured with a BD FortessaX20 flow cytometer (BD Bioscience, Heidelberg, Germany). FACS data analysis was conducted using FlowJo software 10.0 (Tree Star Inc., Ashland, OR). FlowSOM analysis, viSNE plots, and heat maps were generated using the Cytobank platform (Cytobank Inc., Santa Clara, CA). Following dimensionality reduction with viSNE, eight to 11 metaclusters were generated in FlowSOM. As per Cytobank recommendations, the number of clusters and metaclusters was empirically honed until a good resolution and correspondence between the FlowSOM metaclustering and the viSNE islands was reached. Kidney-specific metaclusters were identified and annotated according to their marker expression. A manual gating strategy for identification of the various lymphocyte subsets is illustrated in Supplemental Figure 1A. All FACS datasets were uploaded in the public repository Zenodo (https://zenodo.org/record/4434462#.YCo_c2hKiUk; DOI 10.5281/zenodo.4550735).

Analysis of Antigen-Specific T Cells

For detection of antigen-specific cells, PE-labeled HLA-A*0201 MHC I dextramers containing immunodominant epitopes of polyomavirus-type BK (BKV), influenza virus, Epstein–Barr virus (EBV), and cytomegalovirus (CMV; Immudex, Copenhagen, Denmark) were used (Supplemental Table 2). Peripheral blood and renal mononuclear cells of HLA-A*02–positive patients were stained with multimers according to the manufacturer's protocol. For phenotypic analysis, cells were additionally stained with a mixture of surface antibodies (Supplemental Table 3). PE-labeled control multimers (Immudex) were used to determine gate limits.

Cell Stimulation and Functional Analysis

For functional analysis, 4×10^6 cells were stained with CD69 antibody for 20 minutes at room temperature (RT) before

Table 1. Patient demographics

Variable	*n* (%)	Minimum/ Maximum	Mean	SD
Total no. of included patients	62 (100)			
Age, yr		26/85	63.92	13.58
Sex, men/women	40 (64.52)/22 (35.48)			
Cause of nephrectomy				
Renal cell carcinoma	46 (74.19)			
Ureter tumor	7 (11.29)			
Oncocytoma	1 (1.61)			
Nephrolithiasis	1 (1.61)			
Impaired function	4 (6.45)			
Cystic kidney	3 (4.84)			
Preoperative kidney function (eGFR, CKD-EPI)				
Stage 1, ≥90 ml/min	8 (12.90)			
Stage 2, 60–90 ml/min	24 (38.71)			
Stage 3, 30–60 ml/min	17 (27.42)			
Stage 4, 15–30 ml/min	2 (3.23)			
Stage 5, <15 ml/min	5 (8.06)			
ns	6 (9.68)			
Further diagnoses				
Hypertension	37 (59.98)			
CKD	17 (27.42)			
Diabetes	DM1: 1 (1.61); DM2: 12 (19.35)			
Cardiac disease	11 (17.74)			
Staging by size of tumor				
T1 (thereof 1a, 1b)	23 (50.00[a]);11 (23.91[a]), 13 (28.26[a])			
T2 (all 2a)	8 (17.39[a])			
T3 (all 3a)	13 (28.26[a])			
T4	2 (4.35[a])			
Relapse of patients with tumors				
Renal cell carcinoma remained kidney	1 (2.17[a])			
Lung + lymph nodes	1 (2.17[a])			
Urinary bladder	1 (2.17[a])			
Liver	1 (2.17[a])			
Larynx	1 (2.17[a])			
Prostate	1 (2.17[a])			
No	40 (86.96[a])			
Metastases diagnosed before nephrectomy				
Pulmonary metastases	3 (6.52[a])			
Osseous metastases	2 (4.35[a])			
Adrenal gland metastases	1 (2.17[a])			
Lymph node metastases	2 (4.35[a])			
Lymph node + pulmonary metastases	1 (2.17[a])			
No	37 (80.43[a])			

CKD-EPI, Chronic Kidney Disease Epidemiology Collaboration; ns, not significant; DM1, diabetes mellitus 1; DM2, diabetes mellitus 2.
[a]Percentage of $n=46$ (patients with tumors).

stimulation with PMA (50 ng/ml) and ionomycin (1 μg/ml) for 6 hours at 37°C and 5% CO_2 in the presence of 10 μg/ml brefeldin A. After stimulation, cells were stained with a surface antibody mixture for 20 minutes at RT, fixed, permeabilized (Fixation Permeabilization Kit; BD Bioscience, Heidelberg, Germany), and stained with antibodies against intracellular molecules (Supplemental Figure 1B, Supplemental Table 4).

Tissue Preparation for Multiepitope Ligand Cartography

Multi-epitope ligand cartography (MELC) analysis was performed as described recently.[14] Fresh frozen tissue was cut into 5-µm sections using an NX80 cryotome (ThermoFisher, Waltham, MA) on APES-coated cover slides (24 × 60 mm; Menzel-Gläser, Braunschweig, Germany). Samples were then fixed for 10 minutes at RT with 2% paraformaldehyde (methanol and RNAse free; Electron Microscopy Sciences, Hatfield, PA). After washing, samples were permeabilized with 0.2% Triton X-100 in PBS for 10 minutes at RT and blocked with 10% goat serum and 1% BSA in PBS for at least 20 minutes. Afterward, a fluid chamber holding 100 μl of PBS was created using "press-to-seal" silicone sheets (Life Technologies, Carlsbad, CA; 1.0-mm thickness), which were attached to the coverslip, surrounding the sample.

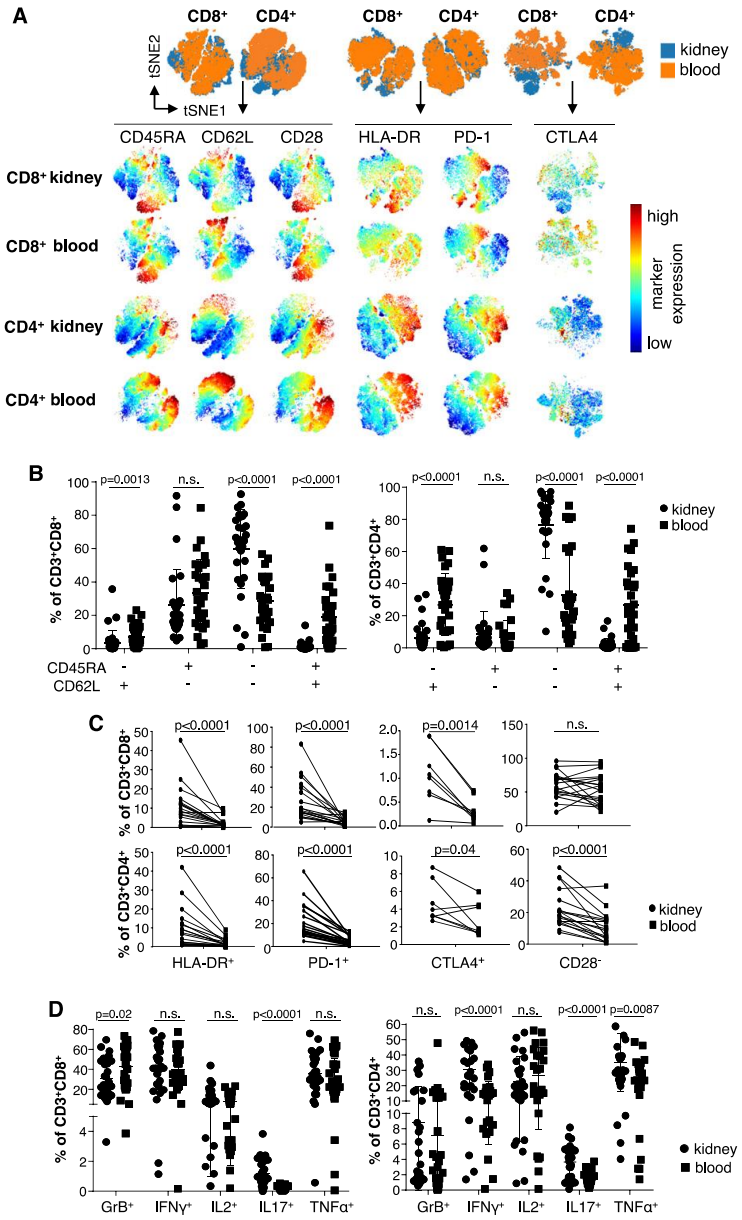

Figure 1. Increased frequencies of effector memory T cells reside in the human kidney. (A) viSNE plots of flow cytometric analysis of viable $CD8^+$ and $CD4^+$ T cells illustrate the separate clustering of kidney and blood. Individual plots for measured markers (CD45RA, CD62L, CD28, HLA-DR, PD-1, CTLA4) are displayed for both kidney- and blood-derived $CD8^+$ and $CD4^+$ T cells using the viSNE algorithm. Expression is shown by color coding in relative intensity. viSNE plots were generated from concatenated FCS files and gated on $CD8^+$ and $CD4^+$ T cells. Displayed markers were measured in three different panels, where three different viSNE plots were generated (CD45RA/CD62L/CD28: $n=19$, considering CD103, CD28, CD45RA, CD49a, CD62L, CD69, NKG2D, Va7.2 [Panel 1]; HLA-DR/PD-1: $n=19$, considering CD103, CD161, CD45RO, CD69, HLA-DR, NKG2D, PD-1, Va7.2 [Panel 2]; CTLA4: $n=8$, considering CD103, CD161, CD25, CD45RA, CD62L, CD69, CTLA-4, FoxP3, HLA-DR, Ki67 [Panel 3]). (B) Frequencies of $CD45RA^-CD62L^+$ central memory T, $CD45RA^+CD62L^-$ terminally differentiated effector, $CD45RA^-CD62L^-$ T_{EM}, and $CD45RA^+CD62L^+$ naïve $CD8^+$ and

MELC Image Acquisition

A modified Toponome Image Cycler MM3 (MelTec GmbH & Co. KG, Magdeburg, Germany) was used. MELC image acquisition was performed as previously shown.[15] This robotic microscopic system consists of (*1*) an inverted wide-field (epi-)fluorescence microscope (Leica DM IRE2) equipped with a CMOS camera and a motor-controlled XY stage, (*2*) a CAVRO XL3000 Pipette/Diluter (Tecan GmbH, Crailsheim, Germany), and (*3*) the MelTec TIC-Control software for controlling the microscope and pipetting system and for synchronized image acquisition. An MELC run consists of a sequence of cycles, each containing the following four steps: (*1*) incubation of the fluorescence-coupled antibody with subsequent washing, (*2*) crosscorrelation-based autofocusing followed by acquisition of the fluorescence image three-dimensional (3D) stack (plus or minus seven *z* steps), (*3*) photobleaching of the fluorophore, and (*4*) a second autofocusing step followed by acquisition of a 3D stack after bleaching the fluorescence image. In each four-step cycle, another fluorescence-labeled antibody is used. Steric hindrance issues that might appear due to this specific labeling order have been ruled out as previously shown.[15] Antibodies used for multiplexed immunofluorescence histology of kidney samples were stained in the indicated order as listed in Supplemental Table 5 (Supplemental Figure 2).

Image Preprocessing

All images were aligned on the basis of the reference phase contrast image taken at the beginning of measurement. Thereafter, each fluorescence MELC image was processed by background subtraction and illumination correction on the basis of bleaching images.[16] Then, an "Extended Depth of Field" algorithm was applied to the 3D fluorescence stack in each cycle.[17] Images were then normalized in ImageJ,[18] where a rolling ball algorithm was used for background estimation,[19] edges were removed (accounting for the maximum allowed shift during the autofocus procedure), and fluorescence intensities were stretched to the full-intensity range (16 bit→2^{16}). The two-dimensional fluorescence images generated in this way were subsequently segmented and analyzed.

Cell Segmentation and Single-Cell Feature Extraction

Segmentation was performed in a two-step process—a signal classification step using Ilastik 1.3.2[20] followed by an object recognition step using CellProfiler 3.1.8,[21] as described elsewhere.[22] Ilastik was used to classify pixels in three classes (nuclei, membrane, and extracellular matrix) and to generate probability maps for each class. A combination of images was summed up and used to classify membranes and extracellular matrix, whereas only the DAPI image was used to classify nuclei. The random forest algorithm (machine learning; Ilastik) was trained by manual pixel classification in a small region of a dataset (approximately 6% of the image). The rest of the dataset as well as seven extra datasets analyzed here was classified without retraining using the random forest algorithm. CellProfiler was subsequently used to segment the nuclei and membrane probability maps and to generate nuclei and cellular object masks, respectively. These masks were superimposed on the individual fluorescence images acquired for each marker in order to extract single-cell information (*i.e.*, mean fluorescent intensity of each marker per segmented cell).

Cluster Analysis

Segmented cells were analyzed in Orange 3.26.0[23] using several algorithms for dimensionality reduction that use the list of mean fluorescent intensity values as single-cell features. K-means clustering of the kidney single-cell data was performed for all segmented cells from eight kidney datasets pooled together (four tumor and four patient-matched peritumor samples); t-distributed stochastic neighbor embedding of $CD69^+CD103^+$ tissue-resident cells was performed with eight principal components and a perplexity of 30 and 1000 iterations.

Data Transformation and Normalization

Fluorescence intensities per pixel were normalized to the full 16-bit range in ImageJ and brought to a zero to one scale in CellProfiler. Data were transformed using the hyperbolic arcsine function with a scale argument of 0.2 previous to cluster analysis. All datasets for MELC were uploaded in the public repository Zenodo (https://zenodo.org/record/4434462#.YCo_c2hKiUk; DOIs: 10.5281/zenodo.4434363, 10.5281/zenodo.4434454, 10.5281/zenodo.4434462, 10.5281/zenodo.4434473, 10.5281/zenodo.4434504, 10.5281/zenodo.4434522, 10.5281/zenodo.4434545, 10.5281/zenodo.4434560, and 10.5281/zenodo.4434596).

Statistical Analyses

Statistical analysis was performed using GraphPad Prism 8 (GraphPad Software, La Jolla, CA). Data were tested for normal distribution using the Kolmogorov–Smirnov test. For comparison of two groups, a paired *t* test or a Wilcoxon signed ranks test was performed for paired samples; for unpaired groups, a Mann–Whitney *U* test or an unpaired *t* test was

$CD4^+$ T cells isolated from paired blood and kidney samples ($n=29$). (C) Frequencies of HLA-DR^+ ($n=19$), PD-1^+ ($n=19$), $CTLA4^+$ ($n=8$), and $CD28^-$ ($n=19$) $CD8^+$ and $CD4^+$ T cells derived from paired blood and kidney samples. (D) Cytokine effector profile (granzyme B [GrB], IFNγ, IL-2, IL-17, TNFα) of $CD8^+$ ($n=27$) and $CD4^+$ ($n=28$) T cells derived from kidney tissue and paired blood samples. Statistically significant differences were tested with the two-tailed paired *t* or the Wilcoxon signed ranks test and are presented as means ± SD. In all tests, a value of $P=0.05$ was considered significant.

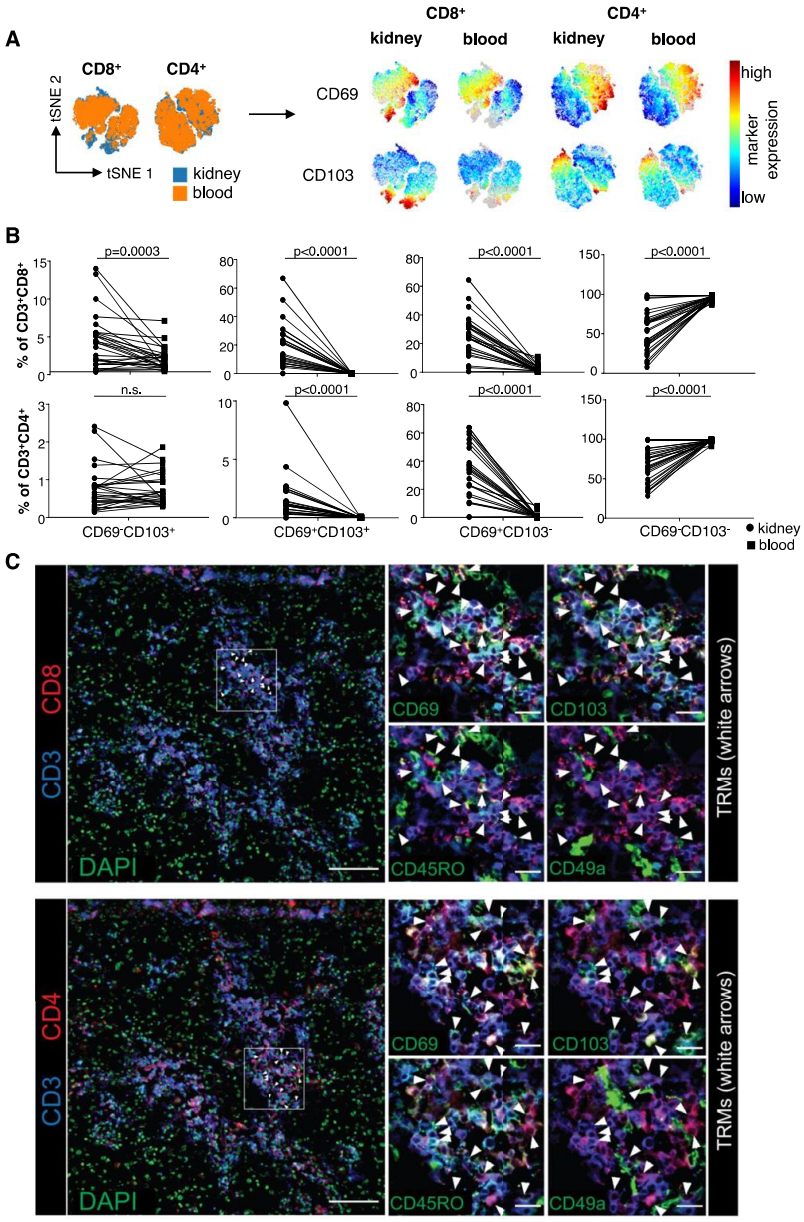

Figure 2. Tissue-resident (TRM) cells can be identified within the human kidney. (A) viSNE plots of flow cytometric analysis of viable $CD8^+$ and $CD4^+$ T cells showing separate clustering of kidney and blood. Individual plots of measured T_{RM} markers (CD69 and CD103, $n=19$) are displayed for both kidney- and blood-derived $CD8^+$ and $CD4^+$ T cells using viSNE algorithm. Expression is shown by color coding in relative intensity. viSNE plots were generated from concatenated FCS files and gated on $CD8^+$ and $CD4^+$ T cells considering CD103, CD161, CD45RO, CD69, HLA-DR, NKG2D, PD-1, and Va7.2 (Panel 2). tSNE, t-distributed stochastic neighbor embedding. (B) $CD8^+$ and $CD4^+$ kidney-derived T cells express the tissue-resident markers CD103 and CD69 as compared with their blood-derived counterparts ($n=28$). Statistically significant differences were tested with the two-tailed Wilcoxon signed ranks test. (C) Overlay of MELC fluorescent images showing marker combinations that allow the identification of T_{RM} cells in the peritumor tissue of

performed. For comparison of three or four groups, a Friedman test or one-way ANOVA was used for paired samples, as well as ordinary one-way ANOVA or the Kruskal–Wallis test for unpaired groups (Supplemental Table 6). Statistical significance was considered for $P=0.05$.

RESULTS

Effector Memory T Cells Are Enriched in the Kidney Displaying a Proinflammatory Phenotype

First, we analyzed frequencies of bulk $CD8^+$ and $CD4^+$ T cells in resected peritumor kidney tissues and paired blood samples by flow cytometry. Significantly more $CD3^+CD8^+$ T cells and double-positive $CD3^+CD4^+CD8^+$ T cell frequencies were detected in the kidney, whereas $CD3^+CD4^+$ T cells were enriched in the blood. No differences regarding the proliferation status of $CD4^+$ and $CD8^+$ T cells reflected by their Ki67 expression were identified (Supplemental Figure 3, A and B). Using a viSNE algorithm approach for dimensional reduction of selected markers analyzed, a clear differentiation between blood and kidney was detected. Both $CD4^+$ and $CD8^+$ T cells derived from blood or kidney were further highlighted for the various surface molecules (Figure 1A). A detailed focus on T cell subset differentiation revealed that both $CD8^+$ and $CD4^+CD45RA^-CD62L^-$ effector memory T (T_{EM}) cells were enriched in the kidney, whereas significantly more naïve $CD8^+$ and $CD4^+CD45RA^+CD62L^+$ as well as $CD8^+$ and $CD4^+CD45RA^-CD62L^+$ central memory T cells were detected in blood samples (Figure 1, A and B, Supplemental Figure 3C). The viSNE map indicated that renal $CD8^+$ was characterized by an elevated HLA-DR expression pointing toward an activated phenotype as well as by higher levels of the coinhibitory molecule PD-1 as compared with peripheral blood (Figure 1A). A detailed analysis using manual gating further revealed higher frequencies of the small CTLA-4^+ population within kidney-derived $CD8^+$ and $CD4^+$ T cells and a higher percentage of $CD4^+$ T cells negative for CD28 in the kidney (Figure 1C), being partially supported by viSNE (Figure 1A). We further applied FlowSOM,[24] an unsupervised technique for clustering and dimensionality reduction of FACS data. Generated viSNE maps were overlayed with metaclusters identified in FlowSOM, allowing the identification of multiple T cell subsets present in the kidney but not in blood (*e.g.*, on the basis of memory and/or tissue residency signatures) (Supplemental Figure 4). With respect to their functional profile, renal $CD8^+$ and $CD4^+$ T cells produced significantly more IL-17, and especially, $CD4^+$ T cells produced significantly more IFNγ and TNFα than did T cells from the peripheral blood (Figure 1D). Kidney-derived $CD8^+$ and $CD4^+$ T cells displayed significantly increased expression of the *α1-subunit of $\alpha1\beta1$-integrin*, CD49a, a marker originally described on a minor fraction of kidney-resident natural killer (NK) cells.[25] Both $CD49a^+$ subsets produced significantly more IL-17 and less granzyme B, whereas $CD49a^+CD4^+$ T cells were additionally characterized by higher IFNγ, IL-2, and TNFα expression than were their $CD49a^-$ T cell counterparts (Supplemental Figure 5A and B).

T_{RM} Cells Reside in the Kidney

The presence of tissue residency for $CD8^+$ memory T cells has been associated with local protection after antigen exposure in multiple tissues.[7–9,26] In order to clarify the presence of T_{RM} cells in the kidney, we investigated classic tissue-resident markers, including KLRG1, CD103, and CD69, for $CD4^+$ and $CD8^+$ T cells. Compared with blood, significantly higher frequencies of renal $KLRG1^-CD103^+$ and double-positive $KLRG1^+CD103^+CD8^+$ T cells were detected, whereas frequencies of $KLRG1^+CD103^-CD8^+$ T cells were decreased. On the contrary, all investigated subsets for $CD4^+$ T cells were enriched in the kidney (Supplemental Figure 6, A and B). It has been demonstrated that $KLRG1^+$ effector $CD8^+$ T cells lose KLRG1 expression after receiving activating signals.[27] Especially $KLRG1^-$-activated $CD8^+$ T cells can develop into $CD103^+CD8^+$ T_{RM} cells in the skin.[28] The analysis by viSNE revealed a clear induction of CD69 and CD103 on $CD4^+$ and $CD8^+$ T cells, thus documenting their T_{RM} phenotype in the kidney (Figure 2A). Interestingly, an enrichment for $CD69^-CD103^+$ single-positive cells was solely observed for renal $CD8^+$ T cells (Figure 2, A and B, Supplemental Figure 6C). Applying MELC, we confirmed the presence of renal $CD8^+$ and $CD4^+$ T_{RM} cells *in situ* on the basis of the coexpression of CD45RO, CD69, CD103, and CD49a in $CD3^+CD4^+$ and $CD3^+CD8^+$ T cell subpopulations (Figure 2C).

Renal T_{RM} Cells Exhibit an Activated Phenotype

Both heat map analysis and manual gating revealed that $CD69^+CD103^+$ T_{RM} and $CD69^+$ single-positive T_{RM} cells were characterized by significantly stronger expression of HLA-DR and PD-1 than were $CD69^-CD103^-$ T cells (Figure 3A). Moreover, $CD4^+$ and $CD8^+$ T_{RM} cells showed a loss of CD28, indicating their antigen experience and differentiation. Interestingly, HLA-DR expression on single-positive $CD69^+CD103^-CD8^+$ T_{RM} cells discriminates this subset from double-negative $CD69^-CD103^-CD8^+$ T cells, whereas PD-1 is significantly more frequently expressed on

the kidney. (Upper panel) CD3 (blue), CD8 (red), and DAPI (green) staining is shown for the whole field of view (FOV). DAPI (green) is exchanged for CD69, CD103, CD45RO, or CD49a in a region of interest (ROI), where $CD8^+$ T_{RM} cells are marked with white arrows. Scale bar: 100 μm in the left panel; 20 μm in the right panels. (Lower panel) CD3 (blue), CD4 (red), and DAPI (green) staining is shown for the whole FOV. DAPI (green) is exchanged for CD69, CD103, CD45RO, or CD49a in an ROI, where $CD4^+$ T_{RM} cells are marked with white arrows. Data represent one of four independent experiments.

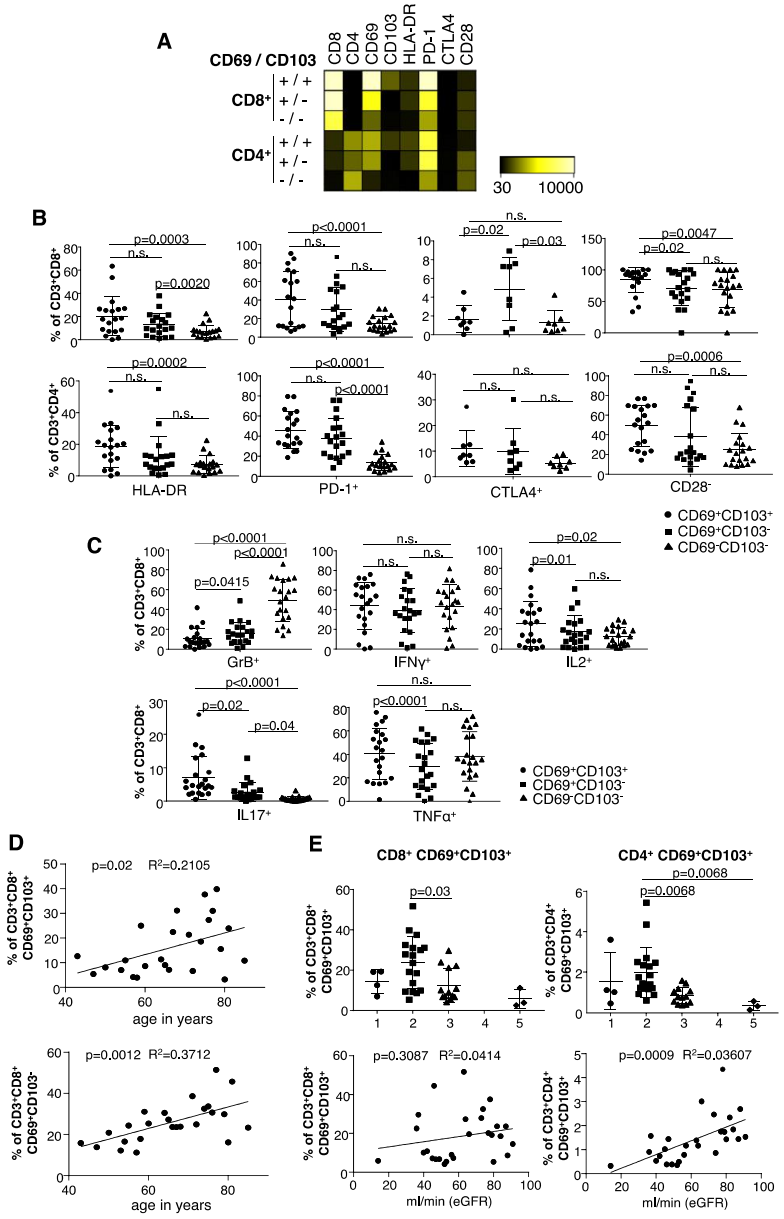

Figure 3. Tissue-resident CD8$^+$ T_{RM} cells in the kidney demonstrate an activated phenotype and accumulate in the aged kidney. (A) Heat map plot of flow cytometric analysis for renal peritumor CD8$^+$ and CD4$^+$ T_{RM} cell populations illustrating mean relative expression levels of measured markers (CD8, CD4, CD69, CD103, HLA-DR, and PD-1 [all n=19]; CTLA4 [n=8]; CD28 [n=19]). (B) Renal peritumor CD69$^+$CD103$^+$, CD69$^+$CD103$^-$, CD69$^-$CD103$^-$CD8$^+$, and CD4$^+$ T cells were analyzed for expression of HLA-DR (n=19), PD-1 (n=19), or CTLA-4 (n=8) or loss of CD28 (n=19). (C) Their functional profile after stimulation with PMA and ionomycin (granzyme B [GrB], IFNγ, IL-2, IL-17, and TNFα; n=21). Statistically significant differences were tested with one-way ANOVA or Friedman test and are presented as mean values ± SD. (D) Correlation analysis of both peritumor-derived CD8$^+$CD69$^+$CD103$^+$ and CD8$^+$CD69$^+$CD103$^-$ cell frequencies with patient age (n=35). Linear regression analysis was performed, and Spearman rank-order coefficients were calculated. (E) Patients were divided according to their stages of CKD by their eGFR (stage 1: n=4; stage 2: n=18; stage 3: n=13; stage 4: n=0; and stage 5: n=3). Peritumor-derived CD8$^+$ and CD4$^+$CD69$^+$CD103$^+$ T_{RM} cell frequencies were compared between the five groups.

$CD69^+CD103^-CD4^+$ T_{RM} versus $CD69^-CD103^-CD4^+$ T cells (Figure 3, A and B). In comparison with the other subsets analyzed, $CD69^+CD103^+CD8^+$ T_{RM} cells showed a significant reduction in frequencies expressing the cytotoxic mediator granzyme B but an enrichment of IL-2–, IL-17–, and TNFα-expressing cells, whereas no difference was detected for IFNγ (Figure 3C). $CD69^+CD103^+CD4^+$ T_{RM} cells displayed a higher proliferative capacity as reflected by Ki67 expression than did $CD69^+CD103^-CD4^+$ T_{RM} cells, an observation not confirmed for $CD8^+$ T_{RM} cells (Supplemental Figure 7A). Renal $CD69^+CD103^+CD8^+$ T_{RM} cells were negative for CD45RA and CD62L, being indicative for T_{EM} cells, and expressed significantly higher levels of CD49a than did $CD69^+CD103^-CD8^+$ T_{RM} cells (Supplemental Figure 7, B and C).

Kidney-Resident $CD8^+$ T_{RM} Cells Accumulate in the Aged Kidney

As it has been proposed that T_{RM} cells accumulate in tissues mediating local immunity,[29] we hypothesized that advanced age leads to an accumulation of T_{RM} in the kidney as with immunosenescence the pool of memory T cells increases. On the basis of $n=35$ patients in our cohort, we defined two age groups according to the calculated mean age of the patients (63 years): $n=13$ being $\leq$63 years (Group I) or $n=22$ being >63 years (Group II). Interestingly, kidneys with an advanced age (Group II) displayed significantly higher frequencies of peritumor-derived $CD69^+CD103^+$ as well as $CD69^+CD103^-CD8^+$ T cells than did Group I kidneys. In contrast, this result was not detected for $CD69^+CD103^+CD4^+$ T cells (Supplemental Figure 8, A and B). An increase of intrarenal peritumor frequencies of both $CD69^+CD103^+$ and $CD69^+CD103^-CD8^+$ T cells significantly correlated with increased age (Figure 3D). Intriguingly, patients diagnosed with CKD stage 2 display significantly higher frequencies of both $CD4^+$ and $CD8^+$ T_{RM} cells than patients diagnosed with stage 3 or 5 CKD. However, only $CD4^+CD69^+CD103^+$ T_{RM} cells significantly correlated with eGFR (Figure 3E).

Renal Mucosal-Associated Invariant T and NK Cells Express T_{RM}-Associated Markers

We further identified the CD69 and CD103 signature for both renal $CD56^{dim}$ and $CD56^{bright}$ NK cells, indicating their tissue residency (tissue-resident natural killer [NK_{TR}]). In addition, although it has already been reported that mucosal-associated invariant T (MAIT) cells displaying a tissue-resident phenotype were detected in renal tissue,[30] we were able to confirm this observation, thus further demonstrating the presence not only of renal MAIT cells but also, of tissue-resident MAIT cells (Figure 4A). We confirmed the presence of these nonconventional tissue-resident populations in the kidney by MELC, demonstrating that $CD3^-CD56^+$ NK cells and $CD3^+CD8^+CD161^+Va7.2^+$ MAIT cells coexpress CD69 and CD103 (Figure 4B).

$CD69^+CD103^+$ Lymphocytes Accumulate in Renal Tumors

Tumor epithelium generally shows enrichment for $CD103^+CD8^+$ T cells, whereas $CD103^-CD8^+$ T cells are found more frequently in tumor stroma.[31,32] Cluster analysis of MELC data from pooled tumor and patient-matched peritumor samples ($n=4$) for 16 analyzed markers revealed the identification of the following clusters: vessels, activated monocytes/macrophages, $CD69^+CD103^+$ tissue-resident cells, $CD69^+CD103^-CD8^+$ T_{RM} cells, $CD69^+CD103^-CD4^+$ T_{RM} cells, and undefined cells (Figure 5A, Supplemental Figure 9). Especially $CD69^+CD103^-CD8^+$ T_{RM} and $CD69^+CD103^+$ tissue-resident cells were found to be significantly enriched within tumors (Figure 5B). Compared with peritumor, $CD69^+CD103^-CD8^+$ and $CD69^+CD103^-CD4^+$ T_{RM} cells were forming groups of at least more than ten cells along the vessel structures in tumor tissues. A microanatomical colocalization between T cells and $CD14^+CD16^+CD163^+$ monocytes/macrophages was particularly observed for $CD69^+CD103^-CD4^+$ T_{RM}, whereas $CD69^+CD103^+$ tissue-resident cells were identified being scattered through the tumor stroma (Figure 5C, Supplemental Figures 10 and 11). Cluster analysis for $CD69^+CD103^+$ lymphocytes identified four different $CD69^+CD103^+$ tissue-resident subclusters: NK_{TR} cluster, T_{RM} cluster, tissue-resident MAIT cluster, and the cluster of proliferating cells expressing Ki67 (Figure 5, D and E). Although all $CD69^+CD103^+$ tissue-resident subclusters accumulated within tumors, the differences were only statistically significant for NK_{TR} cells (Figure 5F).

Tumor-Derived $CD8^+$ T_{RM} Cells Express PD-1 and TOX

Increased intratumor frequencies of $CD69^+CD103^+$ NK_{TR} could also be confirmed for $CD56^{dim}$ and $CD56^{bright}$ NK_{TR} cells by flow cytometry, a result that was not valid for MAIT cells (Figure 6A, Supplemental Figure 12). Both viSNE and FlowSOM analyses of FACS-derived data showed no clear differences between peritumor and tumor tissue (Figure 6B, Supplemental Figure 13). As opposed to $CD69^+CD103^+$ $CD4^+$ T_{RM} cells, we were not able to demonstrate increased frequencies of $CD69^+CD103^+CD8^+$ T_{RM} cells in renal tumor

Statistically significant differences were tested with ordinary one-way ANOVA or the Kruskal–Wallis test and are presented as mean values ± SD. Additionally, a correlation analysis of the same cell population frequencies with patient eGFR (milliliters per minute; $n=42$) is illustrated. Linear regression analysis was performed, and Spearman rank-order coefficients were calculated.

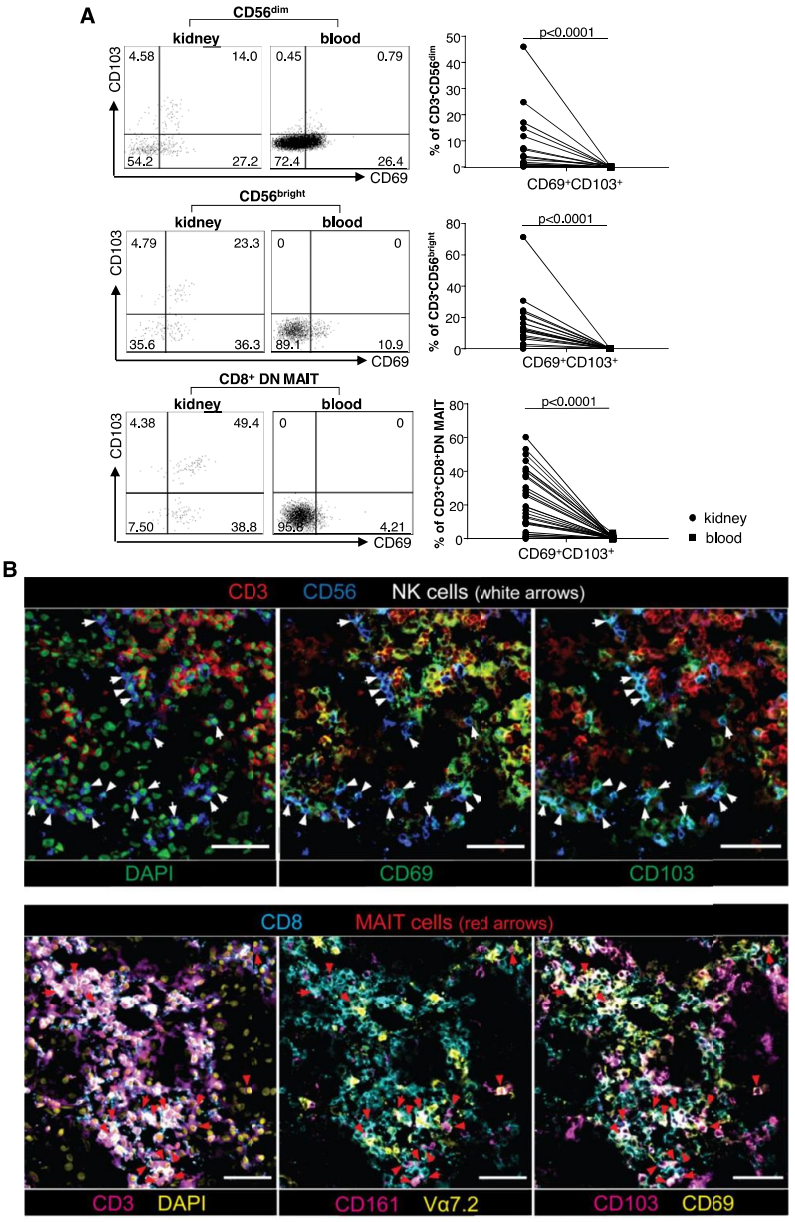

Figure 4. MAIT and NK cells co-expressing CD69 and CD103 reside in renal tissue. (A) Identification of $CD56^{dim}$ and $CD56^{bright}$ NK cells ($n=19$) or $CD3^+CD8^+/CD3^+CD4^-CD8^-$ T cell receptor $V\alpha7.2^+CD161^+$ MAIT cells ($n=29$) in the kidney expressing CD69 and CD103. Statistically significant differences were tested with the two-tailed Wilcoxon signed rank test. (B) Overlays of MELC fluorescent images showing marker combinations that allow the identification of NK_{TR} cells (upper panels; white arrows) and tissue-resident MAIT cells (lower panels; red arrows) in the kidney. For NK cell analysis, CD3 is shown in red; CD56 is shown in blue; and DAPI, CD69, or CD103 is shown in green in the same region of interest (ROI). For MAIT cell analysis, CD8 is shown in cyan; CD3, CD161, or CD103 is shown in magenta; and DAPI, T cell receptor Vα7.2, and CD69 are shown in yellow in a different ROI. Data represent one of four independent experiments. Scale bars: 50 μm.

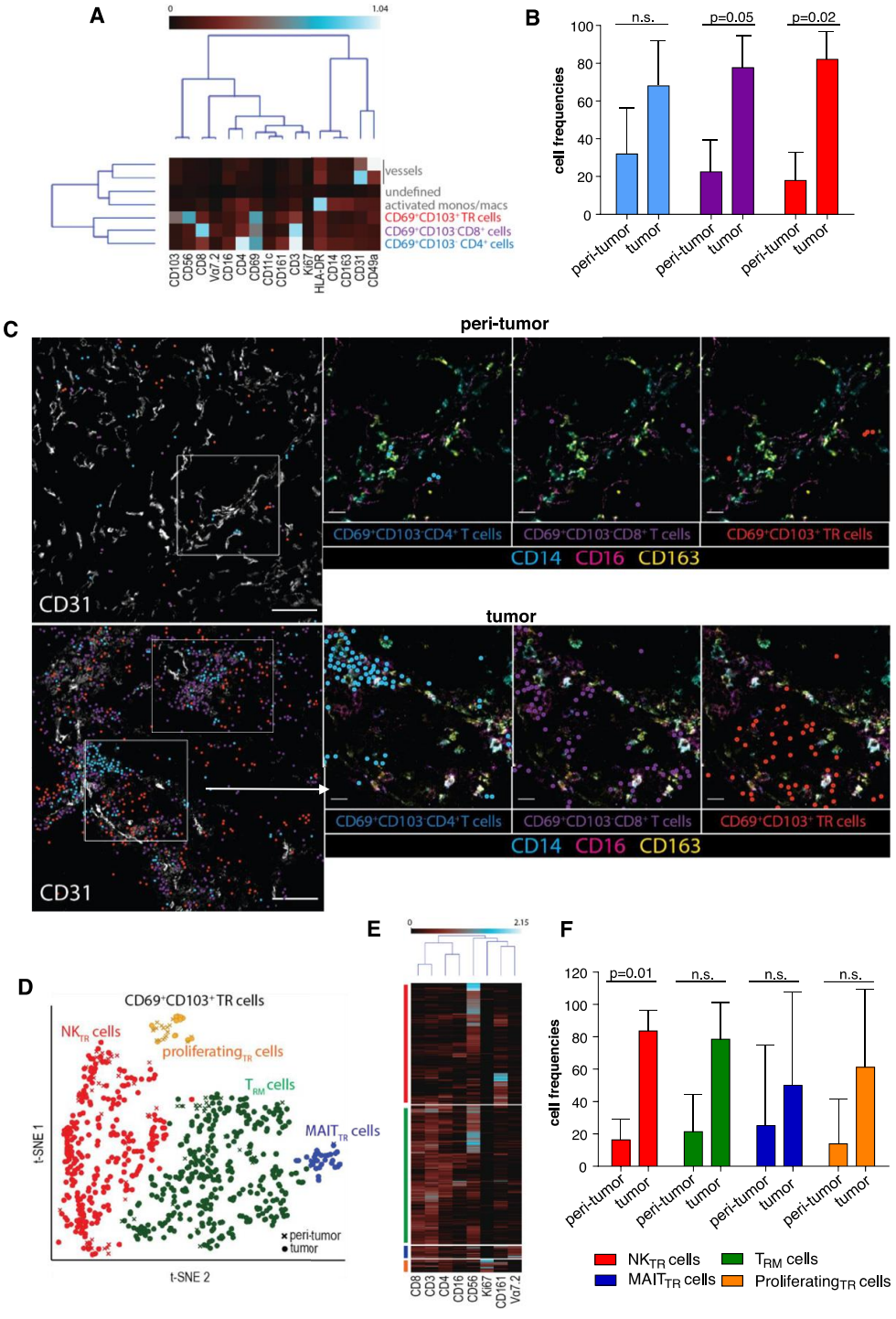
A
0
1.04
vessels
undefined
activated monos/macs
CD69+CD103+ TR cells
CD69+CD103-CD8+ cells
CD69+CD103- CD4+ cells
CD103 CD56 CD8 Vα7.2 CD16 CD4 CD69 CD11c CD161 CD3 Ki67 HLA-DR CD14 CD163 CD31 CD49a
B
n.s.
p=0.05
p=0.02
cell frequencies
100
80
60
40
20
0
peri-tumor
tumor
peri-tumor
tumor
peri-tumor
tumor
C
peri-tumor
CD69+CD103-CD4+ T cells
CD69+CD103-CD8+ T cells
CD69+CD103+ TR cells
CD14 CD16 CD163
CD31
tumor
CD69+CD103-CD4+ T cells
CD69+CD103-CD8+ T cells
CD69+CD103+ TR cells
CD14 CD16 CD163
CD31
D
CD69+CD103+ TR cells
NKTR cells
proliferatingTR cells
TRM cells
MAITTR cells
t-SNE 1
t-SNE 2
peri-tumor
tumor
E
0
2.15
CD8 CD3 CD4 CD16 CD56 Ki67 CD161 Vα7.2
F
p=0.01
n.s.
n.s.
n.s.
cell frequencies
120
100
80
60
40
20
0
peri-tumor
tumor
peri-tumor
tumor
peri-tumor
tumor
peri-tumor
tumor
NKTR cells
TRM cells
MAITTR cells
ProliferatingTR cells

tissue compared with adjacent peritumor tissue. However, we detected a significant accumulation of $CD69^+CD103^-CD8^+$ and $CD69^-CD103^+$ $CD8^+$ T_{RM} cells in the tumor (Figure 6B), thereby confirming MELC data (Figure 5C). Higher frequencies of PD-1^+ cells were demonstrated within both the $CD8^+$ and $CD4^+$ T_{RM} compartments (Figure 6D). No difference was observed for CD49a expression (Supplemental Figure 14).

In chronic infections and tumor diseases, exhausted $CD8^+$ T cells have been identified that demonstrate limited effector function and express inhibitory receptors such as PD-1, illustrating transcriptional changes as compared with effector or memory $CD8^+$ T cells.[33] Recently, the HMG box transcription factor TOX as a central regulator of these exhausted T cells was identified.[34,35] Here, we illustrate for the very first time the significantly induced coexpression of TOX and PD-1 in tumor-derived $CD69^+CD103^+CD8^+$ and $CD69^+CD103^-CD8^+$ T_{RM} cells as compared with peritumor tissue (Figure 7, A and B). Despite significantly higher granzyme B expression, functional assessment of tumor-derived $CD8^+$ T_{RM} and $CD8^+CD69^+CD103^-$ T_{RM} cells showed reduced IL-2 and TNFα as compared with peritumor-derived T_{RM} cells, suggesting at least a functional impairment of these cells (Figure 7C). We further compared patients diagnosed with metastases before nephrectomy with patients without metastases. Interestingly, tumor-derived $CD8^+$ T_{RM} and $CD8^+CD69^+CD103^-$ T_{RM} cells in patients diagnosed with metastases were functionally impaired (IL-2, TNFα, IFNγ) compared with metastases-free patients (Figure 7D).

Antigen-Specific T Cells Reside in the Kidney

Finally, in order to clarify the functional relevance of $CD8^+$ T_{RM} cells in the kidney, we aimed to address whether these cells are characterized by a certain antigen specificity. We, therefore, stained isolated cells with tetramers specific for CMV, EBV, and BKV. We further included influenza A as a representative for a nonpersisting virus. Intriguingly, we were able to identify the presence of $CD8^+$ T cells specific for all four investigated antigens, namely not only in the blood of HLA-A*02–positive patients but also, in the peritumor and tumor tissue (Figure 8, A and B). Antigen-specific T cells made a considerable contribution to the overall memory pool with mean frequencies between 0.6% (BKV) and 2.5% (CMV and EBV) within peritumor tissue. T cells specific for all four antigens predominantly showed a terminally differentiated effector cell ($CD45RA^+CD62L^-$) or T_{EM} ($CD45RA^-CD62L^-$) phenotype in the peritumor tissue. However, we detected, especially for EBV and CMV, significantly higher frequencies of antigen-specific $CD69^-CD103^-CD8^+$ T cells in contrast to $CD69^+CD103^+CD8^+$ T_{RM} cells (Figure 8, C and D).

DISCUSSION

Originally inspired by interest in characterizing tissue-resident cells in the kidney in order to acquire more insight into potential passenger leukocytes migrating out of the graft postkidney transplantation, we present here a detailed identification of T_{RM} cells in the kidney in a further attempt to understand their functional aspects in the organ in relation to tumor pathology and antigen specificity.

Renal T_{RM} cells were able to be identified through the expression of CD69 and the integrins CD103 and CD49a. Especially CD69 limits the egress of T_{RM} cells from tissues by binding to *sphingosine-1-phosphate receptor 1* as its signaling regulates effector T cell residence time in nonlymphoid tissues.[36] Whereas CD69 has been shown to promote early migration and retention in the lung,[37] recent experimental data demonstrated that its expression mainly contributes to T_{RM} cell maintenance in the kidney, suggesting CD69 expression as a consistent marker of $CD8^+$ T_{RM}.[38] Contrarily, it has been found that functional $CD69^-$ T cells can reside in murine kidneys, which led to the conclusion that CD69 is not a definitive marker for distinguishing recirculating cells from T_{RM} cells.[39] However, we were able to identify single-positive $CD69^-CD103^+CD8^+$ T cells in the human kidney, an

Figure 5. Tissue-resident T cells form clusters in renal tumors and colocalize in close proximity to antigen-presenting cells. (A) K-means clustering of pooled MELC data derived from patient-matched peritumor and tumor samples ($n=4$ per each) reveals distinct populations in the kidney. Heat map analysis illustrates the mean relative expression levels of the 16 markers analyzed for each cluster. (B) Bar graph comparing cell frequencies of selected tissue-resident (TR) clusters as (A) in tumor and peritumor samples. Statistically significant differences were tested applying a two-tailed paired *t* test. (C) Overlays of MELC fluorescent images depicting endothelial cells (CD31 in white; left panels) and monocyte/macrophages (CD14 in cyan, CD16 in magenta, and CD163 in yellow; right panels) together with color-coded dots that represent the centroid spatial coordinates of the three TR clusters identified in (A). The images depict the spatial distribution of the $CD69^+CD103^-CD4^+$ T cell cluster (light blue dots), the $CD69^+CD103^-CD8^+$ T cell cluster (purple dots), and the $CD69^+CD103^+$ TR cluster (red dots) in one representative tumor sample (upper panels) and the patient-matched peritumor sample (bottom panels). (D) The t-distributed stochastic neighbor embedding (t-SNE) map of the $CD69^+CD103^+$ TR population identified in (A). On the basis of CD3, CD56, CD161, Va7.2, and Ki67 expression, an NK_{TR} cell cluster (red), a T_{RM} cell cluster (green), a tissue-resident mucosal-associated invariant T ($MAIT_{TR}$) cell cluster (blue), and a proliferating TR cluster (orange) were defined. Each symbol represents one cell. (E) Heat map analysis of the relative expression levels of the eight markers analyzed for the TR cell clusters as in (D), where each row represents one single cell. (F) Bar graph comparing cell frequencies of selected clusters as in (D) in tumor and peritumor samples. Statistically significant differences were tested with the two-tailed paired *t* test and the two-tailed Wilcoxon test.

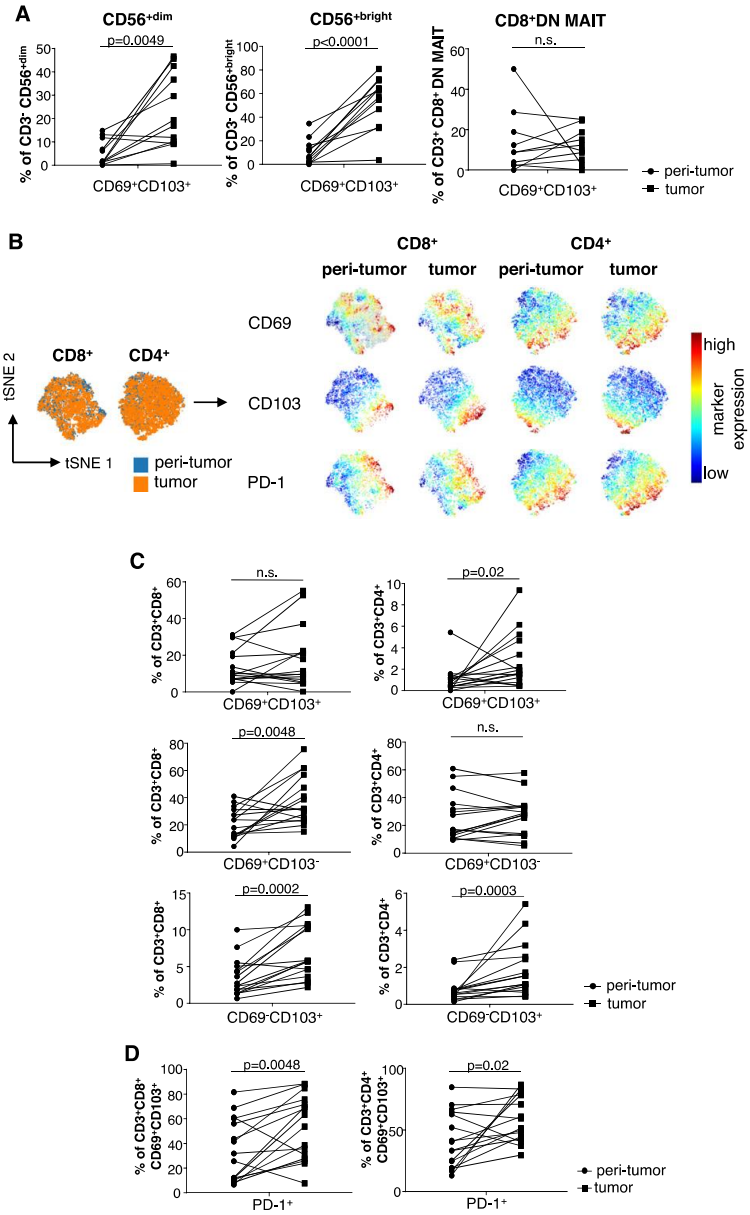

Figure 6. NK_{TR} cells and T_{RM} cells are enriched in renal tumors. (A) Expression of CD69 and CD103 by NK (CD56 dim and bright; $n=12$) and MAIT cells ($n=10$). (B) viSNE plots of flow cytometric analysis of viable $CD8^+$ and $CD4^+$ T cells showing separate clustering of peritumor and tumor tissue. Individual representation of measured markers (CD69, CD103, and PD-1 for $n=7$) is displayed for both peritumor- and tumor-derived $CD8^+$ and $CD4^+$ T cells using viSNE algorithm. Expression is shown by color coding in relative intensity. viSNE plots were generated from concatenated FCS files and gated on $CD8^+$ and $CD4^+$ T cells considering CD103, CD161, CD45RO, CD69, HLA-DR, NKG2D, PD-1, and Va7.2 (Panel 2). tSNE, t-distributed stochastic neighbor embedding. (C) $CD69^+CD103^+$, $CD69^+CD103^-$, and $CD69^-CD103^+CD8^+$ and $CD4^+$ T cell frequencies ($n=16$) derived from renal peritumor and tumor tissue. Statistically significant

observation not confirmed for $CD4^+$ T cells. Although on the basis of experimental murine data,[40] it has been stated that the majority of kidney T_{RM} cells do not express CD103, our results and those of others show the opposite.[13] However, renal $CD103^+$ T_{RM} cell frequencies are clearly lower than those of $CD69^+$ T_{RM} cells.

Kidney-derived $CD69^+$ T_{RM} cells express more HLA-DR and PD-1 and lower levels of CD28 in contrast to $CD69^-CD8^+$ T cells, indicating an activated phenotype reflected by the stronger expression of IL-2 and IL-17. Within this context, a $CD8^+CD2^{hi}CD28^-$ T cell population has been described to contain high numbers of cells with polyfunctional cytokine production and cytotoxic effector molecule expression.[41] In contrast, renal $CD69^+$ T_{RM} cells appear to be less cytotoxic on the basis of their granzyme B expression, an observation already made for hepatic $CD69^+$ T cells.[42] It has been shown that $CD49a^+CD8^+$ T_{RM} cells preferentially localize to regions rich in collagen IV in the lung,[11,43] whereas in nonmucosal organs, the localization within the tissue is less well understood. Here, we demonstrate the coexpression of CD69, CD103, and CD49a on $CD8^+$ and $CD4^+$ T cells in the kidney, showing their colocalization with myeloid cells in the renal parenchyma and suggesting potential interactions with antigen-presenting cells.

In addition to the "classical" $CD8^+$ T_{RM} cells, we were also able to identify $CD4^+$ T_{RM} cells in the kidney, which similar to $CD8^+$ T_{RM} cells, are characterized by the loss of CD28. $CD4^+CD28^-$ T cells have been reported in a number of cardiovascular and autoimmune diseases[44] but also, in the setting of renal transplant rejection.[45] $CD4^+CD28^-$ T cells can be defined as typical T helper 1 cells, which produce a large amount of IFNγ and express the cytotoxic molecules perforin and granzyme B.[46] In general, we cannot rule out the possibility that the gradual loss of CD28 on both renal $CD4^+$ and $CD8^+$ T_{RM} cells can be attributed to renal senescence.[47] However, as we observed a clear correlation at least between $CD69^+CD8^+$ T_{RM} and chronological age, but not for $CD69^+CD28^-CD8^+$ T_{RM} cells (or for $CD69^+CD4^+$ T_{RM} cells) (Supplemental Figure 8B), we propose that the loss of CD28 is a hallmark of this resident T_{RM} subtype in the kidney. In this context, it appears conflicting that $CD4^+$ T_{RM} cells significantly correlate with better kidney function, indicating the necessity for further research on their functional relevance.

Intriguingly, we were also able to identify the combined expression of CD69 and CD103 on MAIT and NK cells, further illustrating that both markers are not unique for $CD8^+$ T cells. Renal-resident MAIT cells have already been described in the kidney, where they contribute to the progression of fibrosis.[30] We here confirm the presence of intrarenal $CD69^+CD103^+Va7.2^+CD161^+$ MAIT cells in a larger number of individuals. However, neither their frequencies nor the frequencies of NK_{TR} correlated with chronological age (Supplemental Figure 8D). Although $CD56^{bright}$ NK cells have been identified as tissue-resident on the basis of their varying expression of CD69, CD49a, and CD103 in combination with NKp44 and the chemokine receptor CXCR6 in human lymphoid tissues, uterus, and liver,[48,49] our data document, to the best of our knowledge, the first description of NK_{TR} on the basis of the combined expression of CD69 and CD103 and their significant increase in renal tumors.

Tumor-derived $CD8^+$ T_{RM} cells have often been described as potential producers of IFNγ, paralleled with the upregulation of CD69, CD103, and CD49a most likely induced by TGFβ in the tumor microenvironment.[50,51] The abundance of $CD103^+CD8^+$ T cells has been shown to correlate with longer disease-free and overall survival of patients[50–52] as $CD103^+$ T cells are supposed to form more stable synapses with target cells than do their $CD103^-$ counterparts, thus resulting in efficient killing of tumor cells.[50] We detected significantly higher percentages of both intratumor $CD69^+CD103^-CD8^+$ and $CD69^-CD103^+CD8^+$ T_{RM} cells. In general, $CD69^+$ T_{RM} cells isolated from the tumor display a significantly strong expression of PD-1, an observation already made for other tumor entities.[53] Renal tumor–derived $CD69^+$ T_{RM} cells are characterized by a significant induction of granzyme B, whereas other cytokines are not affected (IFNγ) or strongly downregulated (*e.g.*, IL-2, IL-17). In principle, the formation of T_{RM} cells in the kidney is promoted by TGFβ, whereas their long-term maintenance was described to be IL-15 dependent.[54,55] Common T_{RM} cell transcriptional programs are active in kidney T_{RM} cells as deficiency in transcription factor Blimp-1, Hobit, or Runx3 leads to impaired maintenance of kidney T_{RM} cells.[55,56] Recently, the transcription factor TOX has been shown to be strongly expressed in dysfunctional tumor-derived T cells, preventing them from overstimulation and activation-induced cell death in settings of chronic antigen stimulation, including cancer.[57] The identification of $TOX^+PD\text{-}1^+CD69^+$ T_{RM} cells in kidney tumors suggests an activated but not exhaustive phenotype as these cells are still producing cytokines, although to a lesser extent. Nonetheless, compared with patients without metastases, patients diagnosed with metastases display impaired functional intratumoral $CD8^+$ T_{RM} cells, suggesting that at least a loss of T_{RM} function is indicative of tumor spreading.

Although the presence of virus-specific $CD8^+$ T cells in human lung and colorectal cancer has been demonstrated,[58] the relevance of antigens for T_{RM} cell formation in the kidney has not yet been determined. Only one study reports BKV-specific $CD69^+CD103^+$ T_{RM} cells in BKVN-affected kidney allografts lacking signs of effector differentiation.[59] Another

differences were tested with the two-tailed paired *t* test or the Wilcoxon signed ranks test. (D) PD-1 expression on $CD69^+CD103^+CD4^+$ and $CD8^+$ T cells ($n=16$). Statistically significant differences were tested with the paired *t* test.

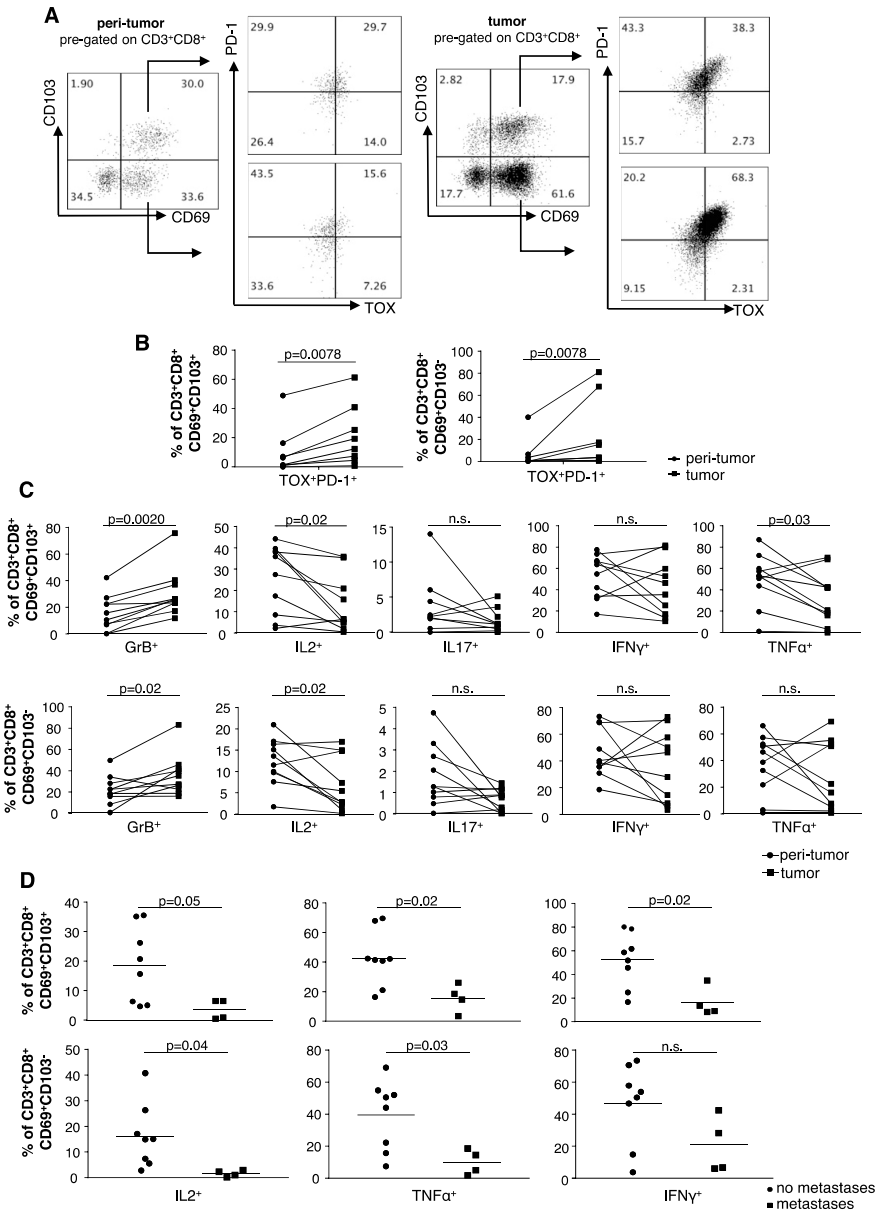

Figure 7. Tumor-derived renal T_{RM} cells express the exhaustion marker TOX and are functionally impaired. (A) Exemplary flow cytometry dot plots of PD-1$^+$TOX$^+$ CD8$^+$CD69$^+$CD103$^+$ and CD8$^+$CD69$^+$CD103$^-$ T_{RM} cells in peritumor and tumor tissue. (B) Identification of PD-1$^+$TOX$^+$ CD8$^+$CD69$^+$CD103$^+$ and CD8$^+$CD69$^+$CD103$^-$ T_{RM} cells (n=8) in renal peritumor and tumor tissue. (C) Cytokine effector profile (granzyme B [GrB], IFNγ, IL-2, IL-17, and TNFα) of CD8$^+$CD69$^+$CD103$^+$ and CD8$^+$CD69$^+$CD103$^-$ T cells (n=10). Statistically significant differences were tested with the two-tailed paired t test or the Wilcoxon signed ranks test. (D) Patients were divided into two groups according to presence of metastases (diagnosed before nephrectomy). The cytokine profile (IL-2, TNFα, and IFNγ) of tumor-derived CD8$^+$ CD69$^+$CD103$^+$ and CD69$^+$CD103$^-$ T_{RM} cells was compared between the groups (no metastases, n=8; metastases, n=4). Statistically significant differences were tested with the two-tailed unpaired t test or the Mann–Whitney test and are presented as mean values ± SD.

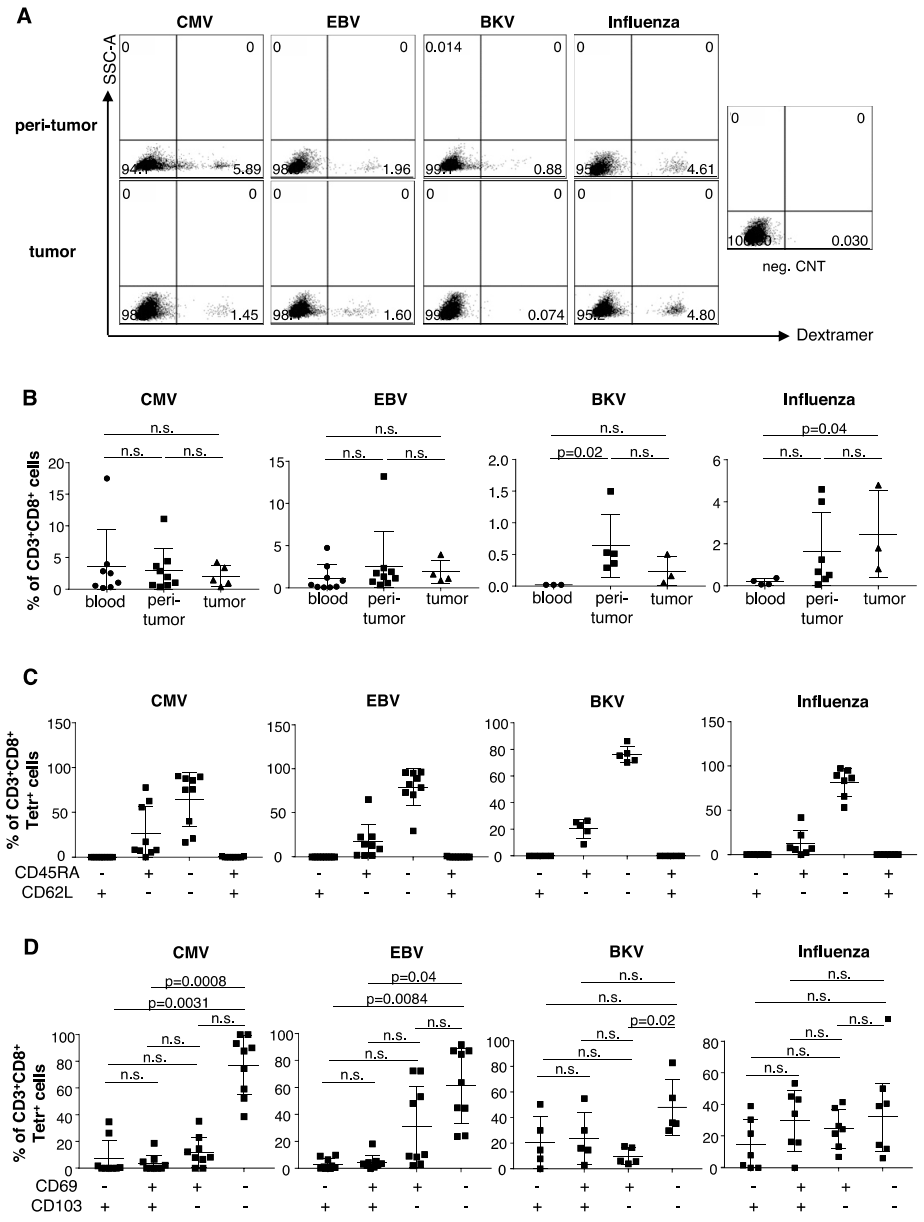

Figure 8. Kidney-derived $CD8^+$ T cells possess a memory phenotype for recall antigens. (A) Representative FACS dot plots for HLA-A2 multimer staining specific for CMV, EBV, BKV, and influenza virus on peritumor and tumor tissue-derived T cells. Control multimer (CNT) was used for gate settings. neg., negative. (B) Detection of antigen-specific $CD3^+CD8^+$ T cells in peripheral blood, renal peritumor tissue, and tumor tissue (CMV: b: $n=8$, p-t: $n=9$, t: $n=5$; EBV: b: $n=9$, p-t: $n=9$, t: $n=4$; BKV: b: $n=3$, p-t: $n=5$, t: $n=3$; and influenza: b: $n=4$, p-t: $n=7$, t: $n=3$). Statistically significant differences were tested with the Kruskal–Wallis test. (C) Antigen-specific $CD3^+CD8^+$ T cells are mainly effector memory T cells in the peritumor tissue (CMV, $n=9$; EBV, $n=9$; BKV, $n=5$; and influenza, $n=7$). (D) $CD69^-CD103^-CD8^+$ T cells constitute the majority of antigen-specific T cells in peritumor renal tissue (CMV, $n=9$; EBV, $n=9$; BKV, $n=5$; and influenza, $n=7$). Statistically significant differences were tested with one-way ANOVA or the Friedman test and are presented as mean values ± SD. b, blood; p-t, peritumor; t, tumor.

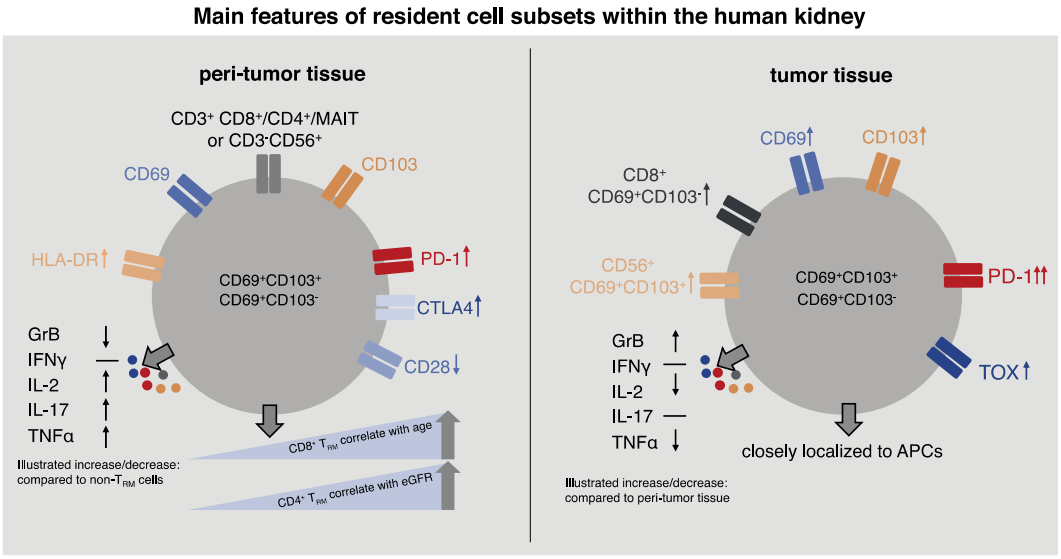

Figure 9. Renal $CD8^+$ TRM cells display an inflammatory phenotype reflected by enhanced IL-2, IL-17 and TNFa expression. Whereas $CD8^+$ TRM cells correlate with increasing age, $CD4^+$ TRM cells correlate with kidney function. Both, mucosa-associated invariant T (MAIT) and Natural Killer (NK) cells expressing CD69 and CD103 were identified in the kidney, with the latter being enriched in renal tumors. Tumor-derived $CD8^+$ TRM cells express high levels of PD-1 and the transcription factor TOX and could be identified in close proximity to APCs. APC, antigen-presenting cell; GrB, granzyme B.

experimental study demonstrates that kidney T_{RM} cells bind to T cell receptors with a 20-fold higher affinity than do splenic memory T cells, suggesting that local antigens may facilitate kidney T_{RM} cell induction.[60] Our data document the presence of T_{RM} cells in human kidneys specific for EBV, CMV, and BKV as well for influenza. Interestingly, the majority of antigen-specific T cells for persistent viruses are negative for CD69 and CD103 expression, suggesting that the lack of both markers enables them to migrate easily as a consequence of ubiquitous virus infection, thus not being organ specific. Alternatively, although T_{RM} cells are identified as effector cells in many tissues and in the kidney, they can maintain their differentiation state in the absence of persistent antigens.[61,62] The role of antigen-specific T_{RM} residing in tumors still remains to be elucidated, but recent research suggests that these T cells can be specifically reactivated via local delivery of adjuvant-free viral peptide for reactivation and tumor targeting.[63]

Although T_{RM} cells are suggested to promote favorable immunity, it needs to be considered that the majority of aspects of T_{RM} cell generation, maintenance, or functionality are derived from infectious mouse models, and data on human T_{RM} cells are limited. We present here a comprehensive overview of T_{RM} cells identified in the human kidney with respect to tumor pathology and viral infections, which is summarized in Figure 9. However, we are aware that our study has several limitations. First, our patient cohort was assembled following the diagnosis of a renal tumor and thus, displayed an advanced age (mean age 63 years) as there was understandably no opportunity to analyze healthy kidneys of a younger age. Second, a lack of sufficient cell numbers prevented us from analyzing the effector profile of antigen-specific T_{RM} and TOX^+ T_{RM}. Third, renal cancer is a slow-growing cancer entity; therefore, we were not able to correlate our findings with long-term outcomes. Despite these limitations, our study reveals a number of novel aspects of tissue-resident lymphocytes in the kidney, and their exact role and relevance (*e.g.*, for CKDs, tumor pathology, or at least transplantation) need to be comprehensively investigated in continuing studies.

DISCLOSURES

All authors have nothing to disclose.

FUNDING

This work was funded by Deutsche Forschungsgemeinschaft grant DFG-Ko2270/4-1 (to K. Kotsch) and a scholarship from Sonnenfeldstiftung (to A.H. Ruhm).

ACKNOWLEDGMENTS

T. Dornieden, K. Kotsch, and A. Sattler were responsible for experiment design and acquisition, analysis, and interpretation of data; Y.S. Bergmann, S. Boral, T. Dornieden, F. Friedersdorff, A.E. Hauser, A.A. Kühl, A. Pascual-

Reguant, A.H. Ruhm, A. Sattler, L.G. Thiel, and L.M.L. Thole performed experiments and data analysis; T. Dornieden and K. Kotsch were responsible for writing the manuscript; and all authors reviewed the manuscript before submission and agreed to be accountable for all aspects of the work.

SUPPLEMENTAL MATERIAL

This article contains the following supplemental material online at http://jasn.asnjournals.org/lookup/suppl/doi:10.1681/ASN.2020101528/-/DCSupplemental.

Supplemental Table 1. Antibodies for phenotypic analysis.

Supplemental Table 2. Multimers.

Supplemental Table 3. Antibodies for phenotypic analysis of antigen-specific $CD8^+$ T cells.

Supplemental Table 4. Antibodies for functional analysis.

Supplemental Table 5. Antibodies for MELC histology.

Supplemental Table 6. Used statistics.

Supplemental Figure 1. Gating strategy.

Supplemental Figure 2. Panel overview of a 19-marker MELC run in human kidneys shows different degrees of T cell infiltration.

Supplemental Figure 3. Quantification of PBMC- and tissue-derived T cell subsets.

Supplemental Figure 4. viSNE and FlowSOM analysis of FACS data.

Supplemental Figure 5. CD49a expression and related cytokine profiles.

Supplemental Figure 6. KLRG1 and CD103 expression of $CD8^+$ and $CD4^+$ T cells.

Supplemental Figure 7. Ex vivo proliferation of $CD8^+$ and $CD4^+$ T_{RM} cell subsets.

Supplemental Figure 8. Patients were divided into two groups according to the calculated mean age of 63 years (n=35).

Supplemental Figure 9. Cluster analysis of MELC data from pooled tumor and patient-matched peritumor samples (n=4).

Supplemental Figure 10. Both $CD69^+CD103^-CD4^+$ and $CD69^+CD103^-CD8^+$ T cells form clusters, whereas $CD69^+CD103^+$ tissue-resident populations tend to be rather scattered across the tumor tissue.

Supplemental Figure 11. Overlays of MELC fluorescent images depicting endothelial cells and monocyte/macrophages together with color-coded dots that represent the centroid spatial coordinates of the three tissue-resident cell clusters identified in Figure 5A for n=3 peritumor/tumor-matched patient samples.

Supplemental Figure 12. Tissue residency of NK cells in peritumor and tumor kidney tissue.

Supplemental Figure 13. viSNE and FlowSOM analysis of FACS data for peritumor and tumor samples.

Supplemental Figure 14. CD49a expression of $CD8^+$ T_{RM} cell subsets.

REFERENCES

1. Masopust D, Soerens AG: Tissue-resident T cells and other resident leukocytes. *Annu Rev Immunol* 37: 521–546, 2019
2. Park SL, Gebhardt T, Mackay LK: Tissue-resident memory T cells in cancer immunosurveillance. *Trends Immunol* 40: 735–747, 2019
3. Fan X, Rudensky AY: Hallmarks of tissue-resident lymphocytes. *Cell* 164: 1198–1211, 2016
4. Clark RA: Skin-resident T cells: The ups and downs of on site immunity. *J Invest Dermatol* 130: 362–370, 2010
5. Purwar R, Campbell J, Murphy G, Richards WG, Clark RA, Kupper TS: Resident memory T cells (T(RM)) are abundant in human lung: Diversity, function, and antigen specificity. *PLoS One* 6: e16245, 2011
6. Smolders J, Heutinck KM, Fransen NL, Remmerswaal EBM, Hombrink P, Ten Berge IJM, et al.: Tissue-resident memory T cells populate the human brain. *Nat Commun* 9: 4593, 2018
7. Hombrink P, Helbig C, Backer RA, Piet B, Oja AE, Stark R, et al.: Programs for the persistence, vigilance and control of human $CD8^+$ lung-resident memory T cells. *Nat Immunol* 17: 1467–1478, 2016
8. Fernandez-Ruiz D, Ng WY, Holz LE, Ma JZ, Zaid A, Wong YC, et al.: Liver-resident memory CD8+ T cells form a front-line defense against malaria liver-stage infection. *Immunity* 45: 889–902, 2016
9. Gordon CL, Miron M, Thome JJ, Matsuoka N, Weiner J, Rak MA, et al.: Tissue reservoirs of antiviral T cell immunity in persistent human CMV infection. *J Exp Med* 214: 651–667, 2017
10. Wu T, Hu Y, Lee YT, Bouchard KR, Benechet A, Khanna K, et al.: Lung-resident memory CD8 T cells (TRM) are indispensable for optimal cross-protection against pulmonary virus infection. *J Leukoc Biol* 95: 215–224, 2014
11. Ray SJ, Franki SN, Pierce RH, Dimitrova S, Koteliansky V, Sprague AG, et al.: The collagen binding alpha1beta1 integrin VLA-1 regulates CD8 T cell-mediated immune protection against heterologous influenza infection. *Immunity* 20: 167–179, 2004
12. de Leur K, Dieterich M, Hesselink DA, Corneth OBJ, Dor FJMF, de Graav GN, et al.: Characterization of donor and recipient CD8+ tissue-resident memory T cells in transplant nephrectomies. *Sci Rep* 9: 5984, 2019
13. Park JG, Na M, Kim MG, Park SH, Lee HJ, Kim DK, et al.: Immune cell composition in normal human kidneys. *Sci Rep* 10: 15678, 2020
14. Pascual-Reguant A, Köhler R, Mothes R, Bauherr S, Hernández DC, Uecker R, et al.: Multiplexed histology analyses for the phenotypic and spatial characterization of human innate lymphoid cells. *Nat Commun* 12: 1737, 2021
15. Holzwarth K, Köhler R, Philipsen L, Tokoyoda K, Ladyhina V, Wählby C, et al.: Multiplexed fluorescence microscopy reveals heterogeneity among stromal cells in mouse bone marrow sections. *Cytometry A* 93: 876–888, 2018
16. Schubert W, Bonnekoh B, Pommer AJ, Philipsen L, Böckelmann R, Malykh Y, et al.: Analyzing proteome topology and function by automated multidimensional fluorescence microscopy. *Nat Biotechnol* 24: 1270–1278, 2006
17. Pertuz S, Puig D, Garcia MA, Fusiello A: Generation of all-in-focus images by noise-robust selective fusion of limited depth-of-field images. *IEEE Trans Image Process* 22: 1242–1251, 2013
18. Abràmoff MD, Magalhães PJ, Ram SJ: Image processing with ImageJ. *J Biophotonics Int* 11: 36–42, 2004
19. Sternberg SR: Biomedical image processing. *Computer* 16: 22–34, 1983
20. Berg S, Kutra D, Kroeger T, Straehle CN, Kausler BX, Haubold C, et al.: ilastik: Interactive machine learning for (bio)image analysis. *Nat Methods* 16: 1226–1232, 2019
21. Carpenter AE, Jones TR, Lamprecht MR, Clarke C, Kang IH, Friman O, et al.: CellProfiler: Image analysis software for identifying and quantifying cell phenotypes. *Genome Biol* 7: R100, 2006
22. Schapiro D, Jackson HW, Raghuraman S, Fischer JR, Zanotelli VRT, Schulz D, et al.: histoCAT: Analysis of cell phenotypes and interactions in multiplex image cytometry data. *Nat Methods* 14: 873–876, 2017
23. Demšar J, Curk T, Erjavec A, Gorup C, Hocevar T, Milutinovic M, et al.: Orange: Data mining toolbox in python. *J Mach Learn Res* 14: 2349–2353, 2013
24. Van Gassen S, Callebaut B, Van Helden MJ, Lambrecht BN, Demeester P, Dhaene T, et al.: FlowSOM: Using self-organizing maps for visualization and interpretation of cytometry data. *Cytometry A* 87: 636–645, 2015
25. Victorino F, Sojka DK, Brodsky KS, McNamee EN, Masterson JC, Homann D, et al.: Tissue-resident NK cells mediate ischemic kidney injury and are not depleted by anti-asialo-GM1 antibody. *J Immunol* 195: 4973–4985, 2015
26. Davies B, Prier JE, Jones CM, Gebhardt T, Carbone FR, Mackay LK: Cutting edge: Tissue-resident memory T cells generated by multiple immunizations or localized deposition provide enhanced immunity. *J Immunol* 198: 2233–2237, 2017

27. Herndler-Brandstetter D, Ishigame H, Shinnakasu R, Plajer V, Stecher C, Zhao J, et al.: KLRG1+ effector CD8+ T cells lose KLRG1, differentiate into all memory T cell lineages, and convey enhanced protective immunity. *Immunity* 48: 716–729, 2018
28. Mackay LK, Rahimpour A, Ma JZ, Collins N, Stock AT, Hafon ML, et al.: The developmental pathway for CD103(+)CD8+ tissue-resident memory T cells of skin. *Nat Immunol* 14: 1294–1301, 2013
29. Szabo PA, Miron M, Farber DL: Location, location, location: Tissue resident memory T cells in mice and humans. *Sci Immunol* 4: eaas9673, 2019
30. Law BMP, Wilkinson R, Wang X, Kildey K, Giuliani K, Beagley KW, et al.: Human tissue-resident mucosal-associated invariant T (MAIT) cells in renal fibrosis and CKD. *J Am Soc Nephrol* 30: 1322–1335, 2019
31. Webb JR, Milne K, Watson P, Deleeuw RJ, Nelson BH: Tumor-infiltrating lymphocytes expressing the tissue resident memory marker CD103 are associated with increased survival in high-grade serous ovarian cancer. *Clin Cancer Res* 20: 434–444, 2014
32. Workel HH, Komdeur FL, Wouters MC, Plat A, Klip HG, Eggink FA, et al.: CD103 defines intraepithelial CD8+ PD1+ tumour-infiltrating lymphocytes of prognostic significance in endometrial adenocarcinoma. *Eur J Cancer* 60: 1–11, 2016
33. Xia A, Zhang Y, Xu J, Yin T, Lu X-J: T cell dysfunction in cancer immunity and immunotherapy. *Front Immunol* 10: 1719, 2019
34. Khan O, Giles JR, McDonald S, Manne S, Ngiow SF, Patel KP, et al.: TOX transcriptionally and epigenetically programs $CD8^+$ T cell exhaustion. *Nature* 571: 211–218, 2019
35. Wang X, He Q, Shen H, Xia A, Tian W, Yu W, et al.: TOX promotes the exhaustion of antitumor $CD8^+$ T cells by preventing PD1 degradation in hepatocellular carcinoma. *J Hepatol* 71: 731–741, 2019
36. Skon CN, Lee J-Y, Anderson KG, Masopust D, Hogquist KA, Jameson SC: Transcriptional downregulation of S1pr1 is required for the establishment of resident memory CD8+ T cells. *Nat Immunol* 14: 1285–1293, 2013
37. Takamura S, Yagi H, Hakata Y, Motozono C, McMaster SR, Masumoto T, et al.: Specific niches for lung-resident memory CD8+ T cells at the site of tissue regeneration enable CD69-independent maintenance. *J Exp Med* 213: 3057–3073, 2016
38. Walsh DA, Borges da Silva H, Beura LK, Peng C, Hamilton SE, Masopust D, et al.: The functional requirement for CD69 in establishment of resident memory CD8+ T cells varies with tissue location. *J Immunol* 203: 946–955, 2019
39. Steinert EM, Schenkel JM, Fraser KA, Beura LK, Manlove LS, Igyártó BZ, et al.: Quantifying memory CD8 T cells reveals regionalization of immunosurveillance. *Cell* 161: 737–749, 2015
40. Ma C, Mishra S, Demel EL, Liu Y, Zhang N: TGF-β controls the formation of kidney-resident T cells via promoting effector T cell extravasation. *J Immunol* 198: 749–756, 2017
41. Lo DJ, Weaver TA, Stempora L, Mehta AK, Ford ML, Larsen CP, et al.: Selective targeting of human alloresponsive CD8+ effector memory T cells based on CD2 expression. *Am J Transplant* 11: 22–33, 2011
42. Stelma F, de Niet A, Sinnige MJ, van Dort KA, van Gisbergen KPJM, Verheij J, et al.: Human intrahepatic CD69 + CD8+ T cells have a tissue resident memory T cell phenotype with reduced cytolytic capacity. *Sci Rep* 7: 6172, 2017
43. Richter M, Ray SJ, Chapman TJ, Austin SJ, Rebhahn J, Mosmann TR, et al.: Collagen distribution and expression of collagen-binding alpha1beta1 (VLA-1) and alpha2beta1 (VLA-2) integrins on CD4 and CD8 T cells during influenza infection. *J Immunol* 178: 4506–4516, 2007
44. Broadley I, Pera A, Morrow G, Davies KA, Kern F: Expansions of cytotoxic CD4+CD28- T cells drive excess cardiovascular mortality in rheumatoid arthritis and other chronic inflammatory conditions and are triggered by CMV infection. *Front Immunol* 8: 195, 2017
45. Shabir S, Smith H, Kaul B, Pachnio A, Jham S, Kuravi S, et al.: Cytomegalovirus-associated CD4(+) CD28(null) cells in NKG2D-dependent glomerular endothelial injury and kidney allograft dysfunction. *Am J Transplant* 16: 1113–1128, 2016
46. Dumitriu IE, Baruah P, Finlayson CJ, Loftus IM, Antunes RF, Lim P, et al.: High levels of costimulatory receptors OX40 and 4-1BB characterize CD4+CD28null T cells in patients with acute coronary syndrome. *Circ Res* 110: 857–869, 2012
47. Pangrazzi L, Weinberger B: T cells, aging and senescence. *Exp Gerontol* 134: 110887, 2020
48. Melsen JE, Lugthart G, Lankester AC, Schilham MW: Human circulating and tissue-resident CD56(bright) natural killer cell populations. *Front Immunol* 7: 262, 2016
49. Lugthart G, Melsen JE, Vervat C, van Ostaijen-Ten Dam MM, Corver WE, Roelen DL, et al.: Human lymphoid tissues harbor a distinct CD69+CXCR6+ NK cell population. *J Immunol* 197: 78–84, 2016
50. Djenidi F, Adam J, Goubar A, Durgeau A, Meurice G, de Montpréville V, et al.: CD8+CD103+ tumor-infiltrating lymphocytes are tumor-specific tissue-resident memory T cells and a prognostic factor for survival in lung cancer patients. *J Immunol* 194: 3475–3486, 2015
51. Ganesan AP, Clarke J, Wood O, Garrido-Martin EM, Chee SJ, Mellows T, et al.: Tissue-resident memory features are linked to the magnitude of cytotoxic T cell responses in human lung cancer. *Nat Immunol* 18: 940–950, 2017
52. Wang ZQ, Milne K, Derocher H, Webb JR, Nelson BH, Watson PH: CD103 and intratumoral immune response in breast cancer. *Clin Cancer Res* 22: 6290–6297, 2016
53. Gros A, Robbins PF, Yao X, Li YF, Turcotte S, Tran E, et al.: PD-1 identifies the patient-specific $CD8^+$ tumor-reactive repertoire infiltrating human tumors. *J Clin Invest* 124: 2246–2259, 2014
54. Schenkel JM, Fraser KA, Casey KA, Beura LK, Pauken KE, Vezys V, et al.: IL-15-independent maintenance of tissue-resident and boosted effector memory CD8 T cells. *J Immunol* 196: 3920–3926, 2016
55. Mackay LK, Wynne-Jones E, Freestone D, Pellicci DG, Mielke LA, Newman DM, et al.: T-box transcription factors combine with the cytokines TGF-beta and IL-15 to control tissue-resident memory T cell fate. *Immunity* 43: 1101–1111, 2015
56. Milner JJ, Toma C, Yu B, Zhang K, Omilusik K, Phan AT, et al.: Runx3 programs $CD8^+$ T cell residency in non-lymphoid tissues and tumours. *Nature* 552: 253–257, 2017
57. Scott AC, Dündar F, Zumbo P, Chandran SS, Klebanoff CA, Shakiba M, et al.: TOX is a critical regulator of tumour-specific T cell differentiation. *Nature* 571: 270–274, 2019
58. Simoni Y, Becht E, Fehlings M, Loh CY, Koo SL, Teng KWW, et al.: Bystander $CD8^+$ T cells are abundant and phenotypically distinct in human tumour infiltrates. *Nature* 557: 575–579, 2018
59. van Aalderen MC, Remmerswaal EBM, Heutinck KM, Ten Brinke A, Feltkamp MCW, van der Weerd NC, et al.: Clinically relevant reactivation of polyomavirus BK (BKPyV) in HLA-A02-Positive renal transplant recipients is associated with impaired effector-memory differentiation of BKPyV-specific CD8+ T cells. *PLoS Pathog* 12: e1005903, 2016
60. Frost EL, Kersh AE, Evavold BD, Lukacher AE: Cutting edge: resident memory CD8 T cells express high-affinity TCRs. *J Immunol* 195: 3520–3524, 2015
61. Casey KA, Fraser KA, Schenkel JM, Moran A, Abt MC, Beura LK, et al.: Antigen-independent differentiation and maintenance of effector-like resident memory T cells in tissues. *J Immunol* 188: 4866–4875, 2012
62. Mackay LK, Minnich M, Kragten NA, Liao Y, Nota B, Seillet C, et al.: Hobit and Blimp1 instruct a universal transcriptional program of tissue residency in lymphocytes. *Science* 352: 459–463, 2016
63. Rosato PC, Wijeyesinghe S, Stolley JM, Nelson CE, Davis RL, Manlove LS, et al.: Virus-specific memory T cells populate tumors and can be repurposed for tumor immunotherapy. *Nat Commun* 10: 567, 2019

Auszug aus der Journal Summary List

Publikation im Journal „American Journal of Transplantation“

Journal Data Filtered By: **Selected JCR Year: 2018** Selected Editions: SCIE,SSCI
Selected Categories: **“TRANSPLANTATION”** Selected Category Scheme: WoS
Gesamtanzahl: 25 Journale

Rank	Full Journal Title	Total Cites	Journal Impact Factor	Eigenfactor Score
1	JOURNAL OF HEART AND LUNG TRANSPLANTATION	12,436	8.578	0.027310
2	AMERICAN JOURNAL OF TRANSPLANTATION	24,285	7.163	0.050970
3	BONE MARROW TRANSPLANTATION	12,031	4.674	0.020710
4	TRANSPLANTATION	24,971	4.593	0.032780
5	NEPHROLOGY DIALYSIS TRANSPLANTATION	25,423	4.198	0.029210
6	LIVER TRANSPLANTATION	10,513	4.159	0.013840
7	BIOLOGY OF BLOOD AND MARROW TRANSPLANTATION	10,501	3.599	0.023950
8	TRANSPLANT INTERNATIONAL	4,868	3.526	0.009180
9	XENOTRANSPLANTATION	1,689	3.484	0.002390
10	CELL TRANSPLANTATION	5,941	3.477	0.009210

Mucosal associated invariant T cells are differentially impaired in tolerant and immunosuppressed liver transplant recipients, Sattler and Thiel et al., Am. J. Transplant., 2021; 21: 87-102

Check for updates

Received: 11 February 2020 | Revised: 12 May 2020 | Accepted: 26 May 2020

DOI: 10.1111/ajt.16122

ORIGINAL ARTICLE

AJT

Mucosal associated invariant T cells are differentially impaired in tolerant and immunosuppressed liver transplant recipients

Arne Sattler[1]* | Lion G. Thiel[1]* | Annkathrin H. Ruhm[1] | Yasmin Bergmann[1] | Theresa Dornieden[1] | Mira Choi[2] | Fabian Halleck[2] | Frank Friedersdorff[3] | Dennis Eurich[4] | Katja Kotsch[1]

[1]Department for General, Visceral and Vascular Surgery, Charité–Universitätsmedizin Berlin, Corporate Member of Freie Universität Berlin, Humboldt-Universität zu Berlin and Berlin Institute of Health, Berlin, Germany

[2]Department for Nephrology and Internal Intensive Care, Charité–Universitätsmedizin Berlin, Corporate Member of Freie Universität Berlin, Humboldt-Universität zu Berlin and Berlin Institute of Health, Berlin, Germany

[3]Department for Urology, Charité–Universitätsmedizin Berlin, Corporate Member of Freie Universität Berlin, Humboldt-Universität zu Berlin and Berlin Institute of Health, Berlin, Germany

[4]Department for Surgery, Charité–Universitätsmedizin Berlin, Corporate Member of Freie Universität Berlin, Humboldt-Universität zu Berlin and Berlin Institute of Health, Berlin, Germany

Correspondence
Arne Sattler
Email: arne.sattler@charite.de

Funding information
Bundesministerin für Wirtschaft und Energie, Zentrales Innovationsprogramm Mittelstand, Grant/Award Number: ZF4245603AJ7; Sonnenfeldstiftung, Grant/Award Number: Personal student award to A.H.R.

Mucosal associated invariant T (MAIT-) cells represent a semi-invariant T cell population responsive to microbial vitamin B metabolite and innate cytokine stimulation, executing border tissue protection and particularly contributing to human liver immunity. The impact of immunosuppressants on MAIT cell biology alone and in context with solid organ transplantation has not been thoroughly examined. Here, we demonstrate that in vitro cytokine activation of peripheral MAIT cells from healthy individuals was impaired by glucocorticoids, whereas antigen-specific stimulation was additionally sensitive to calcineurin inhibitors. In liver transplant (LTx) recipients, significant depletion of peripheral MAIT cells was observed that was largely independent of the type and dosage of immunosuppression, equally applied to tolerant patients, and was reproducible in kidney transplant recipients. However, MAIT cells from tolerant LTx patients exhibited a markedly diminished ex vivo activation signature, associated with individual regain of functional competence toward antigenic and cytokine stimulation. Still, MAIT cells from tolerant and treated liver recipients exhibited high levels of PD1, accompanied by functional impairment particularly toward bacterial stimulation that also affected polyfunctionality. Our data suggest interlinked effects of primary liver pathology and immunosuppressive treatment on overall MAIT cell fitness after transplantation and propose their monitoring in context with tolerance induction protocols.

KEYWORDS
basic (laboratory) research/science, flow cytometry, immunobiology, immunosuppressant, immunosuppression/immune modulation, liver transplantation/hepatology, lymphocyte biology: activation, T cell biology, tolerance, translational research/science

Abbreviations: CyA or C, cyclosporine A; GranB, granzyme B; HC, healthy control(s); IS, immunosuppression; ISD, immunosuppressive drug; KTx, kidney transplant; LTx, liver transplant; MAIT cell, mucosal associated invariant T cell; MPA or M, mycophenolic acid; Pred or P, prednisolone; Tac or T, tacrolimus.

*These authors contributed equally.

This is an open access article under the terms of the Creative Commons Attribution-NonCommercial-NoDerivs License, which permits use and distribution in any medium, provided the original work is properly cited, the use is non-commercial and no modifications or adaptations are made.
© 2020 The Authors. American Journal of Transplantation published by Wiley Periodicals LLC on behalf of The American Society of Transplantation and the American Society of Transplant Surgeons

1 | INTRODUCTION

Mucosal-associated invariant T (MAIT) cells constitute an innate-like T cell subset in mammals[1] that is gaining increasing attention because of its unconventional antigen specificity[2] and an emerging role in host protection[3] and tissue repair.[4] MAIT cells are uniquely identified based on coexpression of a semi-invariant T cell receptor (TCR Vα7.2-Jα33 in humans[5]) along with the C-type lectin CD161 or interleukin 18 receptor alpha;[6] they are restricted by the HLA-Ib major histocompatibility complex (MHC)-related protein I (MR1) presenting vitamin B metabolites produced by a multitude of microbes and fungi that employ the riboflavin synthesis pathway.[2] Accumulating data, including our own,[7,8] indicate that alternative activation modes via inflammatory cytokines exist, positioning MAIT cells in between innate and adaptive immunity. Apart from their abundance in peripheral blood[1] and at mucosal surfaces such as in the intestine[9] or lung,[10] MAIT cells account for up to 45% of intrahepatic T cells[6,11,12] where they likely contribute to an intestine-downstream firewall protecting bile ducts and sinusoids.[13] Several studies have reported a disturbed MAIT cell biology in liver diseases; as a common motif, MAIT cells are significantly depleted from the periphery in autoimmune hepatitis, primary biliary cholangitis, alcoholic liver disease, or chronic hepatitis C, a phenomenon being associated with changes in their functional repertoire.[14-17] So far, it has not been addressed whether MAIT cell homeostasis is restored in transplanted individuals and how diverse immunosuppressive regimens affect its reconstitution. Based on prominent expression of the multidrug resistance protein 1, MAIT cells are protected from xenotoxic stress, for example, induced by common cytostatic therapy.[6] With respect to immunosuppressive agents, however, there is only limited information on how these drugs affect MAIT cell effector functions in vitro and in vivo.

Given their emerging role in host protection, we studied peripheral MAIT cell responses toward bacterial and innate cytokine stimuli in the presence of common immunosuppressive medication in healthy individuals in vitro. Furthermore, we comprehensively extended our analysis to the examination of peripheral blood derived MAIT cell frequencies, activation state, and effector functions in immunosuppressed and tolerant liver transplant recipients ex vivo. Although not exactly reflecting intra-organ biology, our choice of peripheral MAIT cell analysis overcomes experimental limitations imposed by biopsy material, enables repeated sampling, and allows direct comparison with the aforementioned studies on liver diseases. Our data pave the way toward understanding how immunosuppressive therapy and/or the postorgan transplantation state per se affects MAIT cell biology—with possible implications for immunological competence of patients at risk of opportunistic infections.

2 | MATERIAL AND METHODS

2.1 | Study approval

The study protocol was approved by the ethics committee of the Charité-Universitätsmedizin Berlin (No. EA2/028/13, EA2/035/16 and EA4/127/17) and carried out in compliance with its guidelines. All subjects gave written informed consent in accordance with the Declaration of Helsinki.

2.2 | Study participants

Details of individuals enrolled are summarized in Tables 1-3. Liver transplant (LTx) recipients initially diagnosed with hepatitis C virus (HCV) infection did not show viral reactivation at least within 3 years prior to the study. For some analyses, LTx patients treated with immunosuppression (IS) drugs were grouped according to drug levels. Group 1 included patients with serum levels of tacrolimus (Tac) < 3 ng/mL or cyclosporine A (CyA) < 50 ng/mL ± up to 500 mg mycophenolate mofetil (MMF) (1-0-1), Group 2 with Tac 3-5 ng/mL or CyA 50-100 ng/mL ± up to 500 mg MMF (1-0-1), Group 3 with Tac > 5 ng/mL or CyA > 100 ng/mL ± up to 500 mg MMF (1-0-1).

2.3 | Cell isolation

Peripheral blood was collected from liver and kidney transplanted individuals and from healthy controls; peripheral blood mononuclear cells (PBMC) were isolated by Ficoll-Paque™ density gradient centrifugation and freshly analyzed.

2.4 | Stimulation conditions

PMBC were cultured in RPMI1640 media containing 0.3 mg/mL glutamine, 100 U/mL penicillin, 0.1 mg/mL streptomycin, and 10% human AB serum (all Biochrom, Cambridge, UK). In all functional assays, cells were stimulated for 22 hours at 37°C. For cytokine stimulation, a combination of interleukin-12 (IL-12), IL-15 (5 ng/mL each, Miltenyi Biotec, Bergisch Gladbach, Germany), IL-18 (5 ng/mL, R&D, Minneapolis, MN), and TL1A (10 ng/mL, R&D) was used after determining optimal concentrations. Brefeldin A (BrefA, Sigma-Aldrich, St. Louis, MO) was present for the last 4 hours. Bacterial stimulation was performed with formalin-fixed *E. coli* (lab strain DH5α) at a pretitrated multiplicity of infection of 30 in the presence of anti-CD28 (1 μg/mL, 28.2, Biolegend, San Diego, CA) for costimulation. Specificity of bacterial stimulation was controlled by adding anti-MR1 (10 μg/mL, 26.5, Biolegend) or isotype control prior to bacterial stimulation. BrefA and Monensin (GolgiStop™, BD Biosciences, San Jose, CA) were added after 4 hours, enabling optimal CD107a and cytokine staining. In some experiments, PBMC were preincubated with immediate posttransplant consensus concentrations (based on Refs. 18 and 19-21 and according to local hospital guidelines) of tacrolimus (10 ng/mL, Astellas Pharma, Tokyo, Japan, Prograf®), cyclosporin A (120 ng/mL, Cayman Chemical, Ann Arbor, MI), mycophenolic acid (2.7 μg/mL, Sigma-Aldrich), or prednisolone (Prednisolut®, 0.57 μg/mL, Mibe, Sandersdorf-Brehna, Germany) for 2 hours and subsequently stimulated as described previously. Drug concentrations were titrated as indicated.

TABLE 1 Characteristics of LTx patients and healthy donors

Variable	All patients (n = 58)	Tolerant patients (n = 8)	Healthy donors (n = 19)
Age (y ± SD)[a]	61.78 (11.75)	63.8 (10.3)	61.26 (6.51)
Gender (females)[b]	21/58 (36.2%)	1/8 (12.5%)	10/19 (52.6%)
Time since transplantation (y ± SD)[a]	12.59 (7.2)	17.3 (5.5)	
Tolerant group (IS-free)[b]		8/58 (13.8%)	
Tolerant group: mean IS-free time[c]		36.8 (75.6)	
IS group 1[b,d]	20/58 (34.5%)		
IS group 2[b,d]	19/58 (32.8%)		
IS group 3[b,d]	11/58 (19%)		
IS medication[b]			
Tacrolimus + mycophenolate mofetil	19/58 (32.8%)		
Tacrolimus	16/58 (27.6%)		
None	8/58 (13.8%)		
Mycophenolate mofetil	6/58 (10.3%)		
Cyclosporin A + mycophenolate mofetil	5/58 (8.6%)		
Cyclosporin A	4/58 (6.9%)		
Primary disease[b]			
Nutritive-toxic cirrhosis	13/58 (22.4%)		
Hepatitis C	11/58 (19%)	5 (62.5%)	
Hepatocellular carcinoma	9/58 (15.5%)	1 (12.5%)	
Hepatitis B	9/58 (15.5%)	1 (12.5%)	
Primary biliary cholangitis	4/58 (6.9%)		
Cryptogenic cirrhosis	3/58 (5.2%)	1 (12.5%)	
Alpha-1 antitrypsin deficiency	2/58 (3.4%)		
Primary sclerosing cholangitis	2/58 (3.4%)		
Budd–Chiari syndrome	1/58 (1.7%)		
Caroli syndrome	1/58 (1.7%)		
Chemotherapy-induced cirrhosis	1/58 (1.7%)		
Secondary biliary cirrhosis	1/58 (1.7%)		
Wilson's disease	1/58 (1.7%)		

Abbreviations: IS, immunosuppression; LTx, liver transplant.

[a]Mean + SD.

[b]Count (%).

[c]Months + SD.

[d]For characterization of IS groups, see materials and methods section.

2.5 | Flow cytometric analysis

For surface stainings, antibodies against CD3 (SK7, Biolegend), CD4 (SK3, Becton Dickinson), CD8 (SK1, Ebioscience, San Diego, CA), CD8β (SIDI8BEE, eBioscience), CD25 (BC96, Biolegend), CD27 (M-T271, Biolegend), CD38 (HIT2, BD), CD45RA (HI100, Biolegend), CD56 (5.1H11, Biolegend), CD69 (FN50, Biolegend), CD103 (Ber-ACT8, Biolegend), CD161 (HP-3G10, Biolegend), TCRVα7.2 (3C10, Biolegend), IL-18Rα (H44, Biolegend), CCR7 (3D12, BD), KLRG1 (SA231A2, Biolegend), NKG2D (1D11, Biolegend), HLA-DR (L243, Biolegend), and PD1 (EH12.1, BD) were used. Unwanted cells were excluded via a "dump channel" containing $CD14^+$ (M5E2, Biolegend), $CD19^+$ (HIB19, Biolegend) and dead cells (fixable live/dead, Biolegend). The basic gating

TABLE 2 Characteristics of IS-free LTx patients

Patient number	01	02[a]	03[a]	04	05	06	07	08[a]
Age (y)	53	61	75	46	74	64	72	65
Gender (m/f)	m	m	m	f	m	m	m	m
Time since Tx (y)	19	9	14	26	12	22	22	14
IS-free time (mo)	19	6	9	223	9	21	3	4
Primary disease	HCV	Crypt.	HCV	HBV	HCV	HCV	HCC	HCV
Biopsy	Yes	Yes	Yes	Yes	No	Yes	No	No
Rejection	No	No	No	No	n.a.	No	n.a.	n.a.
Liver function[b]								
gGT (U/L)	211	300	52	27	20	17	14	28
AP (U/L)	158	135	56	86	75	62	48	73
Total bilirubin (mg/dL)	0.7	0.8	1.1	1.11	0.63	0.6	1.61	0.15
ALT/AST (U/L)	36/43	38/48	30/31	23/31	18/28	13/21	34/33	23/20
INR	1.03	0.92	1.14	1.35	0.99	1.23	1.12	n.d.

Abbreviations: ALT/AST, aspartate transaminase/alanine transaminase; AP, alkaline phosphatase; gGT, Gamma-glutamyltransferase; HBV, hepatitis B virus; HCV, hepatitis C virus; INR, international normalized ratio; IS, immunosuppression; LTx, liver transplant; n.a., not applicable; n.d. not determined.

[a]Weaned during the study.

[b]At time of cellular analysis.

strategy to identify MAIT cells and other subsets within PBMC is shown in Figure S1A.

After stimulation, cells were fixed in FACS™ Lysing Solution (BD), permeabilized with FACS™ Perm II Solution (BD), and intracellularly stained with anti-tumor necrosis factor alpha (anti-TNFα) (MAb11, Biolegend), anti-interferon gamma (anti-IFNγ) (4SB3, Ebioscience), anti-granzymeB (GB11, BD), and anti-IL-17 (BL168, Biolegend). Where indicated, granzymeB or activated Caspase 3 (C92-605, BD) were intracellularly assessed ex vivo. For assessing expression of FoxP3 (150D, Biolegend), CTLA-4 (BNI3, Biolegend), and/or Ki67 (B56, BD), cells were fixed and permeabilized using the Foxp3 staining buffer set (Ebioscience). Cells were analyzed on a FACS™ Fortessa X20 (BD).

2.6 | Data analysis

FACS data were analyzed with FlowJo 10 (BD); polyfunctionality was assessed via Boolean gating. Statistical analysis and graph creation were conducted using GraphPad Prism 7.0 (GraphPad, La Jolla, CA). The Kolmogorov-Smirnov test was used to evaluate the distribution of each parameter. Depending on Gaussian distribution, analysis of variance (ANOVA) or Kruskal-Wallis test (with Dunn post hoc) was chosen for multiple comparisons; for 2-group comparisons with unpaired samples, *t* test with Welch's correction or Mann-Whitney test was used. For analysis of paired data (eg, titrations), paired *t* test or Wilcoxon matched-pairs signed rank test was performed depending on data distribution. In all tests, a value of $P < .05$ was considered significant with $^{*}P \le .05$, $^{**}P \le .01$, $^{***}P \le .001$, and $^{****}P \le .0001$.

3 | RESULTS

3.1 | Impairment of cytokine-induced MAIT cell functions by immunosuppressive drugs in vitro

To address the functional impact of immunosuppressive agents used in clinical routine after solid organ transplantation on human MAIT cells, PBMC from healthy donors were preincubated with tacrolimus, cyclosporine A, mycophenolic acid, or prednisolone. Thereafter, cells were stimulated with pretitrated (data not shown) concentrations of IL-12, IL-15, IL-18, and TL1A, a cytokine combination robustly inducing the effector molecules TNFα, IFNγ, and granzymeB in MAIT cells in a T cell receptor independent fashion.[7,8] Whereas prednisolone significantly inhibited TNFα and IFNγ secretion but did not reduce frequencies of MAIT cells producing the cytotoxic mediator granzymeB, none of the other drugs affected MAIT cell functionality (Figure 1A-D). Titration of immunosuppressive agents revealed that increasing concentrations by 10-fold further diminished $TNF\alpha^{+}$ MAIT cell frequencies significantly only in the presence of prednisolone (Figure S1B); higher concentrations of immunosuppressants did not show additional effects on frequencies of $IFN\gamma^{+}$ or $granzymeB^{+}$ cells (data not shown). Only prednisolone significantly affected multipotency of MAIT cells as mirrored by diminished portions of cells coexpressing all 3

TABLE 3 Characteristics of KTx patients

Variable	Patients (n = 23)
Age (y ± SD)[a]	58.57 (11.7)
Gender (females)[b]	8/23 (34.8%)
Time since transplantation (y ± SD)[a]	9.3 (5.0)
IS medication[b]	
Tacrolimus + mycophenolate mofetil + prednisolone	11/23 (47.8%)
Cyclosporin A + mycophenolate mofetil + prednisolone	8/23 (34.8%)
Tacrolimus + mycophenolate mofetil	2/23 (8.7%)
Tacrolimus + prednisolone	2/23 (8.7%)
Primary disease[b]	
Hypertensive nephropathy	5/23 (21.7%)
IgA nephropathy	3/23 (13%)
Glomerulonephritis	3/23 (13%)
Pyelonephritis	2/23 (8.7%)
Polycystic kidney disease	2/23 (8.7%)
Unknown	2/23 (8.7%)
Cystinosis	1/23 (4.3%)
Diabetic nephropathy	1/23 (4.3%)
Diabetic + hypertensive nephropathy	1/23 (4.3%)
Focal segmental glomerulosclerosis	1/23 (4.3%)
Obstructive nephropathy	1/23 (4.3%)
Systemic lupus erythematosus	1/23 (4.3%)

Abbreviations: IS, immunosuppression; KTx, kidney transplant.
[a]Mean + SD.
[b]Count (%).

effector molecules (Figure 1E,F), accompanied by an increase of cells expressing only one or no effector molecule (Figure 1F). Unless otherwise stated, live $CD3^+TCRV\alpha7.2^+CD161^+$ $CD8^+$ and $CD8^-CD4^-$ "DN" MAIT cells were identified within PBMC as depicted in the gating strategy in Figure S1A.

3.2 | Impairment of *E. coli* induced MAIT cell functions by immunosuppressive drugs in vitro

To decipher whether immunosuppressants influence MAIT cell functions induced by antigenic triggering, PBMC of healthy individuals were activated with formalin-fixed *E. coli*. IL-17 and the degranulation marker CD107a were included in the analysis being typically induced after TCR-dependent MAIT cell activation. Under these conditions, Tac, CyA, and prednisolone (Pred) significantly diminished frequencies of $TNF\alpha^+$ and $IL\text{-}17^+$ MAIT cells, whereas Tac and Pred also significantly reduced portions of $IFN\gamma^+$ cells; granzymeB expression was impaired only by Pred. Interestingly, the capacity of MAIT cells to release cytotoxic granula, being reflected by CD107a staining, was not affected by any of the drugs applied (Figure 2A-F). A dose dependency of immunosuppressive agents on frequencies of $TNF\alpha^+$ MAIT cells was evident for both Tac, CyA and Pred (Figure S1C). In context with bacterial stimulation, polyfunctionality of MAIT cells was significantly diminished following preincubation with Tac and CyA and moderately affected by Pred, as mirrored by reduced frequencies of cells expressing 4 effector molecules at a time (TNFα, IFNγ, granzymeB, and CD107a) (Figure 2G,H). As frequencies of $IL\text{-}17^+$ MAIT cells were very low, they were excluded from polyfunctional analyses. In line with earlier reports,[22] bacterial activation of MAIT cells proved to be largely, but not completely antigen-specific as mirrored by substantial, but not full abrogation of effector function upon MR1 blockade (Figure S1D).

3.3 | Depletion of peripheral MAIT cells in immunosuppressed and tolerant liver transplant recipients

To address how different immunosuppressive regimens affect MAIT cell biology in vivo, their frequencies were determined in treated liver transplant recipients in comparison to a group of tolerant patients as well as to age-matched healthy controls (Tables 1 and 2). Overall, frequencies of $TCRV\alpha7.2^+CD161^+$ MAIT cells within the $CD3^+$ T cell compartment were significantly reduced in LTx patients as compared to healthy controls (Figure 3B). This observation was largely independent of the type of IS regimen (Figure 3A,C) or the dosage of medication (Figure 3D) and equally accounted for tolerant patients (Figure 3A,C,D). These findings could be reproduced when only MAIT cells within the $CD8^+$ and DN compartment were quantified (Figure 3F-H). For a limited number of LTx patients, we assessed MAIT cells during immunosuppressive therapy and 4-9 months after cessation (Table 2). After successful weaning from medication (as reflected by stable graft function), we did not note consistent changes in MAIT cell frequencies both within the $CD3^+$ and the $CD8^+$/DN compartment (Figure 3E,I). Subset distribution analysis highlighted a significant rise in $CD4^+$ MAIT cells (Figure 3J) in treated, but not tolerant LTx patients at the expense of the $CD8^+$ population (Figure 3K), whereas the DN subset remained unaffected (Figure 3L). There was no significant correlation between MAIT cell frequencies and time since transplantation in all LTx patients (data not shown).

Contrary to MAIT cell subset distribution (Figure 3J,K), we observed an inverted ratio of conventional T cells with increased portions of $CD8^+$ at the expense of the $CD4^+$ population in all LTx patients regardless of being treated or not, as compared to healthy controls (Figure S2A,B). Whereas frequencies of $CD3^-CD56^+$ natural killer (NK) cells were similar in all groups (Figure S2C), we detected a significant drop of $CD3^+CD4^+CD25^+FoxP3^+$ natural regulatory T cells in patients treated with immunosuppressive drugs (ISDs) but not in tolerant patients, as compared to healthy controls (Figure S2D). Natural regulatory T cells (nTregs) of both patient groups were further characterized by significantly reduced portions of CTLA4, higher proliferation as mirrored by Ki67 expression, but no differences in frequencies of activated $HLA\text{-}DR^+$ cells (Figure S2E-G). nTregs from all LTx patients showed a substantial reduction of the naïve $CD45RA^+CCR7^+$ subset, counterbalanced by a rise in $CD45RA^-CCR7^-$ effector/memory nTregs (Figure S2H,I).

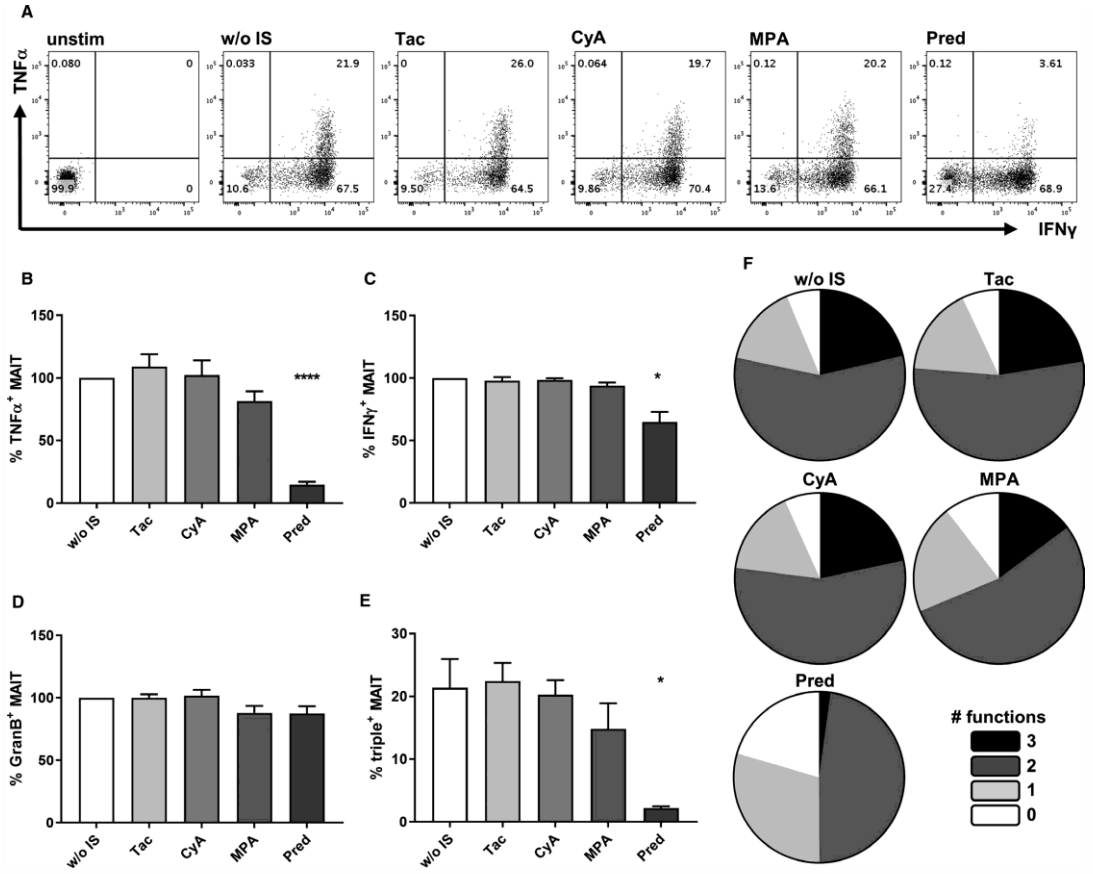

FIGURE 1 Impact of immunosuppressive drugs on cytokine-mediated MAIT cell activation in vitro. Peripheral blood mononuclear cells of healthy donors were preincubated with immunosuppressive drugs as indicated, followed by stimulation with IL-12, IL-15, IL-18, and TL1A. Frequencies of $CD8^+$ and $CD8^-CD4^-$ "DN" MAIT cells expressing TNFα (A,B), IFNγ (A,C), or granzymeB (D) were quantified by FACS. Polyfunctionality was assessed by Boolean gating in MAIT cells that express 3 (E,F), 2, 1, or no functions (TNFα, IFNγ, granzymeB) (F) at a time. Results are based on 5 individual donors obtained in 3 independent experiments. For polyfunctionality analysis (F), the respective means were used. In (B-D), values of stimulated cultures in the absence of ISDs were set to 100%, allowing normalization. All bar graphs show means ± SEM. In all statistical analyses with more than 2 groups, treatment groups were compared to the reference group (w/o IS). CyA, cyclosporine A; FACS, fluorescence-activated cell sorting; IFNγ, interferon gamma; IL, interleukin; IS, immunosuppression; ISD, immunosuppressive drug; MAIT, mucosal associated invariant T; MPA, mycophenolic acid; Pred, prednisolone; Tac, tacrolimus; TNFα, tumor necrosis factor alpha

3.4 | An ex vivo activation signature on MAIT cells distinguishes tolerant LTx patients from those receiving immunosuppressive therapy

To identify cellular signatures that are differentially regulated on MAIT cells isolated from immunosuppressed or tolerant LTx patients, a set of activation and differentiation related molecules was analyzed ex vivo by flow cytometry. First, frequencies of cells expressing the activation markers CD69 (Figure 4A), HLA-DR (Figure 4D), CD38 (Figure 4G), the inducible inhibitor PD1 (Figure 4M), the cytotoxic mediator granzymeB (Figure 4P), or coexpressing CD38 and HLA-DR (Figure 4J) were significantly upregulated in patients as compared to healthy controls. Stratification for treatment regimen, however, revealed that tolerant patients showed no significant differences in frequencies of $CD69^+$ (Figure 4B), $HLA\text{-}DR^+$ (Figure 4E), $CD38^+$ (Figure 4H), or $granzymeB^+$ (Figure 4Q) MAIT cells in comparison to healthy individuals, whereas these markers were significantly upregulated in most treated LTx recipients. Comparing this activation signature in patients during treatment and after cessation of medication, we noted a consistent reduction of MAIT cells being $CD38^+$ (Figure 4I), $CD38^+HLA\text{-}DR^+$ (Figure 4L), and $granzymeB^+$ (Figure 4R). Apart from diminished frequencies of $IL\text{-}18R^+$ MAIT cells in both tolerant and treated patients (Figure S3A) that did now show a distinct

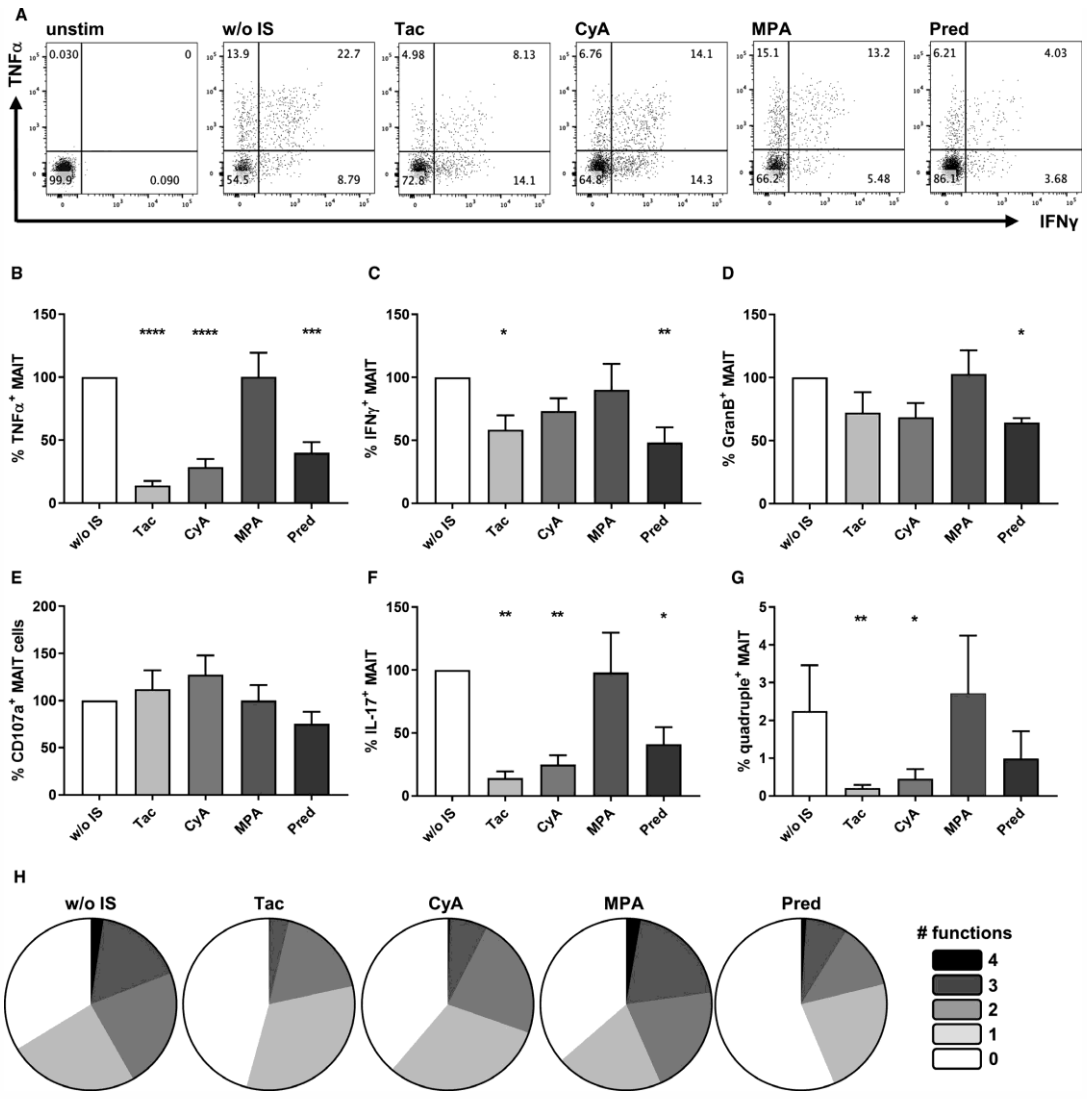

FIGURE 2 Impact of immunosuppressive drugs on bacterial MAIT cell activation in vitro. Peripheral blood mononuclear cells of healthy donors were preincubated with immunosuppressive drugs as indicated, followed by stimulation with fixed *E. coli*. Frequencies of MAIT cells expressing TNFα (A,B), IFNγ (A,C), granzymeB (D), CD107a (E), or IL-17 (F) were quantified by FACS. Polyfunctionality was assessed by Boolean gating in MAIT cells that express 4 (G,H), 3, 2, 1, or no functions (TNFα, IFNγ, granzymeB, CD107a) (H) at a time. Results are based on 6 individual donors obtained in 3 independent experiments. For polyfunctionality analysis (H), the respective means were used. In (B-F), values of stimulated cultures in the absence of ISDs were set to 100%, allowing normalization. All bar graphs show means ± SEM. In all statistical analyses with more than 2 groups, treatment groups were compared to the reference group (w/o IS). CyA, cyclosporine A; FACS, fluorescence-activated cell sorting; IFNγ, interferon gamma; IL, interleukin; IS, immunosuppression; ISD, immunosuppressive drug; MAIT, mucosal associated invariant T; MMF, mycophenolate mofetil; MPA, mycophenolic acid; Pred, prednisolone; TNFα, tumor necrosis factor alpha

expression in subgroups (data not shown), transplant recipients did not exhibit quantitative differences in MAIT cells expressing the pro-apoptotic marker activated caspase 3, or the differentiation related molecules CD56, CD27, or CD8β ex vivo; however, we found the NK-associated activating receptor NKG2D to be slightly upregulated in treated patients (Figure S3B-F).

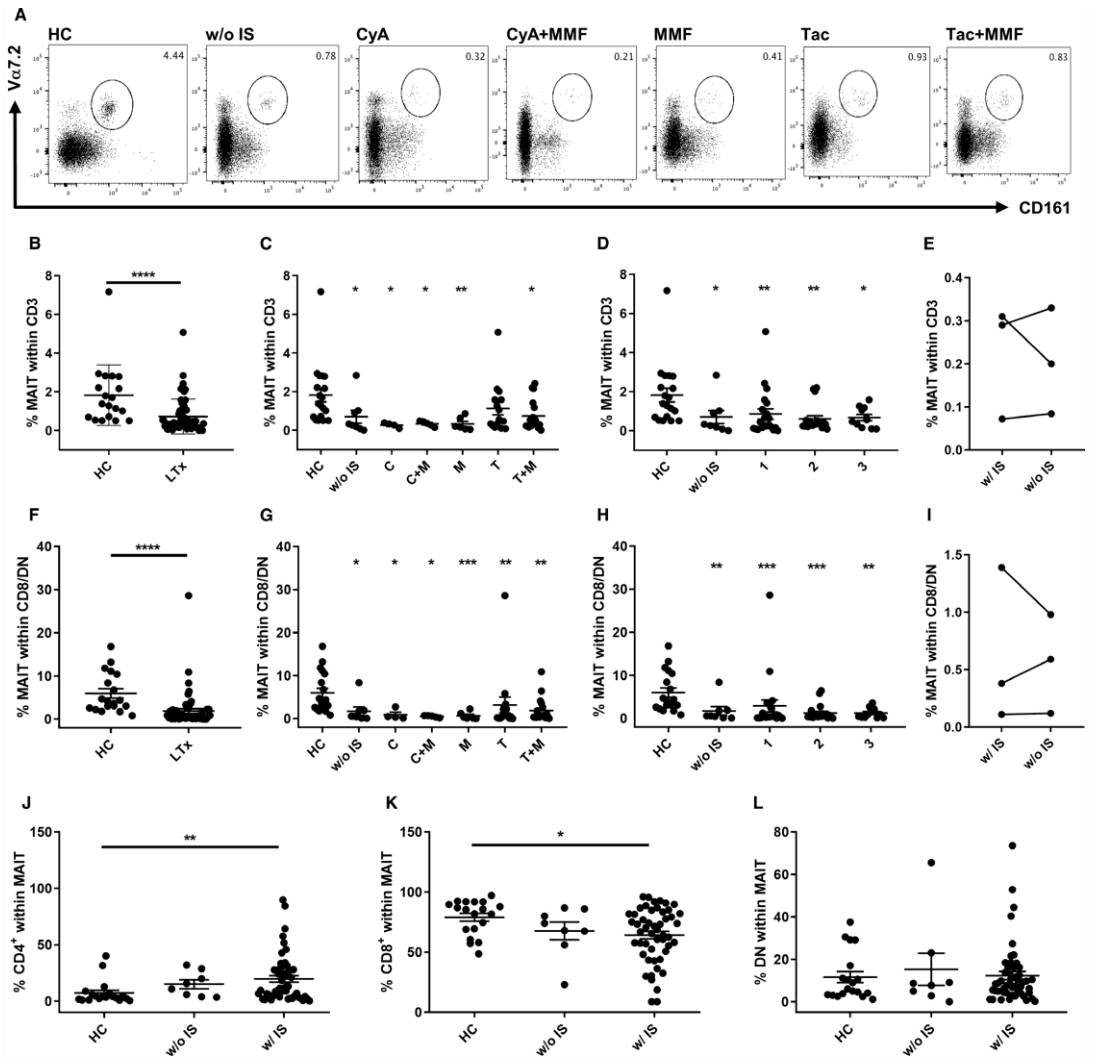

FIGURE 3 Quantitative impairment of MAIT cells in LTx patients. Frequencies of peripheral MAIT cells were determined in tolerant and treated liver transplant recipients and age-matched healthy controls (HC) by FACS within the total $CD3^+$ (B-D) or combined $CD8^+$/DN (A and F-H) compartment. Patients were further stratified according to their type (C + G) or dosage of treatment, or the absence thereof (see Table 1 for details) (D,H). The above mentioned analyses were further conducted in 3 liver transplant recipients during ISD treatment and 4-9 mo after complete drug weaning (E,I). $CD4^+$, $CD8^+$, and DN MAIT cell subsets were individually quantified in tolerant and treated patients and compared to healthy donors (J-L). All bar graphs show means ± SEM. In all statistical analyses with more than 2 groups, treatment groups were compared to the reference group (HC). C or CyA, cyclosporine A; FACS, fluorescence-activated cell sorting; HC, healthy controls; ISD, immunosuppressive drug; MAIT, mucosal associated invariant T; M or MPA, mycophenolic acid; Pred, prednisolone; T or Tac, tacrolimus

FIGURE 4 Tolerant and treated LTx patients are characterized by different activation patterns ex vivo. Frequencies of $CD8^+$/DN peripheral MAIT cells expressing CD69 (A,B), HLA-DR (D,E), CD38 (G,H), $HLA\text{-}DR^+CD38$ (J,K), PD1 (M,N), or granzymeB (P,Q) were quantified ex vivo by FACS in tolerant and treated liver transplant recipients in comparison with age-matched healthy controls. The marker set was further monitored in 3 liver transplant recipients during and after cessation of ISD treatment (C, F, I, L, O, and R). All bar graphs show means ± SEM. In all statistical analyses with more than 2 groups, treatment groups were compared to the reference group (HC). C, cyclosporine A; FACS, fluorescence-activated cell sorting; HC, healthy controls; IS, immunosuppression; ISD, immunosuppressive drug; LTx, liver transplant; M, mycophenolic acid; MAIT, mucosal associated invariant T; T, tacrolimus

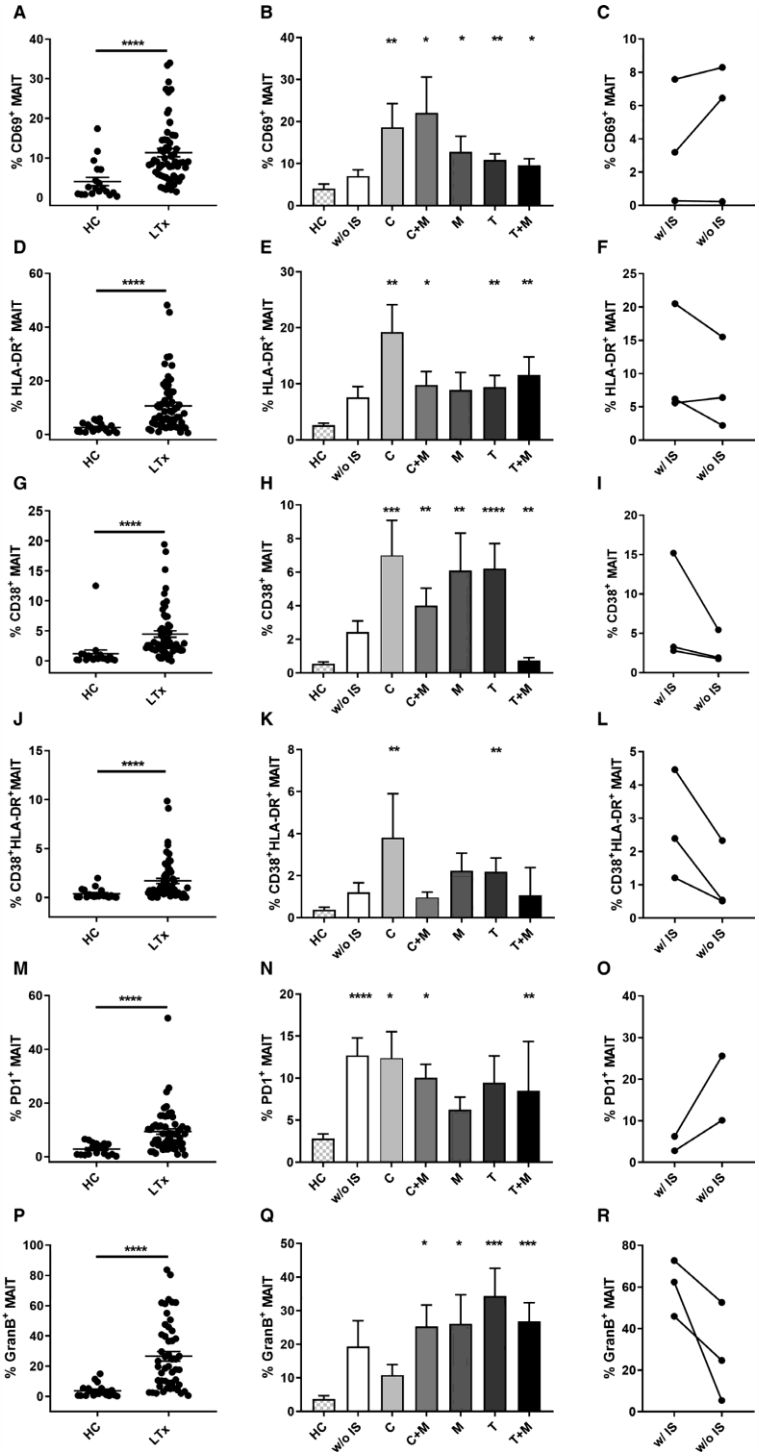
A
% CD69+ MAIT
HC
LTx
B
% CD69+ MAIT
HC
w/o IS
C
C+M
M
T
T+M
C
% CD69+ MAIT
w/ IS
w/o IS
D
% HLA-DR+ MAIT
HC
LTx
E
% HLA-DR+ MAIT
HC
w/o IS
C
C+M
M
T
T+M
F
% HLA-DR+ MAIT
w/ IS
w/o IS
G
% CD38+ MAIT
HC
LTx
H
% CD38+ MAIT
HC
w/o IS
C
C+M
M
T
T+M
I
% CD38+ MAIT
w/ IS
w/o IS
J
% CD38+HLA-DR+MAIT
HC
LTx
K
% CD38+HLA-DR+ MAIT
HC
w/o IS
C
C+M
M
T
T+M
L
% CD38+HLA-DR+ MAIT
w/ IS
w/o IS
M
% PD1+ MAIT
HC
LTx
N
% PD1+ MAIT
HC
w/o IS
C
C+M
M
T
T+M
O
% PD1+ MAIT
w/ IS
w/o IS
P
% GranB+ MAIT
HC
LTx
Q
% GranB+ MAIT
HC
w/o IS
C
C+M
M
T
T+M
R
% GranB+ MAIT
w/ IS
w/o IS

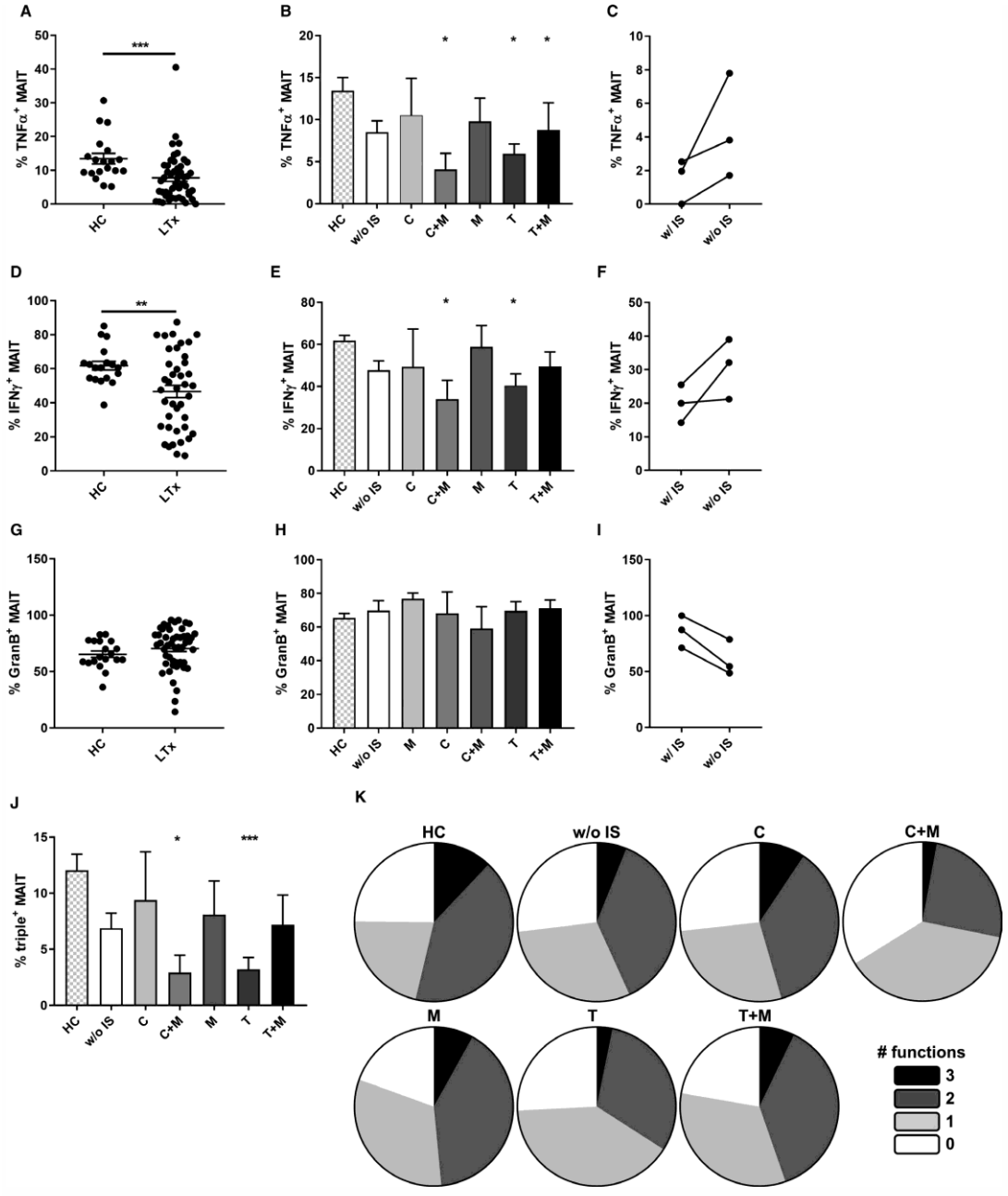

FIGURE 5 Differential impairment of MAIT cells from LTx patients in response to cytokine stimulation. Peripheral blood mononuclear cells from differently treated or tolerant LTx patients and healthy controls were stimulated with IL-12, IL-15, IL-18, and TL1A. Frequencies of MAIT cells expressing TNFα (A,B), IFNγ (D,E), or granzymeB (G,H) were quantified by FACS. MAIT cells from patients before and after ISD weaning were analyzed in an identical fashion (C, F, and I). Polyfunctionality was assessed by Boolean gating in MAIT cells that express 3 (J,K), 2, 1 or no functions (TNFα, IFNγ, granzymeB) (K) at a time. For polyfunctional analysis in (K), the respective means were used. All bar graphs show means ± SEM. In all statistical analyses with more than 2 groups, treatment groups were compared to the reference group (HC). C, cyclosporine A; FACS, fluorescence-activated cell sorting; HC, healthy controls; IFNγ, interferon gamma; IL, interleukin; IS, immunosuppression; LTx, liver transplant; M, mycophenolic acid; MAIT, mucosal associated invariant T; T, tacrolimus; TNFα, tumor necrosis factor alpha

3.5 | Impairment of cytokine-induced MAIT cell functions in LTx patients

To address whether MAIT cells isolated from LTx patients are functionally altered in response to inflammatory cytokines, cells were stimulated directly ex vivo with IL-12, IL-15, IL-18, and TL1A and analyzed for cytokine and cytotoxic molecule production. Collectively, transplanted individuals showed a significant impairment of TNFα and IFNγ production, whereas frequencies of cytokine-induced granzymeB expressing cells were not affected (Figure 5A,D,G). With respect to different treatment regimens, individuals receiving CyA+ MPA or Tac (±MPA with respect to TNFα production) exhibited significantly reduced frequencies of $TNF\alpha^+$ and $IFN\gamma^+$ cells (Figure 5B,E), accompanied by a drop in multipotency (Figure 5J,K). Importantly, whereas MAIT cells of patients weaned from immunosuppression regained their capacity to secrete higher levels of TNFα and IFNγ, they were characterized by a consistent drop in $granzymeB^+$ cells after cessation of medication (Figure 5C,F,I).

3.6 | Impairment of *E. coli* induced MAIT cell functions in LTx patients

In analogy to previous in vitro experiments (Figure 2), we compared the functional capacity of MAIT cells toward bacterial stimulation between LTx patients and healthy controls ex vivo. Overall, frequencies of *E. coli* reactive MAIT cells expressing TNFα (Figure 6A), IFNγ (Figure 6D), and CD107a (Figure 6J) were significantly reduced in patients as compared to controls, whereas those producing granzymeB showed a pronounced increase (Figure 6G). We observed a trend toward reduced frequencies of $TNF\alpha^+$, $IFN\gamma^+$, and $CD107a^+$ MAIT cells in patients regardless of the type of medication (Figure 6B,E,K) that reached significance for IFNγ not only in individuals treated with mycophenolic acid (MPA), Tac-, or Tac+ MPA but also in tolerant LTx patients (Figure 6E), whereas a drop in $CD107a^+$ cells was confined to the 3 aforementioned treatment groups only (Figure 6K). Assessment of polyfunctionality of bacteria-triggered MAIT cells revealed a significant reduction in cells coexpressing all 4 molecules in patients treated with Tac ± MPA as well as in tolerant patients (Figure 6M,N). Withdrawal from immunosuppression led to increased portions of cytokine and CD107a positive cells in all 3 individuals monitored (Figure 6C,F,L) but showed no consistency with respect to granzymeB expression (Figure 6I). Bacterial induction of IL-17 was neither significantly diminished in treated nor in tolerant LTx patients and not included into polyfunctional analyses because of low event counts (data not shown).

3.7 | Kidney transplanted individuals share quantitative and qualitative features of MAIT cells with patients after liver transplantation

To investigate whether prominent features of MAIT cells identified in LTx patients are shared with immunosuppressed individuals after kidney transplantation (KTx, Table 3), cells from a cohort with 23 patients were analyzed ex vivo by flow cytometry. Interestingly, KTx patients exhibited equally diminished frequencies of MAIT cells both within the $CD3^+$ (Figure 7A) and the $CD8^+$/DN (Figure 7B) subsets and we also noted a significant reduction of $CD8^+$ MAIT cells that was counterbalanced by a rise of the $CD4^+$ and DN subsets, although not reaching significance (Figure 7C-E). Whereas portions of $CD69^+$ and $CD38^+$ MAIT cells were similarly increased as observed for LTx recipients in comparison to healthy controls (Figure 7F,G), we could not detect significant changes in frequencies of HLA-DR- or PD1 expressing MAIT cells ex vivo (Figure 7H,I). Also in agreement with our data from liver transplant recipients, we observed an inverted CD4 to CD8 ratio in KTx patients (Figure 7J,K).

4 | DISCUSSION

In this report, we comprehensively examined how peripheral MAIT cell biology is affected by immunosuppressive medication in vitro and in individuals after liver and kidney transplantation ex vivo. Based on a comparison between tolerant or recently weaned LTx patients and treated individuals, we were able to attribute abnormalities in activation state, phenotype, and effector functions partially to the ISD treatment, whereas quantitative impairment is most likely related to the overall post liver transplantation state, because MAIT cell frequencies do not significantly recover after cessation of treatment.

Owing to their innate receptor repertoire, MAIT cells are not solely dependent on TCR mediated activation by bacterial ligands but also respond to cytokines, for example, released in the course of bacterial[23] and viral infections.[3] As recently published by us and others,[8,24] the TL1A containing cytokine combination applied herein robustly and predominantly induces production of the key antimicrobial mediators TNFα, IFNγ, and granzymeB in human MAIT cells. Under these conditions, only prednisolone significantly inhibited cytokine production and polyfunctionality in vitro, whereas cytotoxicity, based on granzyme expression, remained unaffected. In contrast, *E. coli* induced cytokine production and polyfunctionality were diminished both in the presence of calcineurin inhibitors and prednisolone, whereas only the latter significantly reduced frequencies of $granzymeB^+$ MAIT cells. Our data substantially extend the earlier finding that high expression of the multidrug resistance protein 1 does not rescue MAIT cell proliferation from inhibition by IS drugs,[25] because we now provide evidence for both impaired TCR-dependent and -independent effector functions. At the same time, our results mirror the respective signaling pathways required for effector molecule synthesis: whereas cytokine-mediated TNFα and IFNγ production involves phosphorylation of NFκB,[8,26] a component classically targeted by glucocorticoids,[27] *E. coli* induced activation involves TCR downstream calcineurin that is blocked by tacrolimus and cyclosporin A (reviewed in Ref. 28), as well as glucocorticoid targets such as AP-1 (reviewed in Ref. 29). The observation that individual MAIT cell effector functions are differentially regulated by ISD

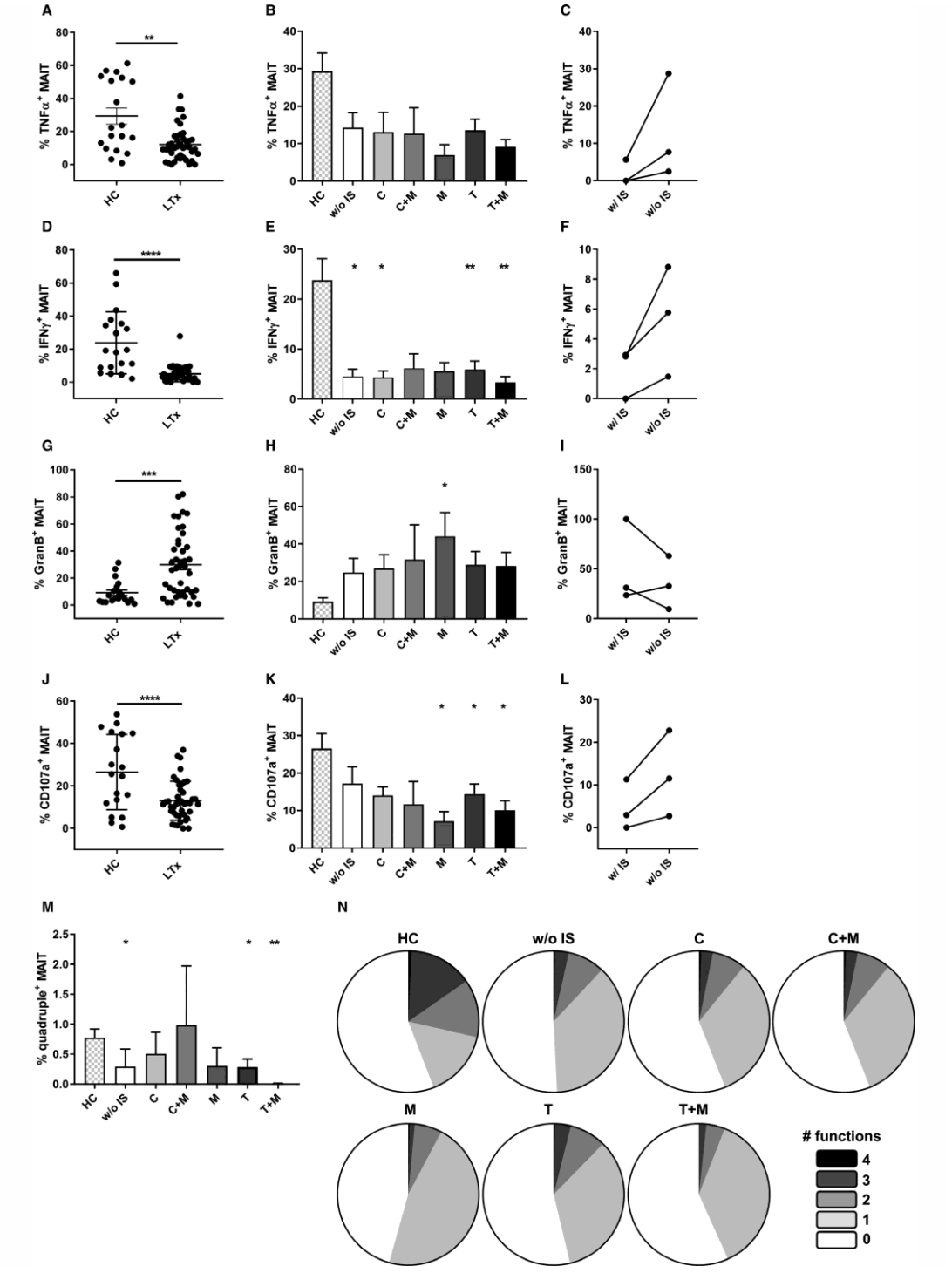
A
% TNFα+ MAIT
HC
LTx
B
% TNFα+ MAIT
HC
w/o IS
C
C+M
M
T
T+M
C
% TNFα+ MAIT
w/ IS
w/o IS
D
% IFNγ+ MAIT
HC
LTx
E
% IFNγ+ MAIT
HC
w/o IS
C
C+M
M
T
T+M
F
% IFNγ+ MAIT
w/ IS
w/o IS
G
% GranB+ MAIT
HC
LTx
H
% GranB+ MAIT
HC
w/o IS
C
C+M
M
T
T+M
I
% GranB+ MAIT
w/ IS
w/o IS
J
% CD107a+ MAIT
HC
LTx
K
% CD107a+ MAIT
HC
w/o IS
C
C+M
M
T
T+M
L
% CD107a+ MAIT
w/ IS
w/o IS
M
% quadruple+ MAIT
HC
w/o IS
C
C+M
M
T
T+M
N
HC
w/o IS
C
C+M
M
T
T+M
functions
4
3
2
1
0

FIGURE 6 Differential functional responses of MAIT cells from LTx patients toward bacterial stimulation. Peripheral blood mononuclear cells from differently treated or tolerant LTx patients and healthy controls were stimulated with formalin-fixed *E. coli*. Frequencies of MAIT cells expressing TNFα (A,B), IFNγ (D,E), granzymeB (G,H), or CD107a (J,K) were quantified by FACS. MAIT cells from patients before and after ISD treatment cessation were analyzed in an identical fashion (C, F, I, and L). Polyfunctionality was assessed by Boolean gating in MAIT cells that express 4 (M,N), 3, 2, 1, or no functions (TNFα, IFNγ, granzymeB, CD107a) (N) at a time. For the latter analysis, the respective means were used. All bar graphs show means ± SEM. In all statistical analyses with more than 2 groups, treatment groups were compared to the reference group (HC). C, cyclosporine A; FACS, fluorescence-activated cell sorting; HC, healthy controls; IFNγ, interferon gamma; IS, immunosuppression; LTx, liver transplant; M, mycophenolic acid; MAIT, mucosal associated invariant T; T, tacrolimus; TNFα, tumor necrosis factor alpha

treatment is supported by data focusing on conventional T cells: similarly to MAIT cells, TNFα production by virus-specific T cells showed a higher sensitivity toward inhibition by immunosuppressants than IFNγ secretion. Furthermore, the cytotoxic potential was only mildly affected by calcineurin inhibitors or prednisolone.[18] At least with respect to IFNγ and granzymeB production, our findings are mechanistically comprehensible as *E. coli* induced effector molecule synthesis in MAIT cells is not solely TCR-dependent, which we confirm in MR1 blocking experiments but could be augmented by cytokines like IL-12 being coreleased in context with bacterial triggering.[22,30] By this means, calcineurin-mediated activation (and thereby consequences of its inhibition by ISD) could be partially bypassed. To allow for translation, drug concentrations in our in vitro assays matched default initial plasma levels recommended for transplant recipients; in addition, titration experiments corroborated effects on MAIT cell functions only for those drugs that already showed potency at therapeutic levels.

As a hallmark, we demonstrate that LTx patients are characterized by a pronounced reduction of peripheral MAIT cells as compared to age-matched healthy controls. This feature comprised all organ recipients regardless of treatment regimen or dosage; surprisingly, it equally accounted for tolerant patients and was reproducible in KTx patients receiving standard IS medication. We cannot not fully exclude that transplantation itself modifies MAIT cell biology, which could, for example, be addressed in an autotransplant setting with nonhuman primates harboring similar MAIT cell frequencies as humans.[31] However, since depletion of MAIT cells is characteristic of severe liver[14-17] and kidney damage,[32] our observation supports the hypothesis that the primary disease likely predetermines the post-transplant MAIT cell pool and that its quantitative replenishment is largely independent from immunosuppression. Peripheral loss of MAIT cells is a common motif in liver diseases of autoimmune-,[14] infectious-[17] and lifestyle-related origin.[16] It further encompasses several nonhepatic pathologies, with HIV being most extensively

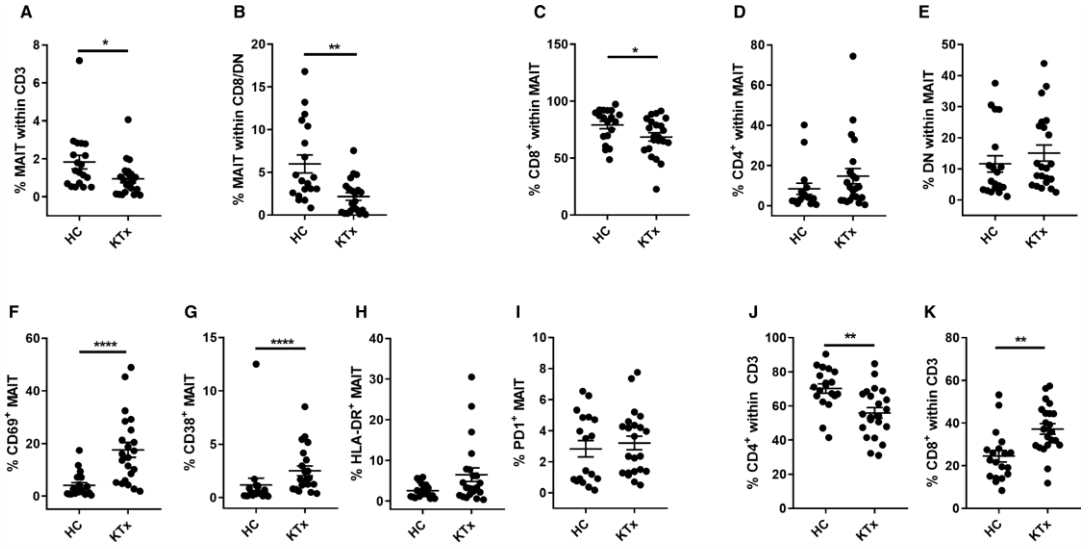

FIGURE 7 Quantitative and phenotypic alterations in MAIT- and conventional T cells from kidney transplanted patients. Frequencies of peripheral MAIT cells were determined in ISD treated kidney transplant recipients (Table 3) in comparison to healthy individuals (HC) by FACS within the total $CD3^+$ (A) or $CD8^+$/DN (B) compartment. Within total MAIT cells, portions of $CD8^+$, $CD4^+$, and DN subsets were further quantified (C-E). For determining the ex vivo activation and exhaustion state, expression of CD69 (F), CD38 (G), HLA-DR (H), and PD1 (I) was analyzed. Frequencies of conventional $CD4^+$ and $CD8^+$ T cells within the CD3 compartment are depicted in (J) and (K), respectively. All bar graphs show means ± SEM. FACS, fluorescence-activated cell sorting; HC, healthy controls; KTx, kidney transplant; MAIT, mucosal associated invariant T

studied.[33] The aforementioned conditions are also interlinked by the general inability to restore MAIT cell homeostasis despite successful treatment, a phenomenon possibly related to their comparatively poor proliferative potential, as reflected, for example, by low portions of peripheral Ki67$^+$ MAIT cells[34] and a high pro-apoptotic propensity.[35] At least with respect to the latter, however, we did not detect elevated frequencies of activated caspase 3 positive MAIT cells, thus questioning the relevance of this mechanism at least within the time frame (on average >10 years since transplantation) of our analyses.

Overall, it still remains obscure what factors promote self-renewal of this unconventional T cell population once thymic output declines and what niches are critical for their survival. Within the transplantation field, the only comprehensive data sets available derive from stem cell transplantation trials. Whereas in an autologous context, MAIT cells recover early,[36] their frequencies do not significantly increase within 2 years after allogeneic stem cell transplantation,[37] suggesting an impact of the inflammatory milieu on their reconstitution. As extra-thymic MAIT cell expansion is possibly depending on interactions with commensals,[38] it is tempting to speculate that in concert with (subclinical) alloinflammation, dysbiosis, established not only during early liver pathology, but also partially maintained after LTx,[39,40] contributes to curtailment of MAIT cell regeneration. Based on data from alcoholic hepatitis, it has already been hypothesized that gut dysbiosis might initially lead to chronic MAIT cell hyperactivation, followed by functional exhaustion, finally promoting their depletion.[16,41] MAIT cells traversing such developmental path are characterized by high expression of CD69, HLA-DR, CD38, PD1, and granzymeB, a signature we observe ex vivo in the majority of treated LTx patients and partially in kidney graft recipients. Interestingly, we demonstrate that this activation pattern is largely downregulated in tolerant individuals, with the exception of PD1, suggesting the possibility of partial normalization of allo- and/or dysbiosis-related triggers. These changes also include the general composition of the MAIT cell pool as the CD4$^+$ subset, being quantitatively expanded in treated patients at the expense of the CD8$^+$ population, was not significantly different from normal donors in treatment-free individuals. For a selected set of markers (CD38, CD38+HLA-DR, granzymeB), examined in patients before and after weaning from IS drugs, attenuation of activation, but not quantitative recovery, was achieved within months, accompanied by a consistent regain of effector cytokine production and cytotoxic capacity. In consequence, our data, together with studies on MAIT cells in severe liver diseases, indicate that transplantation does not entail an environment fostering quantitative regeneration of the MAIT cell pool. Clearly, future studies are needed in order to address whether our findings are restricted to the periphery or mirror local MAIT cell impairment within the liver. Among the few data sets available, a recent report with HCV-infected individuals demonstrated that peripheral MAIT cells might serve as surrogates reflecting the intraorgan situation: patients were characterized by both peripheral and intrahepatic depletion of MAIT cells that equally showed signs of ex vivo hyperactivation,[17] as we also report here.

With respect to patients successfully weaned from medication, it largely remains unclear what predisposes an organ recipient to develop tolerance against the graft, and it is still obscure what characterizes a tolerant immune system. In agreement with the few systematic reports on cellular immunity in operationally tolerant liver recipients,[42] we found normal frequencies of nTregs in tolerant, but not in ISD-treated patients. However, these differences did not extend to ex vivo proliferation, CTLA-4 expression, or differentiation state, thereby not allowing further speculation on their active involvement in the regulation of alloimmunity. Still, despite fingerprints of tolerance within the MAIT- and nTreg compartment, both treated and tolerant organ recipients share an overall attenuated response toward ex vivo stimulation: although not always reaching significance, both patient groups are particularly characterized by impaired cytokine production and cytotoxic capacity (as reflected by CD107a), but elevated portions of granzymeB$^+$ cells after bacterial triggering in comparison to controls. Because high PD-1 levels accompany this partially dysfunctional state also in patients after drug weaning, it needs to be addressed how and when functional exhaustion is imprinted and what consequences arise. Based on experimental limitations in humans, and given the complex individual contribution of alloimmunity, immunosuppression, dysbiosis, and opportunistic infections in our patient cohort, experimental models are needed to decipher in depth the impact of MAIT cells on overall health. However, livers of BALB/c or C57BL/6 mice contain roughly 30-50 times less MAIT cells than humans; furthermore, murine MAIT cells preferentially secrete IL-17 rather than IFNγ.[43] The few experimental studies available provide at least limited translational insights regarding how MAIT cells might contribute to both protective immunity and maintenance of eubiosis. With respect to the latter, MAIT cells are instrumental for regulating gut microbiota in experimental stem cell transplantation.[44] A similar link between quantitative MAIT cell reconstitution and diversity of gut microbiota after allogeneic stem cell transplantation was recently described for humans,[45] arguing in favor of such correlation analyses also after LTx. Infection models further indicated that MAIT cells contribute to decreased bacterial burden in urinary tract infections[46] and mediate protection against mycosis,[47] suggesting a role in these frequent opportunistic infections after kidney[48] or liver[49] transplantation, respectively.

ACKNOWLEDGMENTS

This project was supported by the Bundesministerium für Wirtschaft und Energie (Zentrales Innovationsprogramm Mittelstand, Project ZF4245603AJ7 to KK) and funded by a student award from the Sonnenfeld Stiftung (to AHR).

DISCLOSURE

The authors of this manuscript have no conflicts of interest to disclose as described by the *American Journal of Transplantation*.

DATA AVAILABILITY STATEMENT

The data that support the findings of this study are available from the corresponding author upon reasonable request.

ORCID

Arne Sattler https://orcid.org/0000-0003-2572-5641
Mira Choi https://orcid.org/0000-0002-0286-1491
Frank Friedersdorff https://orcid.org/0000-0002-3104-911X
Katja Kotsch https://orcid.org/0000-0002-3803-0964

REFERENCES

1. Treiner E, Duban L, Bahram S, et al. Selection of evolutionarily conserved mucosal-associated invariant T cells by MR1. *Nature*. 2003;422(6928):164-169.
2. Kjer-Nielsen L, Patel O, Corbett AJ, et al. MR1 presents microbial vitamin B metabolites to MAIT cells. *Nature*. 2012;491(7426):717-723.
3. van Wilgenburg B, Scherwitzl I, Hutchinson EC, et al. MAIT cells are activated during human viral infections. *Nat Commun*. 2016;7:11653.
4. Constantinides MG, Link VM, Tamoutounour S, et al. MAIT cells are imprinted by the microbiota in early life and promote tissue repair. *Science*. 2019;366(6464):eaax6624.
5. Tilloy F, Treiner E, Park SH, et al. An invariant T cell receptor alpha chain defines a novel TAP-independent major histocompatibility complex class Ib-restricted alpha/beta T cell subpopulation in mammals. *J Exp Med*. 1999;189(12):1907-1921.
6. Dusseaux M, Martin E, Serriari N, et al. Human MAIT cells are xenobiotic-resistant, tissue-targeted, CD161hi IL-17-secreting T cells. *Blood*. 2011;117(4):1250-1259.
7. Sattler A, Dang-Heine C, Reinke P, Babel N. IL-15 dependent induction of IL-18 secretion as a feedback mechanism controlling human MAIT-cell effector functions. *Eur J Immunol*. 2015;45(8):2286-2298.
8. Sattler A, Thiel LG, Ruhm AH, et al. The TL1A-DR3 axis selectively drives effector functions in human MAIT cells. *J Immunol*. 2019;203(11):2970-2978.
9. Fergusson JR, Hühn MH, Swadling L, et al. CD161(int)CD8+ T cells: a novel population of highly functional, memory CD8+ T cells enriched within the gut. *Mucosal Immunol*. 2016;9(2):401-413.
10. Wang H, D'Souza C, Lim XY, et al. MAIT cells protect against pulmonary Legionella longbeachae infection. *Nat Commun*. 2018;9(1):3350.
11. Tang X-Z, Jo J, Tan AT, et al. IL-7 licenses activation of human liver intrasinusoidal mucosal-associated invariant T cells. *J Immunol*. 2013;190(7):3142-3152.
12. Jeffery HC, van Wilgenburg B, Kurioka A, et al. Biliary epithelium and liver B cells exposed to bacteria activate intrahepatic MAIT cells through MR1. *J Hepatol*. 2016;64(5):1118-1127.
13. Kurioka A, Walker LJ, Klenerman P, Willberg CB. MAIT cells: new guardians of the liver. *Clin Transl Immunol*. 2016;5(8):e98.
14. Renand A, Habes S, Mosnier J-F, et al. Immune alterations in patients with type 1 autoimmune hepatitis persist upon standard immunosuppressive treatment. *Hepatol Commun*. 2018;2(8):968-981.
15. Seth E, Zimmer CL, Reuterwall-Hansson M, et al. Primary sclerosing cholangitis leads to dysfunction and loss of MAIT cells. *Eur J Immunol*. 2018;48(12):1997-2004.
16. Riva A, Patel V, Kurioka A, et al. Mucosa-associated invariant T cells link intestinal immunity with antibacterial immune defects in alcoholic liver disease. *Gut*. 2018;67(5):918-930.
17. Bolte FJ, O'Keefe AC, Webb LM, et al. Intra-hepatic depletion of mucosal-associated invariant T cells in hepatitis C virus-induced liver inflammation. *Gastroenterology*. 2017;153(5):1392-1403.e2.
18. Weist BJD, Wehler P, El Ahmad L, et al. A revised strategy for monitoring BKV-specific cellular immunity in kidney transplant patients. *Kidney Int*. 2015;88(6):1293-1303.
19. Post DJ, Douglas DD, Mulligan DC. Immunosuppression in liver transplantation. *Liver Transpl*. 2005;11(11):1307-1314.
20. Charlton M, Levitsky J, Aqel B, et al. International Liver Transplantation Society Consensus Statement on immunosuppression in liver transplant recipients. *Transplantation*. 2018;102(5):727-743.
21. Moini M, Schilsky ML, Tichy EM. Review on immunosuppression in liver transplantation. *World J Hepatol*. 2015;7(10):1355-1368.
22. Ussher JE, Bilton M, Attwod E, et al. CD161++ CD8+ T cells, including the MAIT cell subset, are specifically activated by IL-12+IL-18 in a TCR-independent manner. *Eur J Immunol*. 2014;44(1):195-203.
23. Chua WJ, Truscott SM, Eickhoff CS, Blazevic A, Hoft DF, Hansen TH. Polyclonal mucosa-associated invariant T cells have unique innate functions in bacterial infection. *Infect Immun*. 2012;80(9):3256-3267.
24. Leng T, Akther HD, Hackstein C-P, et al. TCR and inflammatory signals tune human MAIT cells to exert specific tissue repair and effector functions. *Cell Rep*. 2019;28(12):3077-3091.e5.
25. Fergusson JR, Ussher JE, Kurioka A, Klenerman P, Walker LJ. High MDR-1 expression by MAIT cells confers resistance to cytotoxic but not immunosuppressive MDR-1 substrates. *Clin Exp Immunol*. 2018;194(2):180-191.
26. Robinson D, Shibuya K, Mui A, et al. IGIF does not drive Th1 development but synergizes with IL-12 for interferon-gamma production and activates IRAK and NFkappaB. *Immunity*. 1997;7(4):571-581.
27. Auphan N, DiDonato JA, Rosette C, Helmberg A, Karin M. Immunosuppression by glucocorticoids: inhibition of NF-kappa B activity through induction of I kappa B synthesis. *Science*. 1995;270(5234):286-290.
28. Azzi JR, Sayegh MH, Mallat SG. Calcineurin inhibitors: 40 years later, can't live without. *J Immunol*. 2013;191(12):5785-5791.
29. Cain DW, Cidlowski JA. Immune regulation by glucocorticoids. *Nat Rev Immunol*. 2017;17(4):233-247.
30. Kurioka A, Ussher JE, Cosgrove C, et al. MAIT cells are licensed through granzyme exchange to kill bacterially sensitized targets. *Mucosal Immunol*. 2015;8(2):429-440.
31. Greene JM, Dash P, Roy S, et al. MR1-restricted mucosal-associated invariant T (MAIT) cells respond to mycobacterial vaccination and infection in nonhuman primates. *Mucosal Immunol*. 2017;10(3):802-813.
32. Juno JA, Waruk JLM, Wragg KM, et al. Mucosal-associated invariant T cells are depleted and exhibit altered chemokine receptor expression and elevated granulocyte macrophage-colony stimulating factor production during end-stage renal disease. *Front Immunol*. 2018;9:1076.
33. Leeansyah E, Ganesh A, Quigley MF, et al. Activation, exhaustion, and persistent decline of the antimicrobial MR1-restricted MAIT-cell population in chronic HIV-1 infection. *Blood*. 2013;121(7):1124-1135.
34. Leeansyah E, Loh L, Nixon DF, Sandberg JK. Acquisition of innate-like microbial reactivity in mucosal tissues during human fetal MAIT-cell development. *Nat Commun*. 2014;5:3143.
35. Gérart S, Sibéril S, Martin E, et al. Human iNKT and MAIT cells exhibit a PLZF-dependent proapoptotic propensity that is counterbalanced by XIAP. *Blood*. 2013;121(4):614-623.
36. Novak J, Dobrovolny J, Brozova J, Novakova L, Kozak T. Recovery of mucosal-associated invariant T cells after myeloablative chemotherapy and autologous peripheral blood stem cell transplantation. *Clin Exp Med*. 2016;16(4):529-537.
37. Solders M, Erkers T, Gorchs L, et al. Mucosal-associated invariant T cells display a poor reconstitution and altered phenotype after allogeneic hematopoietic stem cell transplantation. *Front Immunol*. 2017;8:1861.
38. Garner LC, Klenerman P, Provine NM. Insights into mucosal-associated invariant T cell biology from studies of invariant natural killer T cells. *Front Immunol*. 2018;9:1478.

39. Annavajhala MK, Gomez-Simmonds A, Macesic N, et al. Colonizing multidrug-resistant bacteria and the longitudinal evolution of the intestinal microbiome after liver transplantation. *Nat Commun*. 2019;10(1):4715.
40. Bajaj JS, Fagan A, Sikaroodi M, et al. Liver transplant modulates gut microbial dysbiosis and cognitive function in cirrhosis. *Liver Transpl*. 2017;23(7):907-914.
41. Li W, Lin EL, Liangpunsakul S, et al. Alcohol abstinence does not fully reverse abnormalities of mucosal-associated invariant T cells in the blood of patients with alcoholic hepatitis. *Clin Transl Gastroenterol*. 2019;10(6):e00052.
42. Lau AH, Vitalone MJ, Haas K, et al. Mass cytometry reveals a distinct immunoprofile of operational tolerance in pediatric liver transplantation. *Pediatr Transplant*. 2016;20(8):1072-1080.
43. Rahimpour A, Koay HF, Enders A, et al. Identification of phenotypically and functionally heterogeneous mouse mucosal-associated invariant T cells using MR1 tetramers. *J Exp Med*. 2015;212(7):1095-1108.
44. Varelias A, Bunting MD, Ormerod KL, et al. Recipient mucosal-associated invariant T cells control GVHD within the colon. *J Clin Invest*. 2018;128(5):1919-1936.
45. Konuma T, Kohara C, Watanabe E, et al. Reconstitution of circulating mucosal-associated invariant T cells after allogeneic hematopoietic cell transplantation: its association with the riboflavin synthetic pathway of gut microbiota in cord blood transplant recipients. *J Immunol*. 2020;204(6):1462-1473.
46. Cui Y, Franciszkiewicz K, Mburu YK, et al. Mucosal-associated invariant T cell-rich congenic mouse strain allows functional evaluation. *J Clin Invest*. 2015;125(11):4171-4185.
47. Dias J, Leeansyah E, Sandberg JK. Multiple layers of heterogeneity and subset diversity in human MAIT cell responses to distinct microorganisms and to innate cytokines. *Proc Natl Acad Sci USA*. 2017;114(27):E5434-E5443.
48. Vidal E, Torre-Cisneros J, Blanes M, et al. Bacterial urinary tract infection after solid organ transplantation in the RESITRA cohort. *Transpl Infect Dis*. 2012;14(6):595-603.
49. Hernandez Mdel P, Martin P, Simkins J. Infectious complications after liver transplantation. *Gastroenterol Hepatol*. 2015;11(11):741-753.

SUPPORTING INFORMATION

Additional supporting information may be found online in the Supporting Information section.

How to cite this article: Sattler A, Thiel LG, Ruhm AH, et al. Mucosal associated invariant T cells are differentially impaired in tolerant and immunosuppressed liver transplant recipients. *Am J Transplant*. 2021;21:87–102. https://doi.org/10.1111/ajt.16122

Lebenslauf

Mein Lebenslauf wird aus datenschutzrechtlichen Gründen in der elektronischen Version meiner Arbeit nicht veröffentlicht

Publikationsliste

Signatures and Specificity of Tissue-Resident Lymphocytes Identified in Human Renal Peritumor and Tumor Tissue. Dornieden T, Sattler A, Pascual-Reguant A, Ruhm AH, Thiel LG, Bergmann YS, Thole LML, Köhler R, Kühl AA, Hauser AE, Boral S, Friedersdorff F, Kotsch K. *JASN*. 2021; 32: 2223-2241
IF 9.274

Comparison of three cellular assays to predict the course of CMV infection in liver transplant recipients. Gliga S, Fiedler M, **Dornieden T**, Achterfeld A, Paul A, Horn PA, Herzer K, Lindemann M. *Vaccines.* 2021; 9(2): 88
IF 3.143

Mucosal associated invariant T cells are differentially impaired in tolerant and immunosuppressed liver transplant recipients. Sattler A, Thiel LG, Ruhm AH, Bergmann Y, **Dornieden T**, Chio M, Halleck F, Friedersdorff F, Eurich D, Kotsch K. *Am J Transplant.* 2021; 21: 87-102
IF 7.163

Enhancement of Cytomegalovirus-Specific Cytokine Production after Modulation of the Costimulation in Kidney Transplant Patients. Dornieden T, Wilde B, Korth J, Werner K, Horn PA, Witzke O, Lindemann M. *J Immunol Res.* 2019: 3926175
IF 3.327

The Cytomegalovirus-Specific IL-21 ELISpot Correlates with Allograft Function of Kidney Transplant Recipients. Lindemann M, Korth J, Sun M, Xu S, Struve C, Werner K, **Dornieden T**, Horn PA, Witzke O, Wilde B. *Int J Mol Sci.* 2018; 19(2): 3945
IF 4.556

Danksagung

An dieser Stelle möchte ich allen danken, die es mir ermöglicht haben meine Promotion erfolgreich zu absolvieren. Das Fachgebiet der Immunologie und besonders der Schwerpunkt Transplantation hat mich schon immer sehr interessiert, weshalb ich ausgesprochen dankbar bin, meine Doktorarbeit in diesem Bereich absolviert zu haben.

Daher danke ich besonders meiner Doktormutter Prof. Dr. Katja Kotsch, die es mir ermöglicht hat in Ihrer Arbeitsgruppe zum Thema „Transplantation Immunology“ zu promovieren und mir stets eine umfassende Betreuung ermöglichte. Natürlich bedanke ich mich auch bei der gesamten Arbeitsgruppe Kotsch, die mir bei Fragen immer bei Seite stand, auf deren Hilfe ich immer zählen konnte und die für Spaß bei der Arbeit gesorgt hat, 谢谢 an die chinesischen Mitarbeiter. Besonders dankbar bin ich auch für die vielen Freundschaften, die ich in dieser Zeit im Labor schließen konnte und die mir dabei geholfen haben, auch in schweren Zeiten nicht aufzugeben und zwischendurch abzuschalten. Auch Prof. Dr. Frank Friedersdorff danke ich für die enge und verlässliche Zusammenarbeit, ohne die meine Promotion erst gar nicht möglich gewesen wäre. Ebenso Prof. Dr. Anja Hauser und Dr. Anna Pascual-Reguant, ohne deren Kooperation meiner Arbeit essentielle Experimente und Ergebnisse gefehlt hätten. Ebenfalls danke ich allen anderen Arbeitsgruppen im CBF und CVK für die Zusammenarbeit während dieser Zeit und deren stetiger Aushilfe mit Materialien oder Wissen, sowie generell der Fakultät für Allgemein- und Viszeralchirurgie der Charité-Universitätsmedizin Berlin unter der Leitung von Prof. Dr. Kreis bzw. Dr. Beyer.

Ganz besonders möchte ich mich natürlich auch bei meiner Familie, meinem Freund und meinen Freunden bedanken, die immer hinter mir standen und mich während der gesamten Zeit immer unterstützt und stets aufgemuntert haben.